

UC Merced

UC Merced Electronic Theses and Dissertations

Title

Host-pathogen interactions: Candida albicans infection in the planarian flatworm Schmidtea mediterranea

Permalink

<https://escholarship.org/uc/item/2mf2r3c5>

Author

Maciel, Eli Isael Hernandez

Publication Date

2021

Peer reviewed|Thesis/dissertation

UNIVERSITY OF CALIFORNIA, MERCED

**Host-pathogen interactions:
Candida albicans infection in the planarian
flatworm *Schmidtea mediterranea***

**A dissertation submitted in partial satisfaction of the requirements for the degree
Doctor of Philosophy**

In

Quantitative and Systems Biology

by

Eli Isael Hernandez Maciel

Quantitative and Systems Biology Graduate Program, University of California at Merced,
5200 North Lake Road, Merced, CA 95343, USA

Committee in Charge:

Dr. Néstor J. Oviedo, Advisor

Dr. Clarissa J. Nobile, Chair

Dr. Juris A. Grasis, Member

Dr. Chris T. Amemiya, Member

Dr. Marcos García-Ojeda, Member

Copyright

Eli Isael Hernandez Maciel, 2021

All rights reserved

The Dissertation of Eli Isael Maciel is approved, and it is acceptable
In quality and form for publication on microfilm and electronically:

Dr. Néstor J. Oviedo, Advisor

Dr. Clarissa J. Nobile, Chair

Dr. Juris A. Grasis, Member

Dr. Chris T. Amemiya, Member

Dr. Marcos E. Garcia-Ojeda

University of California, Merced

2021

Dedication Page

I have been fortunate for all the help I have received throughout my career. I did not even know research was an option until my third year of undergrad, and now I am getting my PhD. Thank you for reading my work.

The whole academic journey and process were foreign to me. Being a first-generation student, I relied heavily on outreach programs to teach me and prepare me to apply for universities, scholarships, financial aid, and so on. Specifically, the East Bay consortium and their pre-collegiate academy program, for going through every application, every draft, rejection, and award with me.

To all my friends present and past, every encouragement helped. Some parts of the journey got rough, but the support and distractions made them manageable. Getting me out of Merced and trying new things have created great memories. Even the small talks through the corridors or on the way to the parking lot helped.

To my lab, I am delighted I got to meet all of you. Through all the troubleshooting, stresses, and red lights, we found joy. I have learned so much from everyone and appreciated all the help from all of you. We became very tight, and I will forever have you all as friends.

A mi familia, gracias por siempre apoyarme y ayudarme con cualquier problema. Soy afortunado que he heredado una fraccion de tu disciplina y determinacion. Se que si ustedes tuvieron las mismas oportunidades que yo he recibido, ustedes habrían logrado todo esto con facilidad.

Marcos, you helped start my career in research. You solely got me into the Oviedo lab. After being rejected an abundance of times, you made sure I would be given the opportunity to do research. I am forever grateful for this.

Chris and Juris, both of you contributed immensely to shape my projects, and the advice given was beneficial, especially towards the end of my Ph.D. career. I am glad I had your expertise during discussions of my project and meetings.

Clarissa, if it were not for you and your lab, my whole thesis project would have been something completely different. It was helpful to have you and the support of your lab when exploring the *Candida* field and in accomplishing all of our publications, and now thanks to you, I will join a lab to postdoc in Paris. I enjoyed being a part of your lab.

Nestor, I am grateful to you for believing in me and inviting me to be a part of your lab. You are a great person, and I enjoyed learning from you. I was happy with the research I did and enjoyed the lab environment, and ultimately that is what everyone wants. Thanks for letting me work under your guidance.

Table of Contents

I. List of figures and tables

II. List of abbreviations

III. Curriculum vitae

IV. Abstract

1. Introduction

1.1. Host-pathogen interactions

1.2. *Candida albicans*: Virulence factors and host infection models

1.3. The planarian, *Schmidtea mediterranea*, a new model for host-pathogen interactions

1.4. Interactions between planarians and *Candida albicans*

2. Materials

2.1. Organisms

2.2. Plasmids and primers

2.3. Reagents

2.4. Media, buffers, and solutions

3. Methods

3.1. *C. albicans* culturing

3.2. Infection assay

3.3. Colony forming unit measurements

3.4. Fixation protocols

3.5. Whole mount immunofluorescence

3.6. Cross sections

3.7. Quantitative RT-PCR (qPCR)

3.8. In situ hybridization

3.9. Protein extraction and western blot

3.10. Identification of orthologs

3.11. PCR amplification and gel electrophoresis

3.12. Imaging and data processing

3.13. Statistical analyses

4. Results

4.1. Introducing the planarian, *Schmidtea mediterranea*, as a new host-pathogen model to study *Candida albicans* infections.

4.2. The soaking infection method demonstrates that the hyphal growth form is a highly virulent morphological form of *C. albicans*.

4.3. Visualizing *C. albicans* infection in planarians.

4.4. *Candida albicans* infection induces neoblast division and increases cell death.

4.5 The adherence of *C. albicans* to the planarian leads to a proliferation of neoblasts.

4.6. The ability of *C. albicans* to adhere to the planarian promotes virulence and the proliferation of neoblasts in the planarian.

4.7 The planarian Dectin signaling pathway has a role in the clearance of the *C. albicans* infection.

4.8 The *C. albicans* infection elicits a transcriptional varied neoblast response in the planarian leading to a multi-system response.

5. Discussion

5.1. Development of the planarian infection model for the study of host-pathogen interactions

5.2. The hyphal growth form and adhesins are critical virulence factors of *C. albicans* that elicit a specific neoblast response in the planarian model

5.3. Increased mucus secretion by the planarian counteracts *C. albicans* infection

5.4. Concluding remarks

5.5. Future directions

I. List of Figures and Tables

Figure 1: Common *Candida albicans* cell types.

Figure 2: The anatomy of the *Schmidtea mediterranea* planarian model.

Figure 3: General outline of the planarian immune system.

Figure 4: Different infection assays observed in the planarian model.

Figure 5: Different methods of infecting planarians with *C. albicans*.

Figure 6: The hyper-filamentous *C. albicans* strain is highly virulent.

Figure 7: Visualization of *C. albicans* in planarians during infection.

Figure 8: *C. albicans* penetrates the epithelial layer and infects deeper tissue in the planarian.

Figure 9: The *C. albicans* infection causes neoblast hyper-proliferation and cell death in the planarian model.

Figure 10: Lethal *C. albicans* infection induces early neoblast hyper-proliferation.

Figure 11: *C. albicans* adherence to planarian tissues causes an early wound response.

Figure 12: *C. albicans* genes *ALS3* and *BCR1* are essential for virulence in the planarian model.

Figure 13: The planarian mitotic response decreases during infections using the *C. albicans als3* and *bcr1* mutant strains.

Figure 14: The planarian Dectin signaling pathway plays a role in the clearance of *C. albicans*.

Figure 15: Expression of planarian neoblast subclasses during infection with *C. albicans*.

Figure 16: Specific mesenchymal neoblast and protonephridia markers are upregulated in planarians during *C. albicans* infection.

Figure 17: Cholinergic neurons are upregulated in planarians during *C. albicans* infection.

Figure 18: Summary model of interactions occurring during *C. albicans* infection of planarians.

Table 1: Animal models for *C. albicans*.

II. List of notable abbreviations

1. Planarian - *Schmidtea mediterranea*
2. *Smed* - *Schmidtea mediterranea*
3. Als - Agglutinin-like sequences
4. Sap - Secreted aspartyl proteinases
5. PRR - Pattern recognition receptor
6. CTL - C-type lectin
7. PGRP - Peptidoglycan recognition protein
8. LRR - Leucine rich repeat
9. CHAT - Marker for cholinergic neurons
10. Bcr1 - Biofilm and cell wall regulator 1
11. Efg1 - Enhanced filamentous growth protein 1
12. Nrg1 – Negative regulator of glucose-repressed genes 1
13. SYK - Spleen associated tyrosine kinase
14. TAK1 - Mitogen-activated protein kinase kinase kinase 7
15. CARD - Caspase recruitment domain
16. BCL - B-cell lymphoma
17. MALT1 - Mucosa-associated lymphoid tissue lymphoma translocation protein 1
18. TAB1 - TGF-beta-activated kinase 1
19. NB - Neoblast (planarian stem cell)
20. TBH - Marker for octopaminergic neurons
21. CFU - Colony forming unit
22. H3P- Antihistone-3 phosphorylated antibody

23. TUNEL - Terminal deoxynucleotidyl transferase dUTP nick end labeling
24. RUNT1 - Runt-related transcription factor 1
25. EGR2 - Early Growth Response
26. FISH - fluorescence in situ hybridization
27. PIWI - P-element induced wimpy testis
28. RNAi - RNA interference

III. Curriculum vitae

Eli Isael Maciel	Quantitative and Systems Biology University of California, Merced emaciel@ucmerced.edu
-------------------------	---

Education

2016-08 - present	University of California, Merced Quantitative & Systems Biology, Graduate Division PhD Candidate	2011-08 - 2015-05	University of California, Merced B.S. Biology GPA 3.61 Graduated with honors
-------------------	---	-------------------	---

Awards and Grants

QSB Graduate Student Traveling award 800\$ to travel and present at the International Planaria Meeting	University of California, UC Merced Summer 2018
NSF Graduate Research Fellowships program Fully funded for 3 years (~138,000\$) to work on thesis project	National Science Foundation Fall 2016 - Spring 2019
NSF Traveling Award 1000\$ to travel and present at SCIB conference	National Science Foundation January 2015
NSF REU Friday Harbor Labs Paid summer (2,000\$) for research in larval ecology	University of Washington, Friday Harbor Summer 2014

Publications

1. **Maciel, E. I., Valle-Arevalo, A., Nobile, C., & Oviedo, N. J. (2021).** A Planarian Model System to Study Host-Pathogen Interactions During Fungal Infection. Accepted (MiMB).
2. Barghouth, P.B., Ziman, B., **Maciel, E.I.**, Flores, N., Moua, E., Oviedo, N.J. (2021). Radiation Increases cNeoblasts Plasticity, Allowing Planarians to Tolerate Increased Amounts and Exposures to Gamma-radiation. Manuscript in preparation.
3. Davidian, D., LeGro, M.L., Barghouth, P., Rojas, S., Ziman, B., **Maciel, E.I.**, Ardell, D., Escobar, A.L., Oviedo, N.J. (2021). Restoration of DNA Integrity and Cell Cycle by Electric Stimulation in Planarian Tissues Damaged by Ionizing Radiation. In preparation for submission. Under revision.
4. **Maciel, E. I., Valle-Arevalo, A., Ziman, B., Nobile, C., & Oviedo, N. J. (2020).** Epithelial infection with *Candida albicans* elicits a multi-system response in planarians. *Frontiers in Microbiology*, 11, 3569.
5. Ziman, B., Barghouth, P. G., **Maciel, E. I., & Oviedo, N. J. (2020).** TRAF-like Proteins Regulate Cellular Survival in the Planarian *Schmidtea mediterranea*. *Iscience*, 23(11), 101665.
6. **Maciel, E. I., Jiang, C., Barghouth, P. G., Nobile, C. J., & Oviedo, N. J. (2019).** The planarian *Schmidtea mediterranea* is a new model to study host-pathogen interactions during fungal infections. *Developmental & Comparative Immunology*, 93, 18-27.
7. **Maciel, E. I., & Oviedo, N. J. (2018).** Platyhelminthes: Molecular Dissection of the Planarian Innate Immune System. In Cooper, E. L. (Ed.). (2018). *Advances in comparative immunology*. (pp. 95-115). Springer.

Skills

Aseptic technique	Plasmid transformations	In situ hybridization	Immunohistochemistry
RNA seq analysis	Real Time PCR	Infection assays	Cross Sections via Cryostat
Data analysis	Fluorescent microscopy	RNAi Knockdowns	Microscopy
Biofilm assays			

Research Experience

- 2016-01 - Present Thesis work University of California, UC Merced
Candida albicans is one of the most common fungal pathogens of humans
There are limitations in the evaluation of *C. albicans* infection in existing animal models, especially in terms of understanding the influence of specific infectious stages of the fungal pathogen on the host
I developed the planarian *Schmidtea mediterranea* as a new model to study host-pathogen interactions, and currently investigating the transcriptomic changes in vivo in both the planarian host and the *C. albicans* pathogen during early and late stages of the infection
- 2014-01 - 2015-08 Undergraduate Research University of California, UC Merced
Investigated mechanisms in which cells repair DNA damage after multiple rounds of irradiation
Using the planaria model, I studied how the planaria recovered from multiple rounds of irradiation and how the stem cells recover and proliferate after irradiation.
- 2014-06 - 2015-12 NSF REU Student University of Washington, Friday Harbor
Researched the acclimatization of Sea Star larvae during salinity fluctuations
investigated into the larval behavior in haloclines, and the effect of intense salinity fluctuations on protein expression in *P. ochraceus* larvae.

Teaching Experience

- 2016-01 - Present Lab Instructor (~40-60 students) University of California, UC Merced
Taught the following courses:
 - Introductory biology Laboratory Course (Spring and Summer 2016)
 - Cells, tissues and organs discussion class (Spring 2016)
 - Microbiology laboratory (Fall 2019, Spring 2020, Fall 2020, Spring 2021)
- 2018-02 - Present Private Tutor (~3 students) Merced, California
 - Tutored in all levels of high school math and science.
 - Tutored undergraduates who needed help in biology or chemistry courses.
- 2011-06 - 2013-08 CO-Teacher (~25 students) East Bay Consortium
 - Worked alongside teachers and helped manage a math class of either middle or high school students.
 - Tutored individual students with their assignments.
 - Created and delivered lessons for the class.

Presentations

- 2021-06 Flatworm Fridays Virtual Series, Online
12 minute talk
Transcriptomic changes between the planaria model and *C. albicans* infection
- 2019-04 2019 QSB Annual Retreat University of California, UC Merced
Ten minute talk
Candida albicans epithelial infection elicits an early wound and stem cell response in the planaria model
- 2018-07 2018 Planaria International Meeting Morgridge Institute for Research, Madison WI
Ten minute talk
The flatworm *Schmidtea mediterranea* is a new invertebrate model to study host-pathogen interactions of the human fungal pathogen *Candida albicans*
- 2015-01 2015 SCIB annual conference West Palm Beach, Florida
Poster presentation
Protein Expression in *Pisaster ochraceus* Eggs and Larvae Exposed to Multiple Salinity Fluctuations

IV. Abstract

Candida albicans is one of the most prominent human fungal pathogens. The usage of vertebrate and invertebrate *in vivo* models of candidiasis have provided important insights into the pathogenesis of fungal pathogens. However, there are still limitations with the available animal models used to analyze the early stages of fungal infection and the ensuing response in both the host and the pathogen. Here, I describe the development and characterization of a new model that improves the ability to study the initial stages of a fungal infection. Specifically, I studied early infection stages of *C. albicans* infection using the planarian flatworm, *Schmidtea mediterranea*. I demonstrated that *C. albicans* successfully infects and colonizes planarian tissue. The virulence of *C. albicans* in the planarian model is dependent on the ability of *C. albicans* to adhere to and to form filaments during infection, which is similar to what has been observed in vertebrate infection models. Interestingly, however, I show that adherence of *C. albicans* to the planarian epithelial layer leads to a unique multi-system response (not shown using other models) involving the nervous and excretory systems along with transcriptomic changes resembling the early wound response. I propose that the increased activity of the host excretory system may be mediated by cholinergic neurons to increase mucus secretion leading to a reduction in *C. albicans* adhesion. Mechanistically, I identified that *C. albicans* infection triggers increased expression of the Dectin signaling pathway and stem cell hyperproliferation. Collectively, I demonstrate that planarians are a tractable model system to investigate host-pathogen interactions resembling the virulence and characteristics of an early mucosal fungal infection in mammals. In addition, my work demonstrates that planarians are useful in understanding unique aspects of how fungal pathogens interact with their hosts that are not currently observable using other animal model systems.

1. Introduction

1.1. Host-pathogen interactions

Animals are exposed to a myriad of pathogens throughout their lifetime^{1,2} and as a result have established several lines of defense including barriers, immune cells, and effector proteins³⁻⁵. Pathogens interact with all of these defenses, adapting to the host, surviving within the new environment, and when conditions allow it infecting and invading tissues⁶⁻⁸. The study of host-pathogen interactions investigates the responses of both organisms during the active infection. The goal of these studies is to increase our understanding of infectious diseases and elucidate the different stages of infection to design effective clinical interventions.

Many animal models have been adapted to study host-pathogen interactions and have identified novel immune functions, which may be useful for studying and combating human diseases⁹⁻¹¹. Clearly, a single model that is highly descriptive of humans would be ideal, but organisms differ in their response to diseases and infections; therefore, prioritizing and focusing solely on one animal model decreases the chances of significant scientific developments¹². Thus, analysis of varied immune responses across the animal kingdom may glean life-saving knowledge of interactions fundamental to animal survival in distinct host environments.

Several unique mechanisms have been identified in a variety of animals to prevent the colonization of pathogens^{4,13,14}. For example, a pathogen such as herpes viruses (*Herpesviridae*) can infect both invertebrates and vertebrates even though they possess vastly different immune systems¹⁵. Disparate cellular and humoral responses upon infection are generated by these groups of animals for elimination of the same pathogen. Importantly, studying how different hosts interact with the same pathogen has provided insight into conserved and unique functions of their immune systems. For example, Toll-like receptors, important pattern recognition receptors (PRRs), were first observed in *Drosophila melanogaster*¹⁶. Further, the generation of biofilms was observed on medical devices in rat models¹⁷, and innate immune memory (also known as trained immunity) has been observed in various invertebrate species¹⁸. Moreover, pathogens have developed several tactics for survival in different hosts, enabling them to escape varied strategies used against them. For example, the fungal pathogen *Candida albicans* has different morphological phenotypes that allow it to survive and infect diverse animals and tissues¹⁹.

Non-mammalian model organisms are increasingly used to study infection behaviors of human pathogens²⁰. These are usually invertebrate models, which are used to investigate virulence, biofilm formation, and host-microbe interactions with different pathogens²¹. Invertebrate models for the study of infections have become popular because they are less expensive to culture in laboratory settings, less ethically challenging, provide relatively rapid responses, and these organisms are genetically tractable hosts compared to murine models²². In addition, invertebrate models aid in the discovery of new therapeutic agents and aspects of the innate immune response to pathogens²³. Although some argue that invertebrate models are less valuable than mammalian models, it is increasingly recognized that they serve as powerful tools to classify the development, adaptation, and evolution of infections.

Each animal has unique mechanisms for the identification and elimination of pathogens. Likewise, individual pathogens have specific adaptations for interaction and survival within hosts. Thus, introduction of a novel model can provide new knowledge of important human pathogens, such as *C. albicans*.

1.2. *Candida albicans*: Virulence factors and host infection models

Fungal pathogens are an increasing threat to global public health, as they kill more than 1.5 million and affect over a billion people every year²⁴⁻²⁶. The emergence of antifungal resistance and the ability to adapt to different environments have increased the prevalence of fungal pathogens worldwide. The genus *Candida*, which includes around 500 species, contains a few species that infect humans, several of which are opportunistic pathogens found in the human microbiota²⁷⁻²⁹. These species are responsible for most hospital-acquired fungal infections^{30,31}. The pathogenic species *Candida albicans* is the most prominent human fungal pathogen³². *C. albicans* can quickly adapt to dynamic environments and evade host defenses facilitating tissue colonization. Thus, although there have been advancements in both diagnostics and treatments, *C. albicans* remains challenging to treat³³.

Humans naturally have *C. albicans* in their microbiota as a commensal. More specifically, it is found in the vascular system, skin, oral cavity, esophagus, gastrointestinal tract, and genitalia in the human body³⁴. As a commensal, *C. albicans* asymptotically colonizes mucosal surfaces; however, disruptions in the host environment or presence of immune dysfunction can result in proliferation of *C. albicans* and subsequent invasion of virtually any site in the host. While most of the infections caused by *C. albicans* are superficial, this pathogen can also cause lethal systemic infections. Fatal infections primarily affect immunocompromised individuals with co-morbidities such as AIDS, individuals undergoing treatment with cancer therapeutics, and individuals receiving immunosuppressant drugs⁹.

C. albicans uses its phenotypic switching ability to infect a wide range of tissues. For instance, its ability to change morphologically allows it to adapt to completely different environments like the digestive tract and skin³⁵. These morphological changes depend on environmental cues and conditions that favor one morphology over another. The ability to transition between different growth forms of *C. albicans*, such as the budding yeast form, pseudohyphal and hyphal forms is an important virulence factor for disease progression³⁶ (Figure 1). These growth forms have different virulence capabilities, and their importance depends on the specific environmental niche. In particular, many adhesion proteins are expressed by the hyphal growth form, which is an important growth form for invading host tissues. In addition, the hyphal growth form has the ability to mask pathogen-associated molecular patterns (PAMPs) through rearrangements of the cell wall, making it challenging for the host to identify and eliminate this pathogen^{37,38}. At the same time, *C. albicans* grows in the yeast growth form in the gastrointestinal tract³⁹, which is known to support its colonization as a commensal in that niche.

In addition to transitioning between the yeast and hyphal growth forms, *C. albicans* also can switch between the white and opaque cell states (Figure 1). This transition is epigenetically regulated and controlled by the mating type locus⁴⁰, and affects multiple traits in *C. albicans*, including immunogenicity, pathogenesis and niche specificity⁴¹.

Perhaps the most apparent difference is that the opaque state is stable at 25°C , is metabolically specialized for selective nutritional conditions, and seems to be specialized for skin colonization⁴². In addition, the filamentation response and the genetic wiring are different in both states. Another phenotypic state is the GUT (gastrointestinally induced transition) cell type of *C. albicans*²⁶. GUT cells seem to be attenuated in most mammalian host niches and appear to be specialized for the gastrointestinal tract⁴³. Overall, these various cell states reveal how *C. albicans* uses distinct strategies to transition and adapt to multiple host niches and notably, between being a commensal and invasive pathogen.

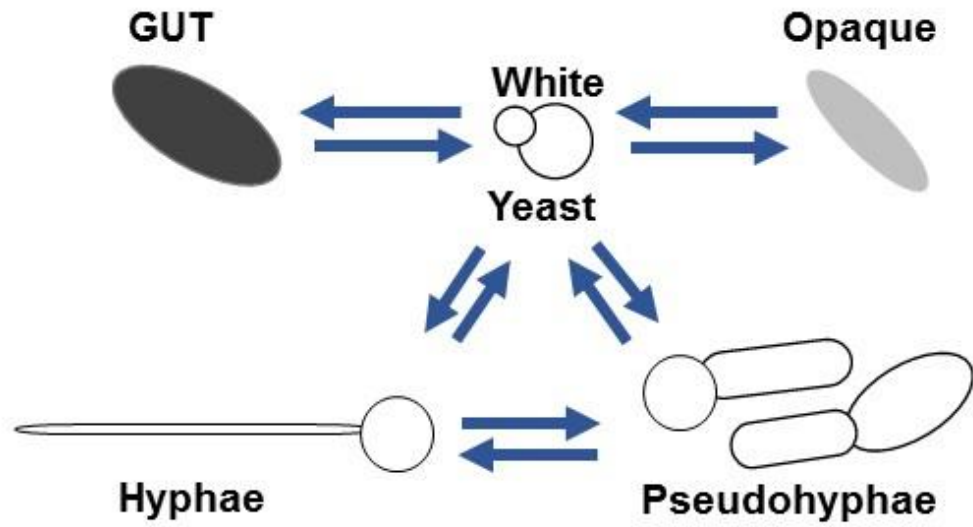


Figure 1: Common *Candida albicans* cell types. Representation of some of the common and reversible cell types of *C. albicans*.

In addition to phenotypic switching, other important virulence factors, such as adhesins, are essential for the early stages of the *C. albicans* infection. Adhesins are specialized proteins that mediate fungal cell adherence to other microbial cells, to abiotic surfaces, and to host tissue^{44,45}. The agglutinin-like sequence (Als) family of proteins consists of at least eight characterized fungal adhesins. The *C. albicans* ALS genes encode glycosylphosphatidylinositol (GPI)-linked cell surface proteins, and Als3, in particular, is crucial for adhesion^{46,47}. Als3 is overexpressed during infections *in vitro* and *in vivo* and is one of the adhesins that contributes to early biofilm formation. Further, disruption of adhesins, and subsequent reduction in *C. albicans* adherence, results in attenuated virulence in murine infection models⁴⁸.

Even after adherence and colonization, *C. albicans* continues to express several virulence factors including secreted aspartyl proteinases (Saps)⁴⁹, which are crucial for oral colonization as they function in adherence to tooth surfaces and in the degradation of proteins. Expression of SAP genes differs and is particular to specific host tissues and environments. *SAP1* and *SAP3* are overexpressed during oral infections, while in epithelial infections *SAP2*, *SAP4*, *SAP5*, and *SAP6* predominate^{50,51}. Saps fulfill different specialized functions during infection that include digestion of host tissues, cell membranes, and molecules⁵². As a result, *C. albicans* expresses different sets of SAP genes depending on the specific animal model or tissue infected.

A wide range of animal models have been used to study the virulence factors and infection processes of *C. albicans*, with murine models being the most common. Virulence is typically assessed in these models through injection of a high concentration of *C. albicans* into the tail vein of the mouse followed by harvesting of organs to analyze infection. In addition, mice and rats provide a variety of infection niches that mimic human colonization sites, such as the vagina, oral cavity, and bloodstream^{10,53}. Although mouse models are often considered to more accurately recapitulate human candidiasis than other models, an immunocompromised mouse must be used⁵⁴. This provides a disadvantage as it eliminates a component of the host immune response and disrupts the natural interactions between the host and pathogen.

In addition, although mouse infection models display similarities with the human system, they currently only recapitulate late stages of infection, hindering the study of early stages of *C. albicans* infection. As an alternative, invertebrate models display a similar course of *C. albicans* infection as observed in humans. Moreover, invertebrate models can reveal unique features of *C. albicans* and host responses not observed in mammals. Therefore, using a variety of models, both vertebrate and invertebrate, provides complementary perspectives and unique advantages due to differences in environmental stressors, immune systems, and tissues. Utilization of animal models to study the development of infection will result in a more comprehensive understanding of how *C. albicans* adapts to and survives in the host environment.

I introduce the planarian *Schmidtea mediterranea* as an alternative invertebrate model to study different stages of *C. albicans* fungal infection. The planarian model has the advantage of allowing observation of infection at early time points, as it can mimic a mucosal epithelial infection (i.e., a skin infection) occurring at room temperature. Due to the ease of infection and exposure to various pharmacological agents, *Schmidtea mediterranea* is an excellent model organism for infection. Further, this model will facilitate

investigation of several *C. albicans* virulence factors, such as morphological transitions, the secretion of proteases, and the expression of adhesins, all of which have been suggested as attractive therapeutic targets. In addition, highly virulent *Candida* species, such as *Candida auris*, are emerging and becoming more prevalent, and further exploring fungal infections with the planarian model may reveal potential solutions for human health issues caused by other fungal pathogens.





Animal model	Advantages	Disadvantages
<i>Mus musculus</i> and <i>rattus rattus</i> 	<ol style="list-style-type: none"> 1. Most resemble human infections 2. Observe infections in medical devices 3. Variety of different tissue to infect 4. Whole genome sequence 5. Creation of Knockout murine models 	<ol style="list-style-type: none"> 1. Must be immunocompromised 2. Infected by injection 3. Long life span and higher cost
<i>Drosophila melanogaster</i> 	<ol style="list-style-type: none"> 1. Fast thrupt model and cost efficient 2. Whole genome sequence 3. RNAi libraires available 	<ol style="list-style-type: none"> 1. Must be immunocompromised 2. Infected by injection 3. Requires specific lab equipment
<i>Caenorhabditis elegans</i> 	<ol style="list-style-type: none"> 1. Fast thrupt model and cost efficient 2. Rapid life cycle 3. Physiologically simplistic 4. Cuticle is transparent 5. Progeny are identical 	<ol style="list-style-type: none"> 1. Does not possess immunocompetent cells 2. Its hard to calculate how many <i>C. albicans</i> cells are consumed when infected through feeding 3. Infecting through injection is difficult because of its small size.
<i>Galleria mellonella</i> (larvae) 	<ol style="list-style-type: none"> 1. Fast thrupt model and cost efficient 2. Can grow in 37 °C 3. Large enough to inoculate without causing too much damage 	<ol style="list-style-type: none"> 1. Not able to produce mutant strains 2. Infected by injection 3. Warmer temperature improves its immune response

Table 1: Animal models for *C. albicans*. Advantages and disadvantages of different animal models used to study *C. albicans* infections. Note, *D. melanogaster*, *C. elegans* and *G. mellonella* are invertebrates and do not possess an adaptive immune system.

1.3. The planarian *Schmidtea mediterranea*, a new model for host-pathogen interactions

Planarians are widely used for the study of fundamental biological questions associated with stem cell-mediated tissue regeneration and maintenance of adult tissues. Planarian are bilaterally symmetrical, triploblastic animals that can reproduce sexually or asexually^{55,56}. Furthermore, the planarian model contains a small genome with a basic anatomy, making it a tractable model (Figure 2A-B). As an invertebrate model, planarians have a complex primordium body plan consisting of a brain, ventral cords, protonephridia, digestive system, immune system, and diverse range of cells (Figure 2C)⁵⁷. In addition, planarian flatworms possess a large pool of adult stem cells called neoblasts, which are instrumental for their regenerative capabilities, developmental plasticity, and cell turnover (Figure 2C)^{58,59}. In recent years, the immune system of planarians has received more attention for its potential to regenerate tissues and the ability to clear a broad spectrum of pathogenic bacteria within a short period of time. Current studies in freshwater planarians are primarily conducted in two species, *Schmidtea mediterranea* and *Dugesia japonica*, which are likely to encounter a wide variety of microbial pathogens in their natural habitats (i.e., ponds, rivers, etc.)^{60,61}.

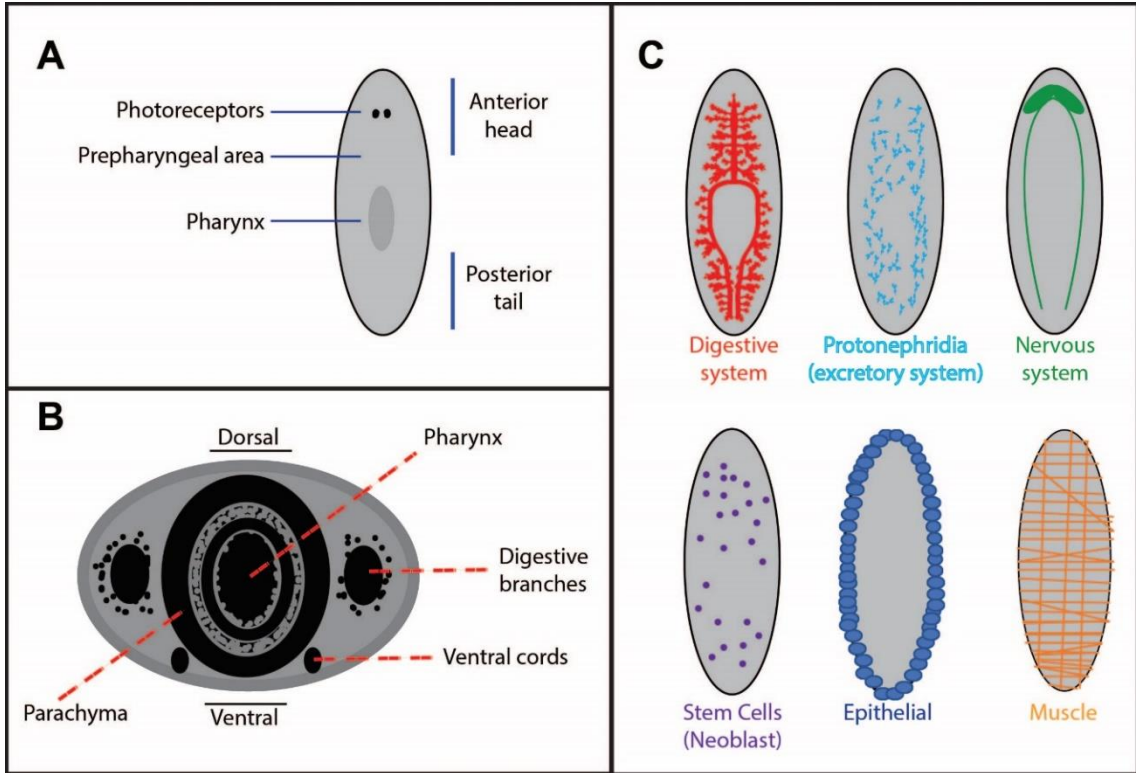


Figure 2: The anatomy of the *Schmidtea mediterranea* planarian model. (A) A general orientation of the planarian in whole-mount images. (B) Model of the transverse cross-sections of planarians. (C) Depictions of multiple systems and stem cells in planarians.

Remarkably, during asexual reproduction or accidental injury, there are little to no traces of infection in open wounds^{62,63}. These observations provide an opportunity to study the role of the invertebrate immune system in clearing and preventing the growth of microbes. In addition, resources exist for data mining and genomic analysis to identify possible human homologs with predicted functions in the immune system of planarians^{60,64,65}. Finally, using a combination of transcriptomic analysis and the ability to disrupt gene expression, fundamental molecular mechanisms and signaling cascades of the planarian immune response can be identified. Exploiting these mechanisms could potentially eliminate pathogens during injury or colonization in humans.

Recent interest in the planarian immune system led to the identification of several molecular structures capable of identifying mucus membranes, phagocytic cells, Pattern Recognition Receptors (PRRs), complement, and natural flora^{60,61,64,66–68}. The first barrier of the immune system is mucus, which contains digestive and immune properties and provides an extra obstacle for pathogens to overcome^{69–71}.

Planarians have a thin mucus layer covering their exterior and lining the digestive system^{72,73}. This mucus layer represents the first physical barrier to pathogenic microorganisms (Figure 3A-B), and aids in digestion, locomotion, adhesion, and immunity. Gland cells, called insunk epithelial cells, are found in the pharynx and subepidermal regions of planarians, which secrete mucus (Figure 3C)⁷⁴. This mucus is a dynamic semipermeable barrier that allows for the movement of vital molecules and obstructs movement of invading pathogens. Proteomic analysis of the planarian mucus revealed a total of 1,604 proteins, some of which are antimicrobial peptides, zymogens, and proteases that possess digestive and immunological roles (Figure 3B-D)^{73,75}. Phenoloxidase is an active zymogen in planarians that originates from its precursor, prophenoloxidase^{61,64}. Phenoloxidase facilitates the formation of the pigment melanin, leading to the sequestration of foreign material when phagocytosed⁷⁶. The mucus within the intestinal system of planarians contain several proteases with predicted roles in activation of PRRs⁷⁷.

The planarian immune system has long been known to recognize and respond to pathogens, while discriminating their own microbial flora. Recent studies show, planarians eliminate prominent, lethal, and evasive human pathogens^{60,66,67}. Moreover, the planarian model has shown impressive recovery when infected via feeding, soaking in, or injection of various pathogens^{60,66,67}. These infection studies and the improvement of the genome's annotation have resulted in increased attention on the immune system of this organism. The planarian's robust immune system was first studied through infections of various bacterial pathogens^{60,78}, including *Mycobacterium tuberculosis* and *Staphylococcus aureus*, which are prevalent human pathogens and the leading causes of death by infection worldwide⁷⁹. For these studies, planarians were infected via feeding of 1×10^5 – 1×10^9 bacterial cells mixed with 50 μ L of liver, and within three to nine days the bacterial infections were cleared⁶⁰. In another case, planarians were incubated with *Pseudomonas aeruginosa* for 24 to 48 hours. While feeding *P. aeruginosa* to planarians did not cause disease, infection through soaking did⁶⁶. In fact, at a concentration of 2×10^8 cells/mL, pseudomonas infection caused morphological phenotypes and even death in some cases. The contradicting results obtained with these infection methods demonstrates the differential immunological responses of the gut and epidermis of planarians. Moreover, these studies resulted in the identification of human homologs relating to autophagy, the immune response, and inflammatory pathways. Nevertheless, knowledge of the planarian

immune system remains incomplete as these recent investigations have only scratched the surface.

Planarian infection studies also resulted in the identification of the immunological roles of phagocytic cells contained in the planarian digestive tract. The presence of these phagocytic cells in the digestive tract suggests the ability to rapidly uptake and eliminate pathogens and foreign particles (Figure 3E-F)⁶¹. In addition, prior studies had found that phagocytic cells can migrate from the digestive tract into other tissues when animals are injected with heat-shocked bacteria⁶⁰. However, these observations were made using an electron microscopy, and no markers or mechanisms of cellular-mediated elimination of pathogens were analyzed. Thus, more research is necessary to understand how phagocytic cells of planarians function. It should be noted that planarians, like other invertebrates, have evolved over long periods of time. Thus, novel effectors against microbial pathogens are likely to be identified in this model.

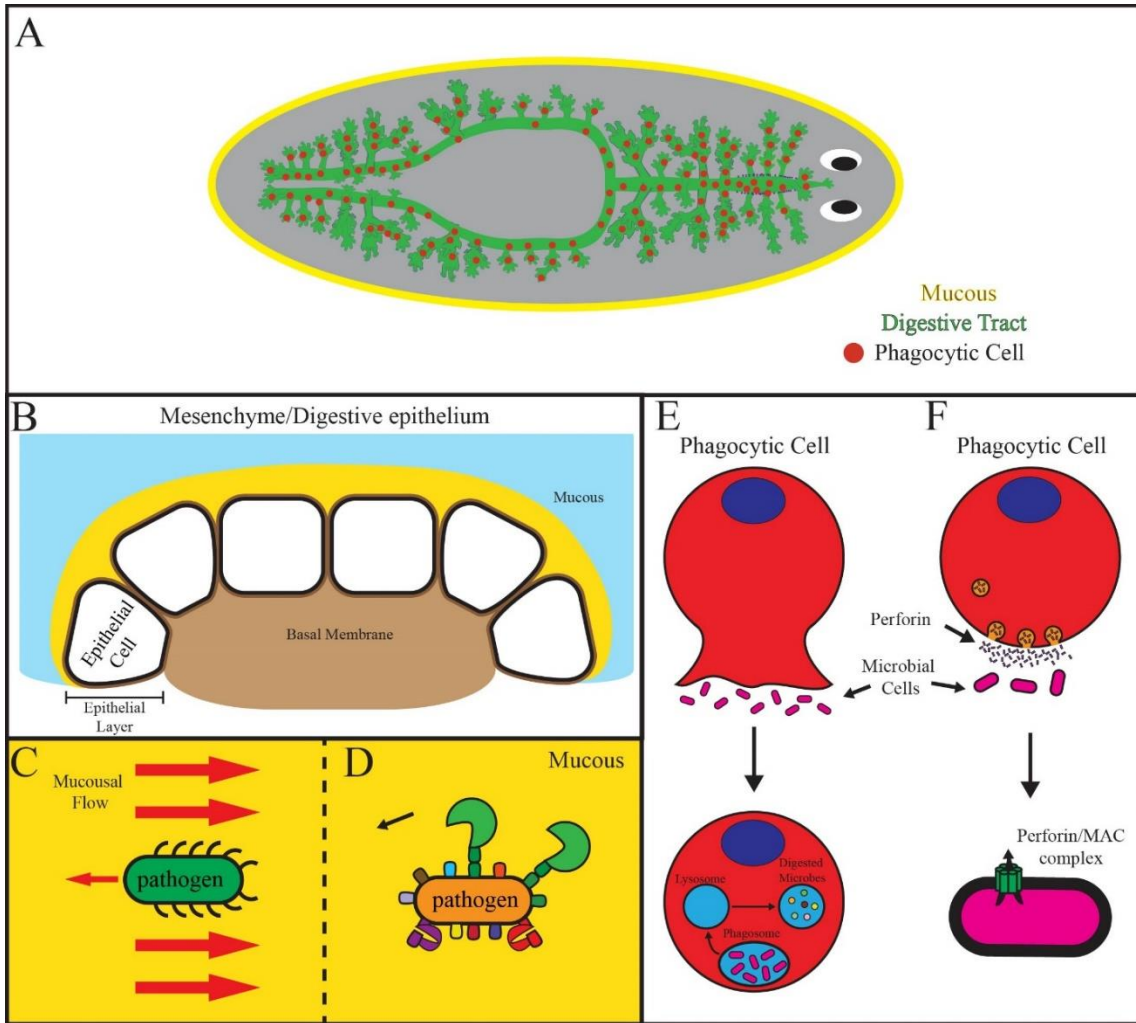


Figure 3: General outline of the planarian immune system. (A) Phagocytic cells along the digestive tract. (B) Magnified illustration of the digestive epithelium and connective tissue underneath (Basal Membrane), highlighting the mucus layer covering epithelial cells (yellow outline). (C) The mucus membrane creates resistance and countercurrent that prevents microbes from colonizing and penetrating the epithelial layer. (D) Mucus proteins: zymogens and protease (purple and red structures, respectively, participate in the degradation of microbes and initiate inflammatory responses. Green shapes are predicted C-type lectin functions that may participate in the elimination of microbes. (E) Representation of the potential mechanisms used by phagocytic cells to eliminate microbes in planarians. The process may involve the fusion of the phagosome with lysosome-containing degradative enzymes. (F) A hypothetical scenario whereby phagocytic cells secrete perforin which binds to microbes and creates a pore structure resulting in diffusion of the cytoplasmic contents.

1.4. Interactions between Planarians and *Candida albicans*

This research aims to establish the planarian flatworm as an infection model for *Candida albicans*. Focus was placed on the planarian's ability to eliminate the fungal pathogens and *C. albicans*' ability to invade planarian tissue. Specifically, I utilized the planarian model to observe different stages of *C. albicans* infection and identify the subsequent host responses. First, a methodology was established to observe the early stages of infection and classify any phenotypes in the planarians resulting from exposure to *C. albicans*. Additionally, I aimed to identify the *C. albicans* virulence factors that are responsible these responses.

I identified that adding *C. albicans* cells to the water where planarians are stored (i.e., soaking) was the best method compared to feeding or injecting the pathogen (Figure 1). Feeding and injecting the pathogen produced inconsistent amounts of adhering *C. albicans*. In addition, it was challenging to inoculate the pathogen in a high enough concentration to cause any morphological changes, and the few cells that did attach would only last two days before being cleared. On the other hand, the success of the feeding method depended on the amount of pathogen and food (i.e., liver paste) each animal consumes. As a result, there was great variance in the number of *C. albicans* cells inoculating the planarians. Further, no morphological phenotypes were observed post-infection using the feeding method. Whereas infecting through soaking was the most consistent, this method showed equal distribution of *C. albicans* cells adhering to the planarian epithelium and demonstrated several morphological phenotypes. Furthermore, I was able to observe *C. albicans* penetrating the epithelium and infecting deeper tissues, resulting in severe and lethal infections. I concluded, the soaking method with *C. albicans* was the most convenient strategy to infect planarian.

I also studied the cellular response planarians mount during *C. albicans* infection. Planarians have pluripotent stem cells called neoblasts that are essential for regeneration and tissue renewal^{59,81}. I identified two time points when there is an increase in neoblast mitotic activity during infection. A similar mitotic response has been described upon injury^{82,83}. Nonetheless, I noticed the spatiotemporal mitotic responses were somewhat different between infection and regeneration.

The *C. albicans* infection-induced neoblast hyperproliferation was specific to a subset of stem cells and geared toward the excretory and neural lineages. This finding led us to examine the transcriptional responses of differentiated tissue related to these systems during infection. I found that the expression of markers in cholinergic (*chat+*) neurons increased during the infection. Moreover, knockdown with RNAi targeting neurotransmitters produced in cholinergic neurons led to an increase in mucus production, suggesting a potential role for these neurons in the regulation of mucus production. Additionally, the expression of markers associated with protonephridia cells, which are critical to balance electrolytes, fluids and other molecules, also increased. This together with the macroscopic observation of increased mucous production upon infection, led me to speculate that antimicrobial peptides are secreted, and the transcriptional increase observed in protonephridia is likely involved in the cellular response to fight the pathogen. These findings suggest that there is a multi-system response involving multiple planarian tissues that lead to effective clearance of the fungal infection in planarians.

Furthermore, I identified that proteins commonly involved in *C. albicans* adherence are mediators of the host cellular response during fungal infection. I tested *C. albicans als*, *sap*, and *bcr1* deletion mutant strains; these genes are responsible for adherence, hyphal formation, production of secreted proteases, and biofilm formation. Using these *C. albicans* mutant strains to infect planarians, I analyzed the resulting mitotic response in the host. I found that the *als3* and *bcr1* mutant strains are avirulent and elicit a lower mitotic response in the host compared to the wildtype strain. Based on these results, I propose that adherence of *C. albicans* to the planarian initiates the immune response and that filamentation enhances virulence of the pathogen during an infection. In addition, this new planarian method of infection provides insights into the host immune response and confirms similar observations made following *C. albicans* infection of other animal models^{67,68}

The host-pathogen model described in this work bears strong resemblance to early mucosal infections in mammals, which could lead to additional understanding about fungal infections. The developed infection method allows numerous experiments to be conducted in a short period of time, as analysis of the pathogen's virulence, host immune response, and the observation of infection can all be accomplished within one week. It also allows systemic analysis of host responses and study of the complex interplay of several tissues in response to a superficial infection. Overall, this new experimental model has produced new knowledge about the planarian immune response to a fungal pathogen and provides a tractable tool to dissect early stages of fungal infections.

2. Materials

2.1. Organisms

Planarians:

Schmidtea mediterranea CIW4 is the planarian species used in all the experiments. The planarian culture was maintained as previously described⁸⁴. All planarians were grown and raised in water with 1x Montjuic salts (planarian water). They were fed liver once a week when not used in experiments. Every experiment used animals that were starving for at least one week, apart from the antibiotic exposed animals that were starved for two weeks.

Microorganisms:

Candida albicans strains:

Candida albicans strain SN250 and SC5314 were used as the wildtype control strains. The hyper-filamentous strain TF125 (*nrg1*)⁸⁵ and non-filamentous strain TF156 (*efg1*)⁸⁵ were used to compare the effects of filamentation on the planarian model. Mutant strains TF137 (*bcr1*)⁸⁵, *asl1*⁸⁶, *als3*⁸⁶, *sap1/sap2/sap3*⁸⁷, and *sap4/sap5/sap6*⁸⁷, were used to assay different virulence factors of *C. albicans*.

Bacterial strains:

NEB 10-beta Competent *E. coli* is the bacterial strain used for cloning.

2.2. Plasmids and primers

All cloning was used with pCR-TOPO from Thermo Fisher.

Primers:

Primers were designed using NCBI primer blast⁸⁸. The designed primers were then ordered through Fisher Scientific using their oligos synthesis services.

List of primers used:

Dectin markers	signaling	qPCR primers	Cloning primers
syk		ACGATTCCAGTGGCTGTCAA	ACAACCCCTGGGGAATACCT
		CGCAGTTGTGACATTGTTTCGT	GCCATTACACGTGCTTCTGC
card		GAGCAATCTAGTGAAGATCCGACT	CAACCACACCCATTCCAGAGA
		CTCTGGAATGGGTGTGGTTGT	AAGACGAATGCACCATCAACG
blc		TGCCACAGGTCCATTGCTAA	TCATTTTGCAGAACCCGAATCA
		CCATCCACCGTGTAGAATGA	TTAGCAATGGACCTGTGGCA

malt1	TGTGCTACACTAGAGACCTCC	TGGAATAAAAACGGCTGGCCT
	AGGCCAGCCGTTTTATTCCA	GCGGTTGCAGAAATAGTCGG
tab1	TTGCGGACTAAACCCGGATG	TGGGGTTATTTTTCGCTGGC
	AATCCCCGACACAACGAGAA	TCCGGGTTTAGTCCGCAATC
tak1	AAGCTGTATGGTGCAGGTCC	ACCGTCAAATCGGTTACGCA
	TCCTTGTGCCAGCGTGAAT	CCGGTCGCTCCTTGATTGA

Neobalst	Neobalst Markers	qPCR primers	Cloning primers
NB2	<i>tspan-1+</i>	TGCTGCGGACGAATCAGTTA	GGTAGCCTGTCGTTGGGAAT
		AGTCGCGTTTAGAACGGCAT	CAGCCGGTGTTCATCGTA
NB3	<i>lmo3+</i>	ATGAGGGCGGGAAGTTTTGT	AACCAGGCCTCTCTGTTGAG
		ACATTTGTCCCCAACGCAA	AACTTCCCGCCCTCATTACC
NB11	<i>ston-2+</i>	TGTTCTTGACCTCACGACA	AAGCATGTTGGAAGCAAGCG
		GTCCTGAAACTGTGCTTGC	CCAGTACCCGTTAGGCCATC
NB9	<i>pou2-3+</i>	TCGGGTTAGCCCTCGGTAAT	GACGAGTTGGAGCAGTTTGC
		TCGGCTTCTTGCAACCACTT	AACCTCAATGCTGGTTCCGT
NB4	<i>pcdh11+</i>	CGAGTGCCGCATACAAATCG	CGAGTGCCGCATACAAATCG
		CGTCATCGGTTGCAATTGGG	GTCGACAGTGTACTTGGCCT
NB7	<i>foxA+</i>	CTTGACCGGAATCGGACCTC	CTTGACCGGAATCGGACCTC
		GTCTCATTCCACCGGCCATT	ACTAGCTTCTTGCGATGCGT
NB5	<i>gata456+</i>	GGTGCCGTCTCAGAATCGT	
		TGTGATTGAAGGGCTGGACT	
NB1	<i>zfp1+</i>	CCCGTGCCTGAACAATTTGAC	
		GCGCATGCCTCTGTAGATTTG	
NB6	<i>atoh8+</i>	CTTACCAGAGAACGCCGAGT	CGCTCAATCGCCGAAAGAAT
		AATAACCAGGCACAGCATGGC	TCGGCGTTCTCTGGTAAGAC
NB8	<i>llgl1+</i>	GCTCATGTGCAATTACCCGC	
		TCTTCTTGCGCTACTGCGAT	
NB10	<i>ascl1+</i>	CGACACGAAGACCGCAGAAA	TAGTGGAGCCATGAGTCGGA
		GTTGACCTGTTCCACCCGTT	GCGTTTCGCTTCGCGATATT

2.3. Reagents

Antibodies and stains

Name	Host	Working dilution in PBSTB	Source
Anti-Candida	Rabbit	1:500	ThermoFischer sci
Anti-Phosphorylated histone H3 (Ser10)	Rabbit	1:500	Millipore
anti-caspase-3	Rabbit	1:500	Thermo Fisher
Anti-Digoxigenin-AP	Sheep	1:2000	Roche

Anti-Digoxigenin-POD	Rabbit	1:1000	Roche
Anti-Fluorescein-POD	Rabbit	1:1500	Roche
Alexa 568 anti-rabbit	Goat	1:800	Invitrogen
HRP anti-rabbit	Goat	1:1000	Millipore
Dapi	NA	1:1000	Thermo Fisher

Enzymes

Name	Source
Proteinase K	Invitrogen
Taq DNA polymerase	Invitrogen
DNase	Promega
T3 RNA Polymerase	Promega
T7 RNA Polymerase	Promega
T3 RNA Polymerase	New England Biolabs
T7 RNA Polymerase	New England Biolabs
RNasin	Promega

Kits and reagents for routine molecular biology applications

Name	Source
SYBR Green PCR Mix	Applied Biosystems
QIAprep Spin Miniprep	Qiagen
1 Kb Plus DNA Ladder	Invitrogen
SIGMAFAST NBT/BCIP	Sigma-Aldrich
Verso cDNA Synthesis	Thermo Fisher
Tyramide Signal Amplification	Invitrogen
TOPO™ TA Cloning™	Thermo Fisher
ApoTag® Fluorescein In Situ Apoptosis Detection Kit	Millipore Sigma

2.4 Media, buffers and solutions

Planarian water

Name	Reagents		
1 x Montjuic Salts for planarian water	1.6	mM	NaCL
	1.0 mM CaCl ₂		
	1.0 mM MgSO ₄		
	0.1 mM MgCl ₂		
	0.1 mM KCl		
	1.2 mM NaHCO ₃		

Microorganism medias

Name	Reagents
2XYT (bacteria media)	16g BactoTryptone 10g BactoYeast extract 5g NaCl ~ Fill to 1L with MilliQ water ~ pH 7.0
Luria Broth (LB)	10g BactoTryptone 5g BactoYeast extract 10g NaCl ~ Fill to 1L with MilliQ water ~ pH 7.0
Yeast Peptone Dextrose (YPD)	20g of BactoPeptone 10g of BactoYeast extract 20g Dextrose ~ Fill to 1L with MilliQ water ~ pH 7.4
Rosewell Park Memorial Institute (RPMI)	Sigma-Aldrich
Other Reagents added to media	10g/L of Agarose 50 µg/mL carbenicillin

Solutions for mucus removal, fixations, and permeability

Name	Reagents
HCl Solution	570 µL 10 mL MilliQ Water
NAC Solution	.75g N-acetyl cysteine 10 mL MilliQ Water
Carnoy's solution	6 mL Ethanol 3 mL Chloroform 1 mL Glacial acetic acid
10X PBS	80g NaCl 2g KCl 14.4g Na ₂ HPO ₄ 2.4g KH ₂ PO ₄ 1L MilliQ Water ~ pH 7.2
4% Fix	1.1 mL 36.5% formaldehyde ~ 10 mL with MilliQ Water
Reduction Solution	500 mL 1M DTT 500 mL 10% SDS 200 µL NP40 ~ 10 mL with 1 X PBS
PBSTx	3 mL Tritonx-100 ~1L of 1X PBS
SDS solution	1 mL of 10% SDS 9 mL of 1X PBS
Proteinase K	1 µL Proteinase K 100 µL 10% SDS 1 mL 10X PBS ~ 10 mL with MilliQ Water
Formamide Solution	

Bleaching solution in 1X PBS	2 mL 30% H ₂ O ₂ 8 mL MeOH
Bleaching solution in Methanol	
Formamide solution	300 μL of formamide 9.7 mL

Solutions for immunohistochemistry or in situ hybridization

Name	Reagents
PBSTx	100 mL 10X PBS 3 mL Triton X-100 ~1L of MilliQ Water
PBSTB	1.25 g BSA 50 mL PBSTx
PBSTI	500 μL 1 M Imidazole 50 mL PBSTx
Tyramide Solution	1:1000 FITC or 1:1000 Rhodamine 50 mL PBSTI
Quench	1% NaN ₃ 50 mL Water
20x SSC	175.3 g NaCl 88.2 g Trisodium Citrate ~ pH 7 ~ 1L of MilliQ Water
Wash Hybe	50% DI Formamide 20% 20X SSC 10% 20% Tween 20 20% Water
Hybe Solution	50% DI Formamide 20% 20X SSC 10% 20% Tween 20 10% Dextran Sulfate 10% Water
MABT	11.6 g Maleic Acid 12.5 mL 20X SSC 1 mL Denhardts 10 mL 10% Tween ~ 50 mL with MilliQ Water
MABTB	9 mL MABT 1 mL Inactivated Horse Serum 0.1g BSA
AP Buffer	100 mM Tris pH 9.5 50 mM MgCl ₂ 100 mM NaCl ~ 10mL of MilliQ Water
NBT/BCIP	1 NBT/BCIP Tablet 10 mL 10% PVA
Tyramide FISH Solution	Tyramide solution 4IPBA

Western blot solutions

Name	Reagents
-------------	-----------------

1X RIPA Buffer	100 uL 10X RIPA Buffer 100 10 uL 1mM DTT 150 uL Protease Inhibitor cocktail 10 uL 100mM PMSF 10 uL Phosphatase Inhibitor ~ 1L of MilliQ Water
6X Laemmli Buffer, pH 6.8	1.47g Tris base 1.5g SDS 1.2 100% Glycerol 2.25 mL 2-Mercaptoethanol 7.5mg Bromophenol blue 7.5mg ~ pH 6.8 ~25 mL pf MilliQ Water
Protease Inhibitor cocktail	1 cOmplete mini tablet ~ 1.5 mL of MilliQ Water
10X Running Buffer	30.3g Tris Base 144g Glycine 50 mL 20% SDS ~ 1L of MilliQ Water up to
10X Transfer Buffer	30.3g Tris Base 144g Glycine ~ 1L of MilliQ Water
1X Running Buffer	100 mL 10X Running Buffer ~ 1L of MilliQ Water
1X Transfer Buffer	100 mL 10X Running Buffer 100 mL MeOH ~ 1L of MilliQ Water
Blocking Solution primary	.05g BSA ~ 10mL of TBS-T
Blocking Solution Secondary	0.5g Nonfat Dry Milk ~ 10mL of TBS-T/SDS
TBS-T	50 mL 1M Tris, pH7.4 30 mL 5M NaCl 1 mL Tween-20 ~ 1mL of MilliQ Water
TBS-T/SDS	50 mL 1M Tris, pH7.4 30 mL 5M NaCl 2 mL Tween-20 .5 mL 20% SDS ~ 1L of MilliQ Water

3. Methods

3.1. *C. albicans* culturing

C. albicans strains are streaked and grown in yeast extract peptone dextrose (commonly known as YPD) agar at 30°C for 48 hours. Single colony overnights are grown by shaking at 30°C for 12-16 hours before the infection assay. This culturing condition was used to grow all *C. albicans* strains, including wildtype, mutant, and clinical isolates strains, before all experiments.

3.2. Infection assay

Injecting

The animals were placed in a cold plate to immobilize planarians⁸⁹. An overnight culture was prepared the night before and used after 12 to 14 hours of growth to infect. The overnight culture was centrifuged at 5,000 rpm for 5 minutes and resuspended in 1mL of planarian water. A few microliters were used to infect all animals using a microinjection dispensing one nanoliter. However, you can also use a glass capillary and pick up a *C. albicans* colony from a 48-hour YPD plate and stab the animal gently in the prepharyngeal area (Figure 3). The animals were then placed in clean petri dishes with planarian water and collected for specific experiments at desired time points.

Feeding⁶⁰

An overnight culture of *C. albicans* was prepared and used between 12 to 14 hours. Allocate 10 million cells and centrifuged at 5,000 rpm for 5 minutes. Afterwards, decant the supernatant and keep the pellet. The pellet will be mixed with 50 µL of liver paste, then pipetted to a petri dish containing the animals⁹⁰. The animals should have 2 to 4 hours to feed and will turn a slight pink or red tint, indicating they have eaten. Once the planarians have finished eating, the animal's petri dishes will be cleaned or moved to a clean petri dish. Unfortunately, the planarians will regurgitate some parts of the mixture eaten, so they must be cleaned the next day again.

Soaking⁶⁷

Ten animals were kept in 6 mL plastic wells containing 3 mL of planarian water to which specific concentrations of *C. albicans* cells were added, and the total volume was adjusted to 4 mL. The animals were kept in the infected media for three days. After the three-day exposure, the planarians were washed daily with fresh water and observed under the microscope to record any behavioral or macroscopic defects until collected for specific experiments at various timepoints. All procedures during and after the infection with *C. albicans* were performed at room temperature, the ideal temperature for planarian. Under these conditions, *C. albicans* are not actively dividing in the media, and thus the infection period was extended to three days.

Exposure of cell free filter sterilized infected planarian media

The media from 6 hours post-infection assays was removed from the planarian wells and filter sterilized using a Corning vacuum system with 0.22 μm pore-size 13.6 cm^2 PES Membrane. Uninfected animals were then inoculated with the cell-free filter sterilized media using the soaking infection assay described above.

3.3. Colony Forming Unit measurements

Planarians were collected at the indicated time points during or after the infection and rinsed with planarian water. The animals were homogenized in 500 μL of planarian water and diluted in 10 mL of planarian water. After homogenization, 100 μL of the homogenate was plated onto YPD media agar plates containing a cocktail of broad-spectrum antibiotics. The colonies were counted to obtain CFUs after being incubated at 30°C for 48 hours. The number of colonies were then multiplied by 100 and divided by the number of planarians to calculate colony forming units per planarian.

3.4. Fixation Protocols

NAC fixation

This fixation is used for planarians that will be used in WISH or FISH experiments.

Animals were selected at certain timepoints and placed in 20 mL scintillation vial. Planarians were sacrificed by removing the planarian water and replacing it with 5% NAC solution. N-acetyl cysteine (NAC) is a mucolytic (gets rid of mucus and kills the animals). Rotate vials at room temperature for 5 minutes. Remove NAC solution and add 4% fixative. 4% fixative is a cross-linking fixative. Rotate vials at room temperature for 15-20 minutes. Remove 4% fixative and rinsed twice with .3% PBSTx. Add 37°C preheated reduction solution and leave vials in 37°C water bath for 10 min, agitating occasionally. The reduction was carried out in a water bath with intermittent gentle agitation (specimens are fragile at this step). Reduction aids with permeabilization to allow probe penetration of prepharyngeal region. Remove the reduction solution and rinsed twice with .3% PBSTx. Add 1:1 (MeOH: 0.3% PBSTx) solution. Rotate at room temperature for 7 minutes. Replace 1:1 (MeOH: 0.3% PBSTx) solution with 100% MeOH. Rotate at room temperature for 7 minutes. Rinsed once with 100% MeOH and store vials in -20°C for at least 1 hour or long term for up to several months. Replace MeOH with bleaching solution and leave vials under direct light at room temperature overnight. The bleaching step removes pigment from the animal and increases permeabilization to help visualize the signal. Remove bleaching solution and rinse two times with 100% MeOH. Use immediately or return the specimen to -20°C.

Carnoy's fixation

This fixation is for planarians that will be used for whole-mount immunostaining with anti-phospho-histone H3 (ser10) or anti-caspase-3 antibodies. This stains the neoblasts or cell death of the planarian respectfully.

planarians were placed in 20 ml scintillation vial. Make the appropriate fixing solutions and leave them in ice to become cold before fixation. Planarians were sacrificed by removing all the water and add 5.7% HCl solution. Leave on ice for 5 minutes. Remove HCl solution and add Carnoy's solution. Leave on ice for 2-3 hours. Remove the Carnoy's solution and rinse once with cold 100% MeOH. Replace with cold 100% MeOH and place in -20°C for

at least 1 hour or long term. Remove the MeOH and add 6% bleaching solution. Place under a light source overnight or until entirely bleached. Remove the bleaching solution and rinse twice with 100% MeOH. Use immediately or place in -20°C for long term storage.

SDS fixation

This fixation is for planarians that will be used for whole-mount immunostaining with anti-*Candida* antibody or TUNEL assay. This will stain the *C. albicans* infecting the planarians or cell death respectfully.

animals were placed in 20 mL scintillation vial. They were sacrificed in 7.5% NAC diluted in PBS for 5 minutes. The liquid was removed, and then the planarians were fixed in 4% formaldehyde in 0.3% PBSTx for 20 min. The fixative was then removed, and the animals were rinsed once with 1X PBS. Afterward, the planarians were permeabilized with 1% SDS for 20 min. Remove the SDS and rinse three times with 1X PBS. Lastly, the animals were bleached in 6% H₂O₂ in 1X PBS for 4 hours. Then afterward, the bleached solution was removed and replaced with 1X PBS and stored at 4°C for a week.

Formamide fixation

This fixation is for planarians that will be used for whole-mount immunostaining with anti-*Candida* antibody only after infected through the feeding method.

Planarians were collected in 20 mL scintillation vials. First, the animals were sacrificed in 7.5% NAC diluted in PBS for 5 minutes. Next, the liquid was replaced and fixed with 4% formaldehyde in 1X PBS for 20 min. The fixative was removed and replaced with a 1X PBS wash. After the wash, the planarians were permeabilized with formamide solution for 20 minutes. Afterward, the samples were washed multiple times with 1X PBS and bleached in 6% H₂O₂ in 1X PBS for 4 hours. Lastly, rinse the bleach off and store it in 1X PBS at 4°C for a week.

3.5. Whole mount immunofluorescence

H3P staining

Animals were sacrificed and fixed via carnoys fixation. Worms were then rehydrated in series from 100% MeOH to 100% PBST and blocked for 4 Hours in PBSTB. Planarians were then incubated with the antibody Anti-Phosphorylated histone H3 (Ser10) for 4 Hours at RT or 8 Hours at 4°C. After incubation, antibody was removed and washed every 20 minutes for 2.5 Hours and then replaced with secondary antibody. Alexa 568 anti-rabbit or HRP anti-rabbit was incubated for 4 Hours at RT or 8 Hours at 4°C. The secondary was removed and washed every 20 minutes for 2.5 Hours. For Alexa the staining can then be mounted and viewed, but HRP secondary will then require tyramide amplification. In tyramide amplification, FITC labeled tyramide will be diluted to 1:1000 with PBSTx and added for 20 minutes. After 20 minutes, the tyramide was activated by adding 30% H₂O₂

to have a final concentration of 0.01% of H₂O₂ for 15 minutes. The worms can then be washed several times for 2 hours and then mounted for viewing.

Anti-Candida staining

Animals were sacrificed and fixed via SDS fixation. Planarian were blocked for 4 Hours in PBSTB. Planarians were then incubated with the antibody Anti-Candida for 4 Hours at RT or 8 Hours at 4°C. After incubation, the antibody was removed and washed every 20 minutes for 2.5 Hours and then replaced with secondary antibody. Alexa 568 anti-rabbit for 4 Hours at RT or 8 Hours at 4°C. The secondary was removed and washed every 20 minutes for 2.5 Hours; for Alexa the staining can then be mounted and viewed.

Caspase staining

Animals were sacrificed using the SDS Fixation. Next, the Planarians were blocked for 4 Hours in PBSTB. Planarians were then incubated with the antibody Anti-Caspase-3 (1:500) for 4 Hours at room temperature or 8 Hours at 4°C. After incubation, the antibody was removed and washed every 20 minutes for 2.5 Hours and then replaced with secondary antibody, Anti-HRP (1:1000), for 4 Hours at room temperature or 8 Hours at 4°C. The secondary was removed and washed every 20 minutes for 2.5 Hours; the solution was replaced with FITC tyramide and activated with .01% H₂O₂ for 15 minutes. The solution was then washed off with six washes of PBSTx, each wash being 20 minutes. The animals will then be mounted and viewed.

TUNEL staining

Animals were sacrificed via SDS Fixation. Worms were prepared for TUNEL or immunostaining identically to those designed for *C. albicans* staining. TUNEL was then performed with ApopTag® Fluorescein In Situ Apoptosis Detection Kit as previously described⁹¹. During the double staining, the animals were also fixed for TUNEL staining.

3.6. Cross sections

Animals were stained the same as mentioned before in whole-mount Immunostaining with additional steps after completing the secondary stain. The addition steps compose of prepping the sample for the cryostat. Following a 2-hour soaking period with 15 % sucrose solution in 1X PBS and then replaced with 30% sucrose overnight at 4°C. Next, one single animal was placed in an embedding mold with all the liquid removed and replaced with cryostat embedding media. The animal was positioned accordingly to make transverse cuts. Once the animal's position was finalized, the embedding mold was placed with a solution of dry ice and ethanol for rapid freezing. The samples were then stored at -80°C until ready for cross-sections via cryostat.

3.7. Quantitative PCR (qPCR)

RNA was extracted with Trizol. The quantitative real-time PCR (qPCR) was performed as previously described⁹². The ubiquitously expressed gene Tata box was used as the

control. Each experiment consisted of triplicates per time point and gene. The investigations were independently repeated at least twice. RNA was extracted from uninfected and infected animals (>15 per condition) and converted to cDNA using the Verso cDNA synthesis kit. Gene expression is expressed as fold change in comparison to the control. Average gene expression at each time point was generated from triplicate replications and divided by the average of the control for that experiment.

3.8. *In situ* hybridization

The protocol is a three-day procedure⁹³

Day 1:

To start, transfer NAC fixed worms from glass vials into a 24 well plate. Replace 100% MeOH with 50% MeOH in PBSTx and then 100% of PBSTx for 5 minutes each step. PBSTx and treat with proteinase K solution for 10 minutes. Replace Proteinase K solution with 4% formalin and fix for 10 minutes. Rinse twice with PBSTx. Incubate samples with 1:1 Wash Hybe: PBSTx for 15 minutes. Replace 1:1 with Wash hybe and place in rotator at 56°C for 2 hours. Prepare riboprobes in Hybe solution and heat them at 72°C for 2 minutes. Return the probes to 56°C. Replace prehybe with riboprobe mix. Cover top of wells with aluminum seal and tape the outside. Incubate in rotator at 56° for at least 16 hours.

Day 2:

For the second day, remove riboprobes and store them at -20°C for re-use if possible. Perform the following washes with preheated solutions in the 56°C rotator, two 30 min washes with Wash Hybe, two 30 min washes with 1:1 Wash hybe, three 20 min washes with 2X SSC, and 0.1% Tx and three 20 min washes with 0.2X SSC and 0.1% Tx. Move to 23°C for the final wash. Wash two times for 10 min with MABT. Block for 1 hr in MABTB. Dilute appropriate antibody in MABTB and incubate samples overnight at 4°C while rocking.

Day 3:

For the last day, remove the antibody and discard it. Rinse twice with MABT. Perform 6 x 20 min washes with MABT. Develop worms as per selected development procedure. For NBT/BCIP Colorimetric development: Equilibrate with two, five minutes washes in AP Buffer and 5 min in AP Buffer (5% PVA). Suspend an NBT/BCIP tablet in 10 mL of 10% PVA and add to wells to initiate development. When the stain has reached appropriate levels, rinse two times in PBSTx. Fix in 4% paraformaldehyde fixative for 30 min. Rinse 2X in PBSTx. If desired, use 100% EtOH for 10 min at room temperature to eliminate background staining in NBT/BCIP animals. Clear samples in 80% glycerol overnight at 4°C and mount them onto slides.

On the other hand, for Tyramide Amplification Fluorescent development, incubate samples in 300 uL of FITC tyramide solution for 30 min. Add 6 uL of .15% H₂O₂ directly into the tyramide solution. Cover the well plate and incubate for 45 min. Rinse twice with PBSTx. Add 300 uL of peroxide quench and incubate for 45 min. Rinse twice with PBSTx. For double FISH, incubated in antibody overnight and repeat previous steps. Clear

samples in 80% glycerol overnight in 4°C and mount them onto slides. Re-clear in 80% glycerol and mount.

3.9. Protein extraction and western blot

Animals were dissociated until no tissue fragments were visible and incubated in 1× RIPA buffer Complete Mini Protease Inhibitor Cocktail; 1 mM PMSF; 1 mM DTT) for 30 min on ice. Volume-to mass ratio for this was as follows: 20 dissociated planarians were incubated in 300 µl of 1× RIPA and protease cocktail mixture. Samples were spun at 20,800g for 15 min at 4°C. The supernatant was transferred to a new tube and immediately placed on ice. A 25 µl aliquot of the supernatant was used to measure protein concentration. The remaining solution was mixed with equal volumes of 2x Laemmli buffer (4% SDS, 10% 2-mercaptoethanol, 20% glycerol, 0.004% bromophenol blue, 0.125 M Tris-HCl) and incubated at 95°C for 5 min (or boiled at 100°C) to denature and reduce. Protein lysates were stored at -20°C. A Bio-Rad protein assay was used to determine protein concentration. Western blot Protein lysate aliquots of 40 µg were heated at 80°C for 5 min and loaded in 12.5-15% SDS-PAGE gel along with a molecular weight marker. Samples were transferred to a 30 s methanol-activated PVDF membrane overnight in 1x Tris-glycine transfer buffer [25 mM Tris base, 192 mM glycine, 10% (v/v) methanol, pH 8.3] at 4°C. The membrane was blocked with 5% milk for 1 h and incubated in the primary antibodies overnight at 4°C on a rocker. Primary antibodies: anti-tubulin (1:500), anti-RAD51 (1:5000) and anti-caspase (1:5000). The membrane was washed three times for 30 min before the addition of the secondary antibodies: HRP-conjugated goat anti-rabbit antibody (1:2000) for anti-RAD51 and anti-caspase, HRP-conjugated goat anti-mouse antibody (1:2000) for anti-tubulin. The membrane was washed three times for 30 min and developed using Luminata Forte Western HRP substrate.

3.10. Identification of orthologs

Using the NCBI BLAST tool, selected gene targets were identified with human annotations to find the ortholog using genomic resources for *S. mediterranea*^{65,94,95}. The chosen sequences went through translations and multiple well annotated alignments through different protein databases UNIPROT, PFAM, and NCBI conserved domain to analyze the protein conservation.

3.11. PCR amplification and gel electrophoresis

Half reaction of a PCR reaction is composed of a master mix containing 5µL of PCR buffer with magnesium chloride, 1µL of dNTPs, .5µL of TAQ DNA Polymerase, 41.74µL of water, and .625µL of both the specific forward and reverse primer. The cocktail was placed in a thermocycler where the following cycles occur repeatedly: 94°C denaturing step, 57 to 62°C annealing step, and 75°C elongation step.

To image the size of the amplified sequence, a 1% agarose gel is made with 1X TBE and 2µL of ethidium bromide to stain the DNA. Then, 5µL of each reaction was mixed 2µL of loading dye to load and run in the gel accompanied with a one kB DNA ladder to measure the size. The gel ran at 100V and 0.05A for 40 minutes afterward it was ready to image with a UV camera set to the EtBr filter.

3.12. Imaging and data processing

Animal morphological phenotypes and digital pictures were recorded using a Nikon AZ-100 multi zoom microscope and NIS Elements AR 3.2 software. Area measurements were calculated with ImageJ. Brightness and contrast were adjusted with Adobe Photoshop. Neoblasts were counted and normalized to the area (mm²) using ImageJ. Caspase-3 signal was quantified by measuring levels of fluorescence using ImageJ.

3.13. Statistical analyses

Data are expressed as mean \pm standard error of the mean (SEM) or fold change \pm SEM. Statistical analyses were performed in Prism, GraphPad software Inc. (<http://www.graphpad.com>). Two-way ANOVA was used to determine significance due to multiple conditions within each experiment (ant/post, days 10,15,25, etc.). Power analysis was used to determine if the sample size was adequate to establish the robustness of the statistical analysis.

4. Results

4.1. Introducing the planarian, *Schmidtea mediterranea*, as a new host-pathogen model to study *Candida albicans* infections.

To understand the *Candida albicans* infection, both host and pathogen will need to be observed and analyzed throughout the course of the infection. The first step to study the infection was to establish an infection protocol. The two different methods previously described in planarian literature were to infect the planarians by using either the injection or feeding method⁶⁰. The injection method appeared to be the least effective as it was only mentioned in one study and the results were not described⁶⁰. The same study abandoned the injection method in favor of the feeding method. The majority of studies that use the planarian flatworm as an infection model use the feeding method (Figure 3B)^{60,77,80,96,97}. In this work, both the feeding and infection models were used, in addition to a soaking method. All three of these models are illustrated and described in Figure 4. All of the infection methods mentioned have previously only been applied to bacterial pathogens. They were reproduced with *C. albicans* to compare and standardize their effectiveness.

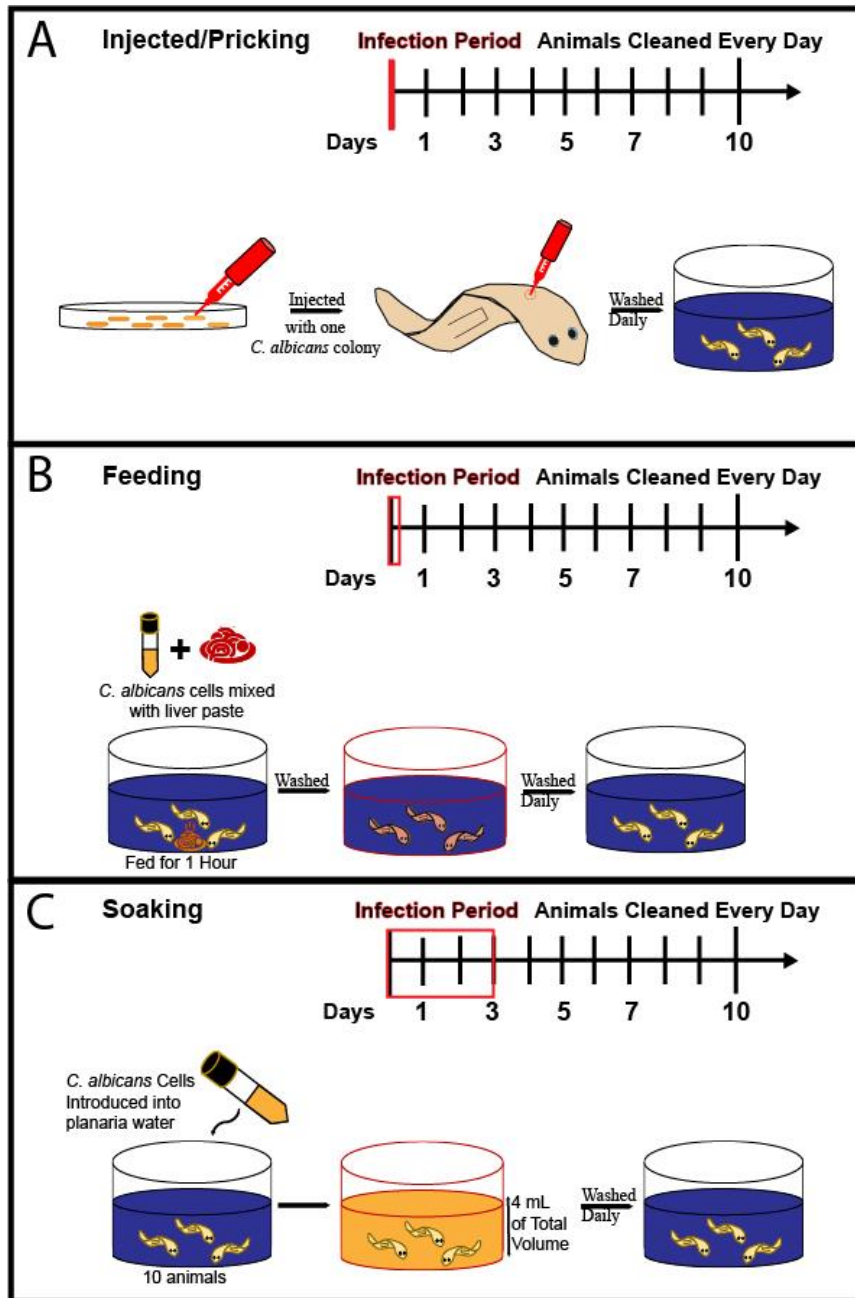


Figure 4: Different infection assays observed in the planarian model. (A) Infection by Injection/pricking, a single microbial colony was pricked with a capillary. The planarian was then pricked with the capillary. The planarian was then placed in a well and observed or collected at specific time points. (B) Infection by feeding, overnight cultures were diluted to the desired concentration and pelleted. The pellet was mixed with liver paste and dispensed to the planarians. After one hour the planarians were washed. Animals that had eaten will have a slight red tint in their body and were successfully infected. The worms were then observed or collected at specific time points. (C) Infection by soaking, from overnight cultures, the desired concentration of cells was calculated and dispensed into a well containing planarians, with the media totaling 4 mL. The planarians remained in the media for three days; after the three days, the planarians were cleaned daily. The worms were then observed or collected at specific time points.

When using the injection method to infect the planarians, I also applied a pricking technique with glass capillaries as typically used to infect flies (Figure 4A)⁹⁸. Both protocols showed similar results, and both were very inconsistent. The *C. albicans* cells had difficulty adhering to the planarians, and the few cells that did adhere only persisted a few days (Figure 5A-B). As the results demonstrate, it appears that *C. albicans* can't properly infect the planarians by injection or pricking, and consequently, this method was abandoned in favor of the feeding method.

Although the feeding method appears practical and repeatable, it can be inconsistent as it is impossible to predict how much each worm will eat. Additionally, the virulence of the consumed pathogens is not assured. The Planarians have evolved as scavengers. They introduce various microbes to their digestive system when they eat, which is why they possess a large population of phagocytic cells in their digestive tract. This evolutionary adaptation may explain why there has not been a study using the feeding method where the pathogen has colonized or killed a planarian. Therefore, pathogen clearance can be assayed, but not pathogenicity and virulence.

When using the feeding method, I observed similar results to previous studies that used the feeding method to infect the planarians with bacteria^{60,78,99}. There was variation in how much *C. albicans* and liver mixture was consumed, but all of the planarians had large amounts of *C. albicans* cells after one day post-feeding (Figure 5C-D). These infected planarians eliminated all the *C. albicans* within a week without displaying any disease-associated phenotypes (Figure 5D). In addition, the planarians behaved normally, it seems as though *C. albicans* did not cause any behavior changes within the host.

The soaking method was the most recently introduced and revealed to be the most effective in observing virulence and infection characteristics of the pathogen (Figure 4C). The soaking method displayed the ability of *C. albicans* to cause a variety of morphological phenotypes in the planarians (Figure 6D). Furthermore, with the soaking protocol, morphological changes of *C. albicans* were able to be visualized within the planarians. An indiscriminate portion of *C. albicans* cells changed from the yeast growth form to the hyphal growth form after the second day (Figure 5E). Thus, the soaking infection method provided more insight into the interactions of both organisms and was therefore used to establish the planarian-*C. albicans* infection model.

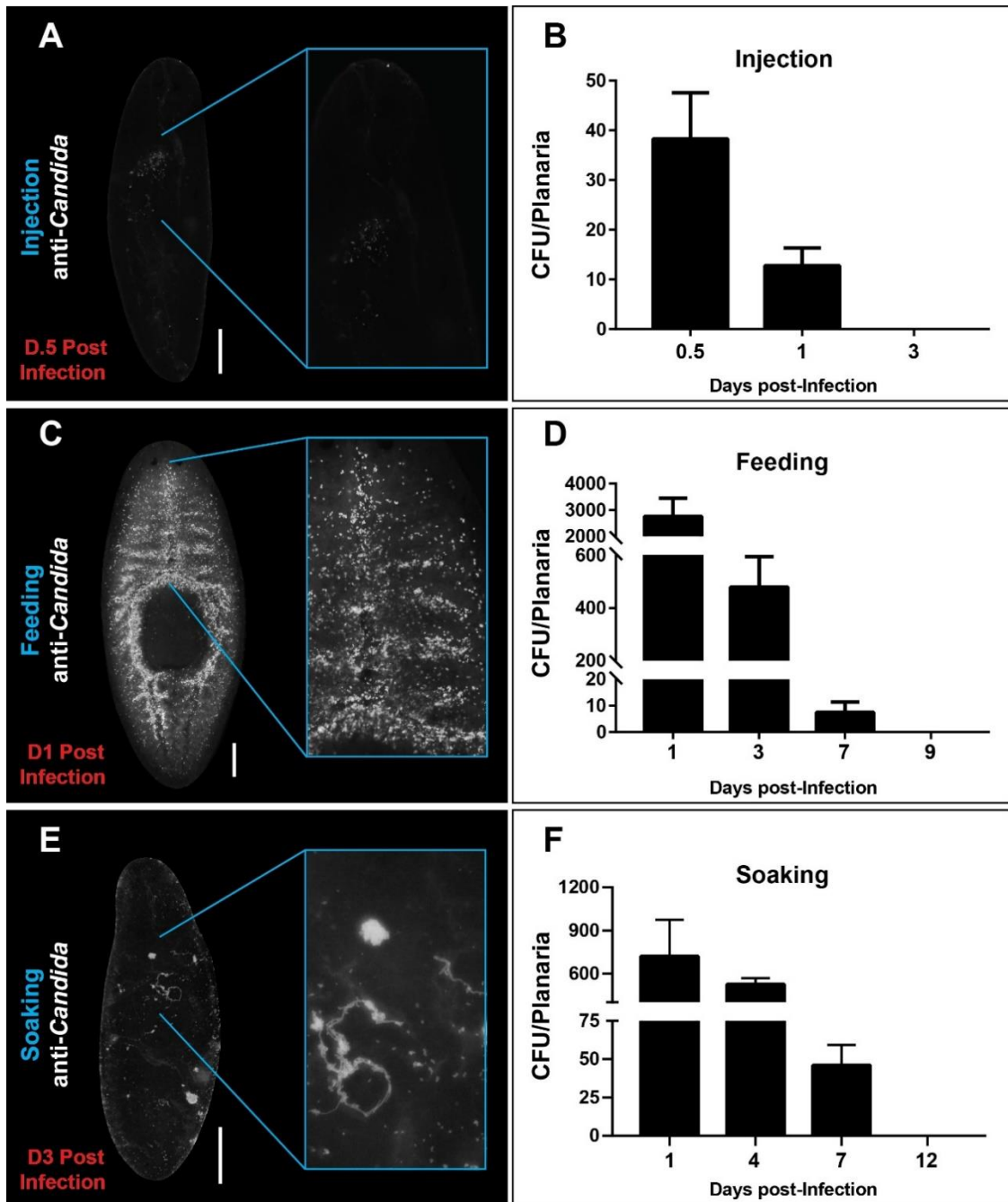


Figure 5: Different methods of infecting planarians with *C. albicans*. (A) Visualization of *C. albicans* infection 6 hours post-injection/prick a colony of *C. albicans* cells in the prepharyngeal area of the planarians. (B) Measurement of colony forming units (CFUs) after pricking the planarians with *C. albicans* colony. (C) visualization of 100 million *C. albicans* cells after 1-day post-infection through feeding. (D) Measurement of colony forming units after infecting the planarians with 100 million *C. albicans* cells through feeding. (E) Visualization of the soaking infecting method using 15 million cells/mL of *C. albicans*. (F) Measurement of CFUs after soaking the animals with 15 million cells/mL of *C. albicans* for three days. All scale bars are 200 μm .

4.2. The soaking infection method demonstrates that the hyphal growth form is a highly virulent morphological form of *C. albicans*.

The following three strains of *C. albicans* were used: wildtype (SN250), non-filamentous (*efg1* mutant), and hyper-filamentous (*nrg1* mutant). The non-filamentous strain is attenuated for virulence, whereas the hyper-filamentous strain is highly invasive in both bloodstream infections in the mice and *C. elegans* models^{100,101}. The difference in the morphology is that the non-filamentous strain is locked in the yeast growth form while the hyper-filamentous strain is locked in the hyphal growth form and seen in (Figure 6A). Measuring the virulence of these strains at a variety of concentrations over a three-day period, I observed different survival rates.

The wildtype strain required around 25 million cells per mL to kill all the planarians (Figure 6B). The non-filamentous strain was the most avirulent. It required more than twice the concentration that the wildtype strain needed to kill all of the planarians. The hyper-filamentous strain was the most virulent, only needing a concentration of 10 million cells per mL to kill all the planarians (Figure 6B). To further analyze the infection response solely from life and death, I focused on the surviving planarians from an infection of 7.5 million cells per mL after three days post-infection of all three strains. I examined the clearance of the infection after the initial three days, using colony forming units (CFU) to dictate how long the planarians took to eliminate the infecting *C. albicans*. All three strains were cleared within ten days (Figure 6C). Notably, the non-filamentous strain had the most cells after the third day.

The morphological defects in the planarians that the *C. albicans* strains caused after three days post-infection were also studied. To that end, I observed that all three *C. albicans* strains caused different rates of morphological defects (Figure 6D-E). The hyper-filamentous strain was the only one that caused 10% of the planarians to partially lyse, while all three strains caused the head regression phenotype (Figure 6D-E). The non-filamentous strain seemed only to cause head regression in planarians, implying that the transition to hyphal is needed to cause lesions or lyse the planarians (Figure 6D-E). Death was observed only in the wildtype and hyper-filamentous strains, with the hyper-filamentous strain killing more than 50% of the planarians, confirming that it is the most virulent. These studies confirm that the hyper-filamentous strain is the most aggressive to the planarian model.

4.3. Visualizing *C. albicans* infection in the planarians

The antibody anti-*Candida* was used to evaluate the effects and distribution of *C. albicans* in planarians. Using three different time points, during an early infection time point (1-day post-infection), a late infection time point (3 days post-infection), and a recovery time point (10 days post-infection). The immunostaining also provided the opportunity to distinguish the morphological forms of *C. albicans* in the planarian tissue and assess their abundance (Figure 8 & 9).

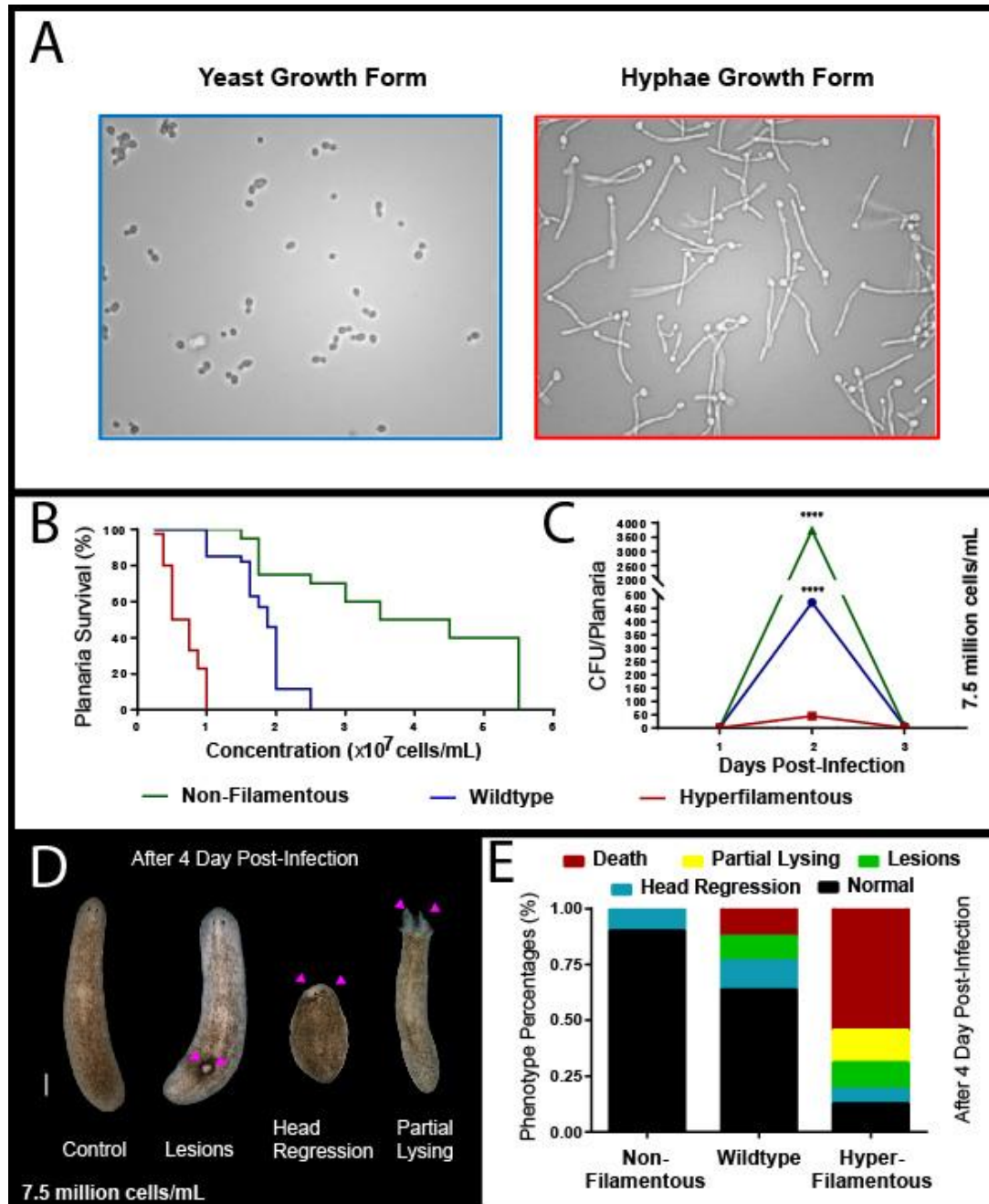


Figure 6: The hyper-filamentous *C. albicans* strain is highly virulent. (A) Demonstration of the yeast growth form and the hyphal growth form from the two mutant strains, the yeast locked and hyphal locked strains, respectively. (B) Planarian survival under different infection concentrations of wildtype, non-filamentous, and hyper-filamentous strain after 3 days post-infection. (C) The number of *C. albicans* cells (three different strains) in planarians during infection time points as colony forming units (CFUs) over time. Note that *C. albicans* growth peaks during the first few days of incubation, but by day 10 post-infection, the presence of fungi is dramatically reduced. The experiment was replicated three times with 10 animals per experiment infected with a concentration of 7.5×10^6 cells/mL for all *C. albicans* strains. Two-Way-ANOVA, **** $P < 0.0001$ (D) Live images are representing morphological defects observed after infecting the planarians with the three different *C. albicans* strains at 7.5×10^6 cells/mL after four days of infection. Scale bar is 200 μ m. (E) Distribution of morphological defects based on the different *C. albicans* strains after four days post-infection at 7.5×10^6 cells/mL. Two independent replicates were performed with 20 animals each.

The amount of *C. albicans* cells adhering to the planarian gradually increased during the beginning of the infection and peaked at 3 days post-infection for all strains (Figure 7). As seen with the planarian survival rates, the infections with the wildtype and hyper-filamentous strains were more severe and prolific than those of the non-filamentous strain. *C. albicans* was found throughout the entire bodies of the planarians, showing no preference to either the dorsal or ventral side of the planarians (Figure 7 & 8). It was observed that the wildtype and hyper-filamentous strains tended to form aggregates as the infection progressed. These aggregates were seen in both 1 and 3 days post-infection (Figure 7). The function of the aggregates is uncertain but may be related to biofilm development, a top virulence factor of *C. albicans*^{102,103}. It was also observed that the wildtype strain had some cells transitioned from the yeast growth form to the hyphal growth form at 3 days post-infection (Figure 7F). The hyper-filamentous strain had hyphal cells surrounding the entire animal, demonstrating a strong adherence ability (Figure 7E). Interestingly, at 10 days post-infection all the *C. albicans* strains were dramatically reduced or absent from the planarians (Figure 7A-C).

I performed transverse cross sections at 1 and 3 days post-infection to visualize the depth in which the *C. albicans* cells infect the planarians. As seen in the cross-section model (Figure 2B), planarian cross sections are taken from the pharyngeal area (Figure 8). All three *C. albicans* strains were observed to adhere to the epithelial layer at day 1 post-infection and will gradually penetrate the epithelial layer, eventually reaching the deeper tissues of the planarians (Figure 8). The difference among the three strains was in the number of cells breaking the epithelial layer and infecting the deeper tissues of the planarians. Specifically, the planarians infected with wildtype and hyper-filamentous strains had the more significant presence of *C. albicans* cells and tissue damage, compared to the non-filamentous strain. It was observed that the planarians that survived 3-day post-infection fully recovered, no matter how many *C. albicans* cells were present or how severe the infection. These results demonstrate that *C. albicans* can attach and penetrate the planarian tissue, and that planarians can remove the *C. albicans* cells and recover shortly after.

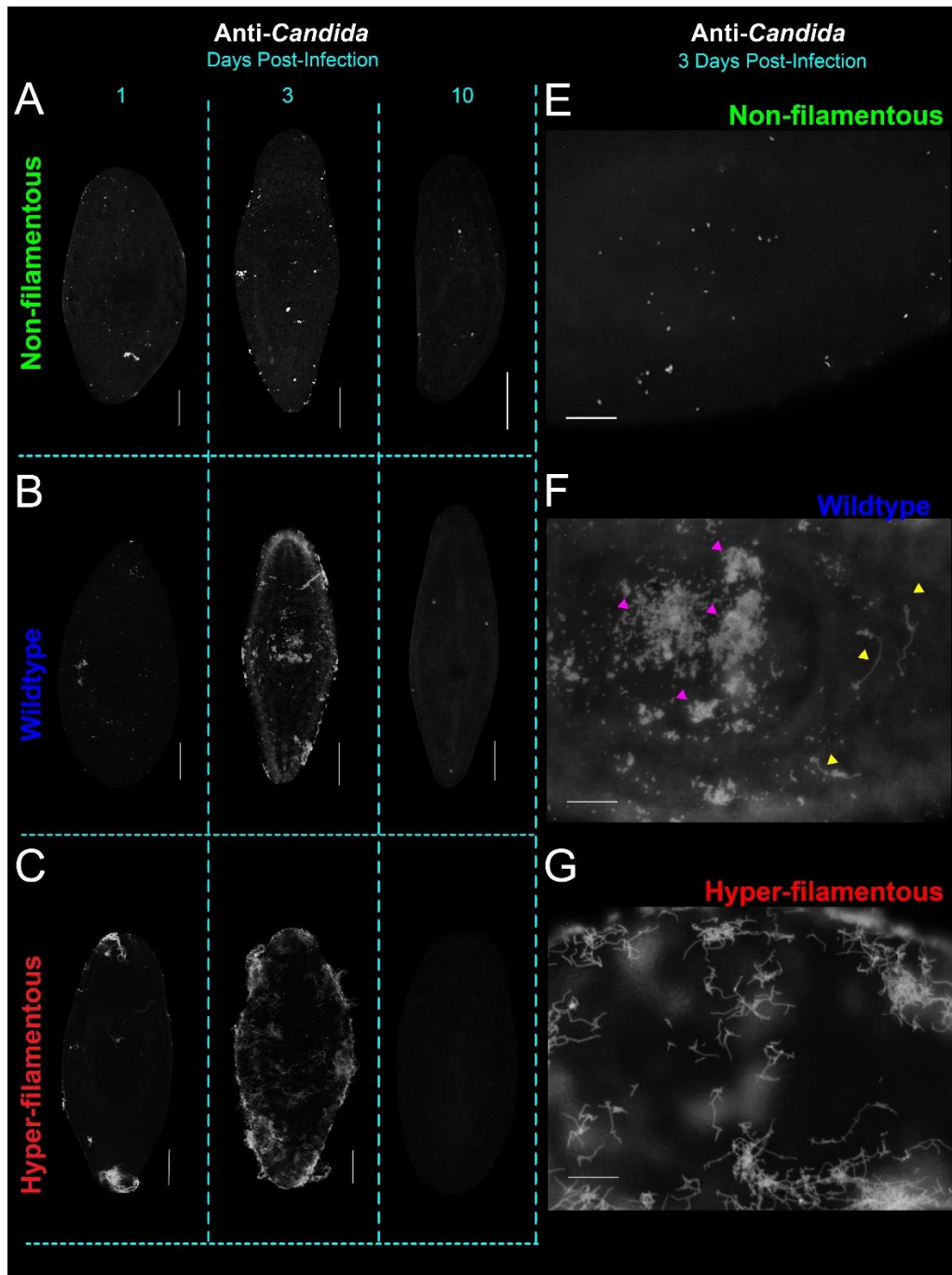


Figure 7: Visualization of *C. albicans* in the planarians during infection. (A-C) Images represent whole-mount anti-*Candida* antibody immunostaining during 1, 3, and 10 days post-infection of three different *C. albicans* strains. Animals were infected with 2×10^7 cells/mL for the non-filamentous, 1.5×10^7 cells/mL for the wildtype, and 5×10^6 cells/mL for the hyper-filamentous *C. albicans* strains. (D-F) High-magnification images of planarian pharyngeal area of the whole-mount at 3 day post-infection. The yellow arrows indicate the presence of hyphae in tissue infected with the wildtype strain. The purple arrows point towards aggregates of *C. albicans* cells and the yellow arrows indicate the presence of hyphal cells. The scale bar in all images is $200 \mu\text{m}$. Three independent replicates were performed using 10 animals each.

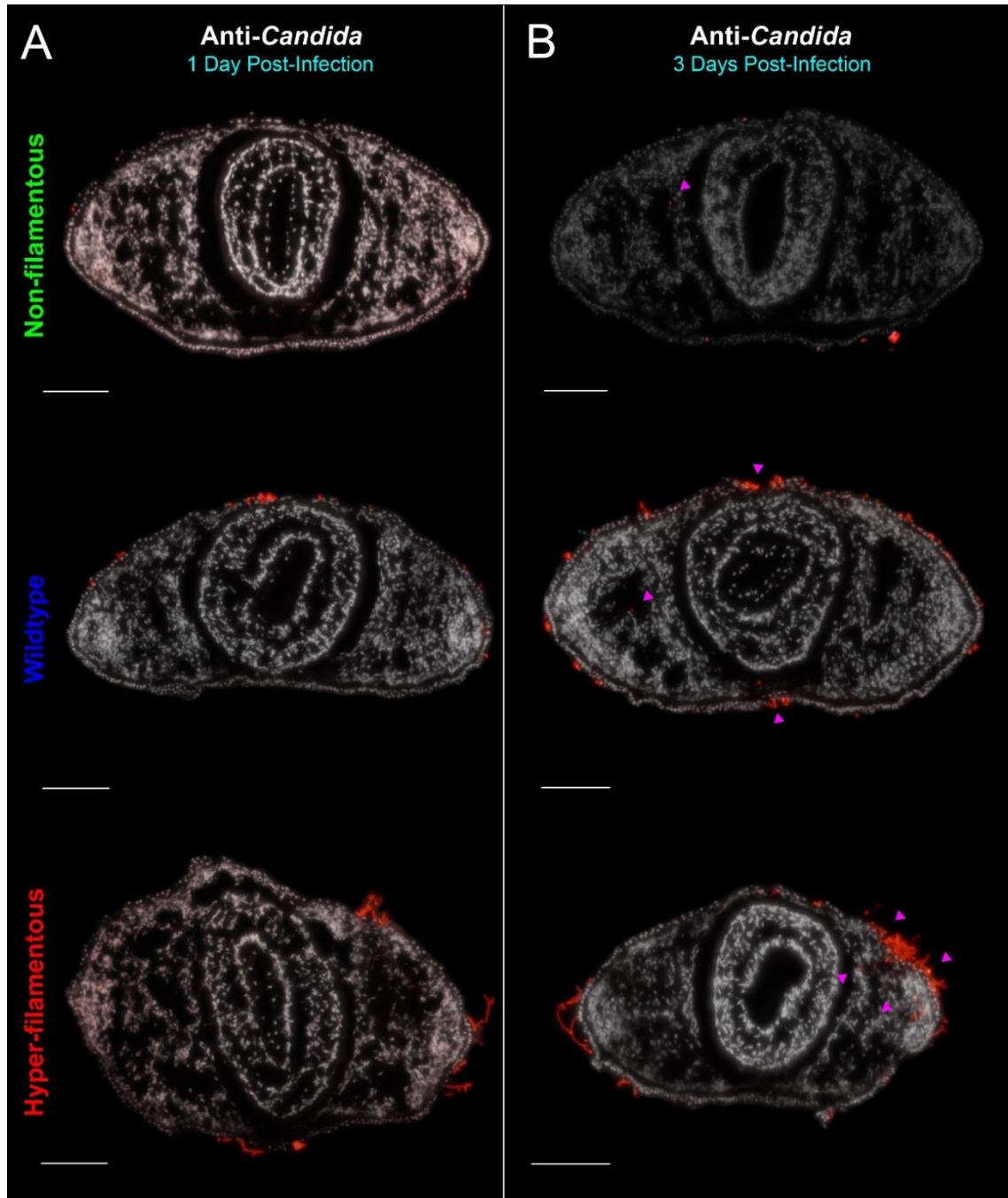


Figure 8: *C. albicans* penetrates the epithelial and infects deeper tissue in the planarians. (A, B) Transverse cross-section of anti-Candida antibody immunostaining images were taken from the middle of the planarian body exposed to *C. albicans* strains (red signal) at 1 and 3 days post-infection. The pharynx is the circular structure in the middle of the section. The purple arrows point towards the *C. albicans* cells breaking the epithelial layer or in the deeper tissues of the planarian. The planarian tissue is counterstained with DAPI (White). Animals were infected with 2×10^7 cells/mL for the non-filamentous, 1.5×10^7 cells/mL for the wildtype and 5×10^6 cells/mL for the hyper-filamentous *C. albicans* strains. The scale bar is $200 \mu\text{m}$ for all images. The thickness of the sections was $10 \mu\text{m}$. Two independent replicates were performed using 5 animals each. Two independent replicates were performed using 4 animals each.

4.4. *Candida albicans* infection induces neoblast division and increases cell death

Neoblasts are stem cells in the planarian body and are the only cells that can divide^{55,81}. I investigated if the planarian neoblasts, crucial for tissue repair and regeneration, has a role during the *C. albicans* infection. Using anti-histone-3 phosphorylated antibody (H3P), a specific neoblast antibody, the neoblasts were observed during the infection of all three *C. albicans* strains. The hyper-filamentous and wildtype strain infections were accompanied by an increase in neoblast proliferation.

The wildtype strain demonstrated an increase in neoblast proliferation during 1-day post-infection (Figure 9A-D). Infection samples with both, hyper-filamentous and wildtype strains, showed increased mitotic activity but then returned to uninfected levels soon after, during the recovery time point (Figure 9A-C). The hyper-filamentous strain was the only strain for which a rise in neoblast division was seen for both 1 and 3 days post-infection. The non-filamentous strain did not cause any mitotic changes during the infection, neoblast levels were close to those in uninfected planarians (Figure 9D).

Simultaneously, whole-mount immunostaining was conducted with both TUNEL (terminal deoxynucleotidyl transferase dUTP nick end labeling) and anti-caspase-3 antibody. The double staining allowed me to observe the amount of cell death caused by *C. albicans* (Figure 9D-E). Since the TUNEL assay labels both *C. albicans* and planarian cell death, using the anti-caspase-3 antibody allowed me to distinguish host cell death and *C. albicans* cell death.

Increase in cell death was observed for all three *C. albicans* strains during 3 days post-infection (Figure 9D-E). Furthermore, the cell death levels differed greatly. The most virulent strain, the hyper-filamentous, demonstrated the highest increase in cell death, followed by the wildtype (Figure 9D-E). The non-filamentous strain did show a twofold increase in cell death but was not seen to affect neoblast proliferation (Figure 9A-C). Overall, the results demonstrate that the hyphal growth form elicits the highest mitotic and cell death response in the host.

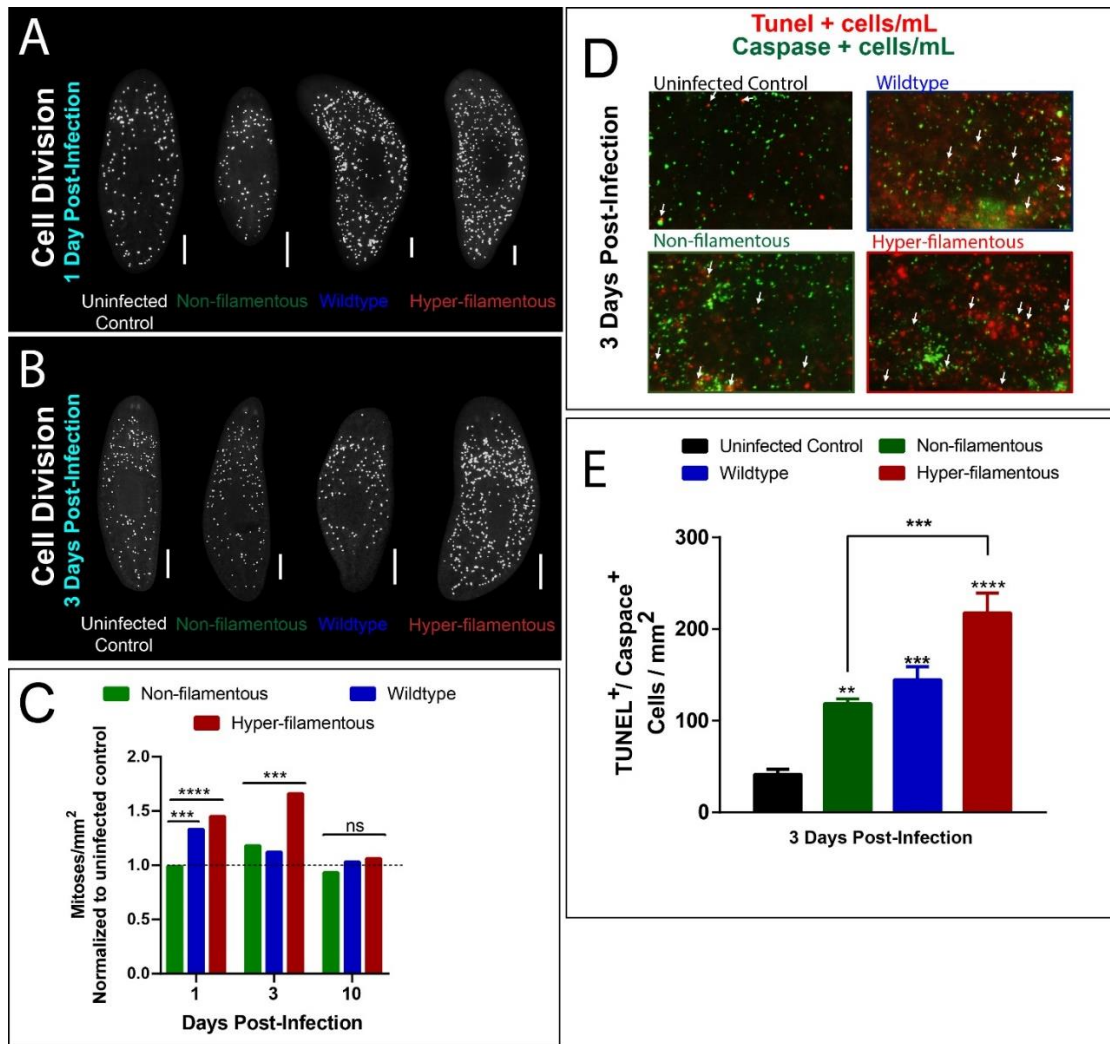


Figure 9: The *C. albicans* infection causes neoblast hyper-proliferation and cell death in the planarians. (A-B) Whole-mount immunostaining with anti-phospho-histone H3 (Ser10) antibody labeling mitotic cells (white foci) at 1 and 3 days post-infection. Planarians infected with *C. albicans* strains: non-filamentous (2×10^7 cells/mL), wildtype (1.5×10^7 cells/mL) and hyper-filamentous (5×10^6 cells/mL). Scale bar is 200 μ m. (C) Amount of mitosis at three different time points of infection (1, 3 and 10 days post-infection) of three different *C. albicans* strains normalized to an uninfected control. (D) Double staining with anti-caspase-3 antibody (green signal) and TUNEL positive cells (red signal) in planarian tissue at day 3 post-infection. White arrows indicate TUNEL and Caspase positive cells. Planarians infected with *C. albicans* strains: non-filamentous (2×10^7 cells/mL), wildtype (1.5×10^7 cells/mL) and hyper-filamentous (5×10^6 cells/mL). (E) Levels of double positive cells for caspase+/TUNEL+ in planarian tissue at day 3 post-infection with *C. albicans* strains (7.5×10^6 cells/mL) compared to an uninfected control. Cell division experiments consisted of three biological replicates using 10 animals each. Cell death experiments consisted of two biological replicates using 4 animals each. All graphs represent mean \pm SEM. All statistical comparisons are against control unless noted with bars. Two-Way ANOVA, * $P < 0.05$; ** $P < 0.01$; *** $P < 0.001$; **** $P < 0.0001$ and ns = no significant.

4.5. The adherence of *C. albicans* to the planarian leads to a proliferation of neoblasts.

To further evaluate the mitotic response observed in Figure 9, I focused on the wildtype strain and infected the planarians with a lethal concentration (25×10^6 cells/mL). The infection of the *C. albicans* was analyzed temporally through a time course of 48 hours post-infection (Figure 9). During this time course, no morphological defects or phenotypes were observed between infected and uninfected animals.

I found two specific mitotic peaks occurring at 6 and 24 hours post-infection, and as previously described, it was followed by a decrease in mitotic activity (Figure 10B). The mitotic peaks at 6 hours post-infection were, by far the largest, with a 75% increase compared to the uninfected control (Figure 10A-B). There was no specific tissue location for the mitotic peaks, suggesting that this dispersed expression is a system-wide response (Figure 10A). Planarians are known to respond to increased cell death with mitotic proliferation⁹¹. The planarians induce a regenerative neoblast proliferation response occurring at 6 hours post-amputation that followed a spike in cell death⁹¹.

Due to a similar time response to amputation, I measured cell death to understand if it was the cause of the mitotic proliferation in response to the damage of the infection or a specific response to *C. albicans*. Surprisingly, using the TUNEL assay during the infection, no increase in cell death was observed before the neoblast mitotic peak at 6 hours post-infection (Figure 10C-D). In Figure 10C-D, only 2 and 4 hours post-infection are shown because those are the time points established to demonstrate a rise in cell death after amputation⁹¹. Only the TUNEL assay was used because there isn't enough *C. albicans* cell death at these time points to misinterpret as the host cell death. Overall, there is no connection to cell death and the mitotic peak observed with the infection, so I proceeded to discern how *C. albicans* elicits the mitotic response.

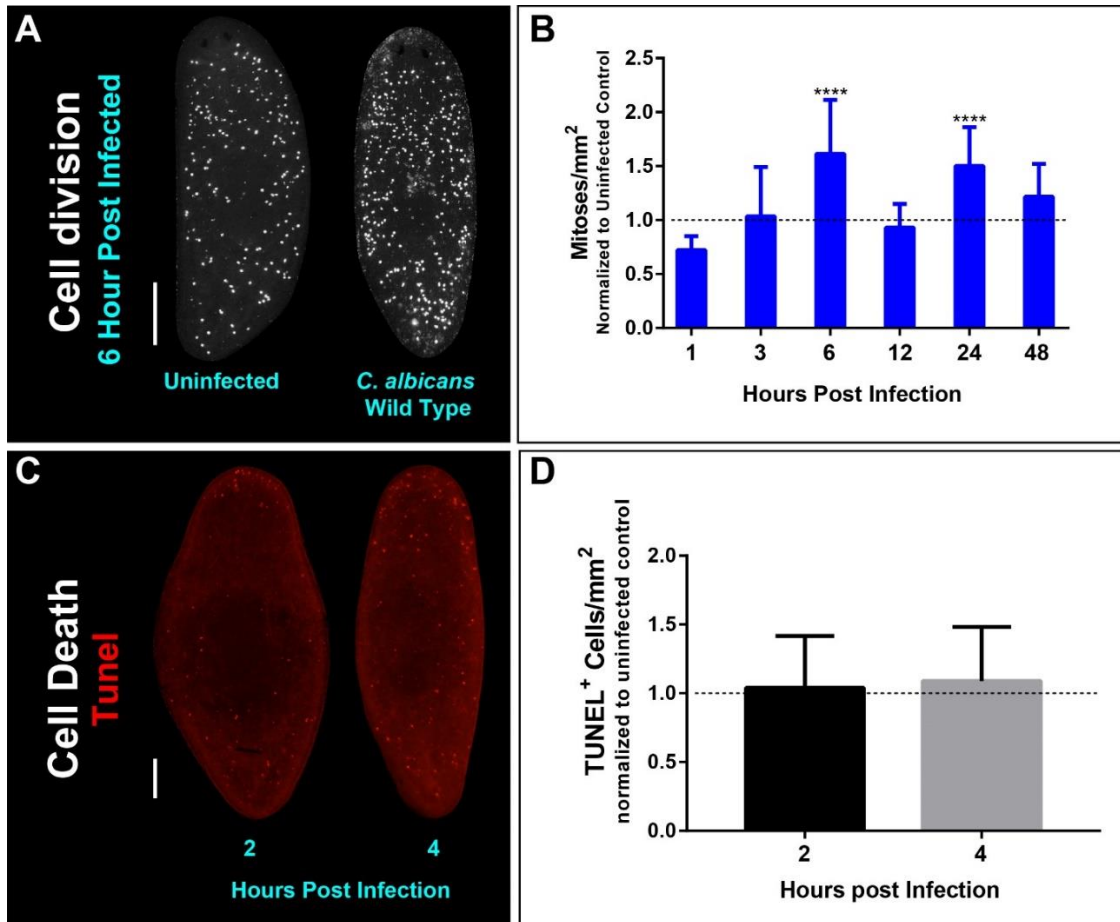


Figure 10: Lethal *C. albicans* infection induces early Neoblast hyper-proliferation. (A) Whole-mount immunostaining with anti-phospho-histone H3 (ser10) antibody for planarians, which labels mitotic cells (white foci) at 6 h post-infection with the *C. albicans* wildtype strain. (B) Number of mitosis between one to 48 hours post-infection normalized to an uninfected control. Cell division experiments consisted of three biological replicates using 10 animals each. (C) Staining of TUNEL (red foci) was done in animals infected during 2 and 4 hours post-infection at 25 million cells/mL using the wildtype strain. (D) Levels of TUNEL positive cells in planarian tissue at 2 and 4 hours post-infection normalized to an uninfected control. Cell death experiments consisted of two biological replicates using 4 animals each. All graphs represent mean \pm SEM. Scale bars are 200 μ m in all figures. Statistical comparisons are against the uninfected control. Two-Way ANOVA, **** $P < 0.0001$.

I performed immunostaining on whole-mounts and cross sections to observe how early *C. albicans* cells begin to adhere to planarian tissue and if the cells penetrate the epithelial surface. These experiments demonstrated that as early as 1 hour post-infection, a few *C. albicans* cells began to adhere to the planarian tissue. From there, more cells adhered to the tissue, gradually increasing every hour (Figure 11A-B). During the first 6 hours post-infection, the *C. albicans* cells began to form small aggregates over the surface of the animal (Figure 11A). I also quantified the amount of *C. albicans* cells during the early infection time period by measuring the CFUs within the planarians (Figure 10B). These measurements confirm the gradual increase of yeast cells attaching to the planarians from as low as roughly ten *C. albicans* cells 1 hour post-infection to a drastic ~900 cells after 6 hours post-infection (Figure 11B). To distinguish if the adhered *C. albicans* cells are also penetrating the epithelial during the earlier time points, the yeast cells were also assessed in transverse cross sections. Just as previously seen in Figure 8, no anti-*Candida* signal was found in the deep tissue before 1-day post-infection (Figure 8A & 11C). These findings suggest that adherence to the surface is all that the *C. albicans* cells are able to do during this early infection time period.

Another response that planarians has been shown to express during physical injury is a set of wound response genes^{83,94}. I measured the expression levels of *Smed-runt1* (*runt1*) and *Smed-egr2* (*egr2*) using Real-Time Quantitative Reverse Transcription PCR (qRT-PCR). The two, *runt1* and *egr2*, are early wound response genes in planarians necessary for regeneration, during the early time period of the infection. Significant increase in the expression of *egr2* was observed in all the early time points. However, *runt1* was either slightly reduced or showed no changes in expression during the infection (Figure 11D). The gene expression differences in early wound response demonstrate a specific set of wound response genes with slight similarities to regenerative responses.

Furthermore, to reconfirm the gene expression of *egr2*, the planarian extracellular regulated kinase (ERK) was investigated. ERK is known to be activated via phosphorylation (pERK) ~ 15 min post-injury¹⁰⁴⁻¹⁰⁶. Further, pERK activates the *egr* family genes. Therefore, pERK protein levels were evaluated using western blots during early infection period. These pERK measurements demonstrated a gradual increase from the earliest time point, having a threefold increase at 0.5 hours post infection to a fourfold increase during 6 hours post-infection (Figure 11E). These results suggest that the adherence of *C. albicans* cells to the epithelial layer activates early wound response genes, which will then lead to the proliferation of neoblasts.

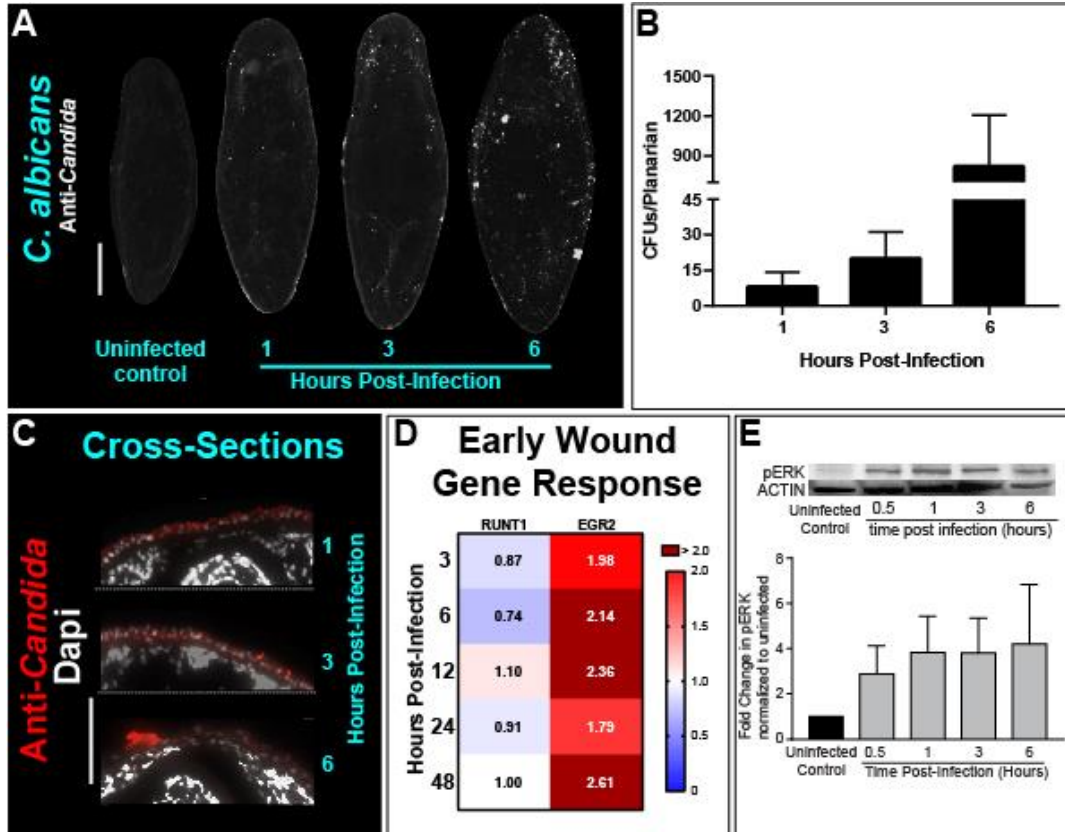


Figure 11: *C. albicans* adherence to planarian tissues causes an early wound response. (A) Whole-mount anti-Candida antibody stain at 1, 3, and 6 h post-infection (white foci) in planarian tissue. (B) *C. albicans* colony forming units (CFUs) normalized per planarian. Ten animals were used per infection time point. (C) Transverse cross section images from the dorsal side of the planarian body showing the adherence of the *C. albicans* wildtype strain (red signal) at 1, 3, and 6 h post-infection. Two biological replicates were used with a total of eight planarians. (D) Gene expression levels represented in a heat map of wound-induced response planarian genes *runt1* and *egr2* at the different infection time points. Gene expression is represented by fold change normalized to an uninfected control. Color scale depicts red as upregulation and blue as downregulation; burgundy demonstrates upregulation greater than twofold. (E) Western blot of planarian phosphorylated-ERK (p-ERK) and quantification at different time points of a *C. albicans* infection. β -tubulin was used as an internal control. Early wound response experiments were obtained in triplicate per experiment for at least two biological and technical replicates. *C. albicans* infections were performed using 25 million cells/mL. All graphs represent mean \pm SEM. Comparisons are against the uninfected control. The scale bar for all images is 200 μ m.

4.6. The ability of *C. albicans* to adhere to the planarian promotes virulence and the proliferation of neoblasts in planarians.

The adherence of *C. albicans* was examined to observe if it alone contributed to the planarian mitotic response. Additionally, secreted proteases of *C. albicans* were also examined to measure their impact on host response. Both adhesion and secreted proteases are known virulence factors of *C. albicans* that provide an increase in virulence⁴⁶. Through genetic disruption of *C. albicans*, the virulence factors were analyzed during the infection. I focused on two gene families of *C. albicans* virulence factors, the agglutinin-like sequence (*ALS*) family associated with adherence, filamentation and biofilm formation, and the secreted aspartyl protease (*SAP*) family important for degrading the epithelial layer⁵².

The Als family of cell surface glycoproteins are essential for *C. albicans* adherence and mediate cell–cell and cell-substrate adherence¹⁰⁷. Specifically, Als1 and Als3 are the two major Als proteins that are critical for adherence, filamentation and biofilm formation¹⁰⁸. Moreover, biofilm and cell wall regulator 1 (*Bcr1*) is a known master regulator of biofilm development that controls the expression of *ALS1* and *ALS3*¹⁰⁹. Aside from adherence, *C. albicans* also contains ten different Saps that have different importance depending on the environment of the infection^{52,110}. Therefore, I focused on the ability of two triple deletion *SAP* mutant strains, the *sap1/sap2/sap3* and the *sap4/sap5/sap6* mutant strains, which encompass the significant Saps involved in virulence, to observe if they contributed to the host mitotic responses.

Using anti-*Candida* immunostaining during the 6 hours post-infection with a lethal concentration, all *C. albicans* mutant cells were able to adhere to the planarian surface, but with different abundance of *C. albicans* cells (Figure 12). Comparatively, the *als3* and *bcr1* *C. albicans* mutant strains displayed a lower number of cells capable of adhering to the host. Also, the *als3* and *bcr1* mutant strains did not form any of the small aggregates observed in the wildtype strain (Figure 7F and 12A). In addition to these observations, planarians survived additional days when infected with the *als3* and *bcr1* mutant strains compared to the wildtype and the other mutant strains (Figure 12B). However, the *sap* mutant strains did not hinder the ability of *C. albicans* to adhere to the planarian, and the virulence was slightly more if not equal to the wildtype. Through qRT-PCR, it was also observed that when the wildtype strain infects the planarians, there is a large increase in gene expression of *ALS1*, *ALS3*, and *BCR1* (Figure 12C). Essentially, the results of the *als3* and *bcr1* mutant strains and those of Figures 6 to 8 demonstrate that the adherence to planarian tissue with the ability to transform to the hyphal growth form is vital for *C. albicans* to infect and colonize the planarians.

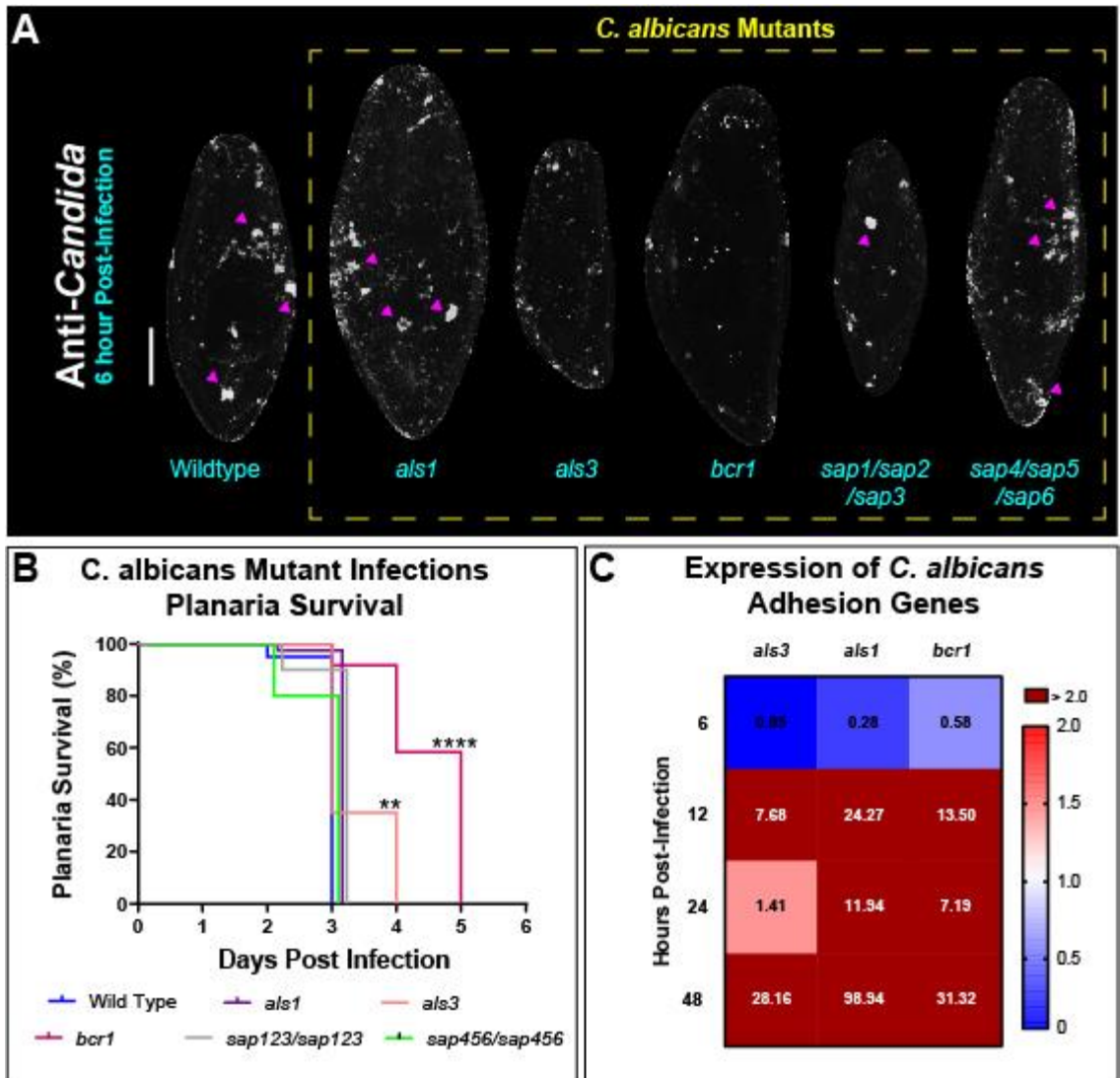


Figure 12: *C. albicans* genes *ALS3* and *BCR1* are essential for virulence in the planarian model. (A) Whole-mount anti-Candida antibody stain of *C. albicans* mutant strains 6 hours post-infection. All mutant strains are capable of adhering to the planarian epithelial surface. Purple arrows indicate notable *C. albicans* aggregates. Scale bar is 200 μ m. (B) Planarian survival after infection with 25 million cells/mL of the different *C. albicans* mutant strains. Logrank test, ** $P < 0.01$; **** $P < 0.0001$. (C) Gene expression levels represented in a heat map of *C. albicans* genes *ALS3*, *ALS1*, and *BCR1* at the different infection timepoints. Gene expression is represented by fold change normalized to an uninfected control. Color scale depicts red as upregulation and blue as downregulation; burgundy demonstrates upregulation greater than twofold. Data were obtained in triplicate per experiment using three biological and technical replicates of a total of 30 planarians.

Furthermore, in addition to virulence, the *C. albicans* mutant strains were able to cause a mitotic response in the planarians during the 6 hours post-infection peak. All *C. albicans*

mutants elicited a mitotic response to that of the wildtype strain except for two. The *als3* and *bcr1* mutant strains were the only ones that displayed a reduced mitotic response at 6 hours post-infection (Figure 13A-B). Thus, the data suggest Als3 and Bcr1 are important for *C. albicans* virulence and the ability to induce the planarian mitotic response during the infection. Additionally, *C. albicans* secretes a variety of virulence factors, which may also contribute to the mitotic response of the planarians^{34,35}. To analyze the secretions of *C. albicans*, the planarians were exposed with filtered sterilized media from water obtained at 6 hours post-infection. There was no difference in mitotic activity between planarians exposed to the filtered infected media and unexposed animals (Figure 13C-D). These results further indicate that the *C. albicans* secretions are not essential when infecting planarians. Thus, adherence and hyphal development are the most important in *C. albicans* during early infection in the planarian model.

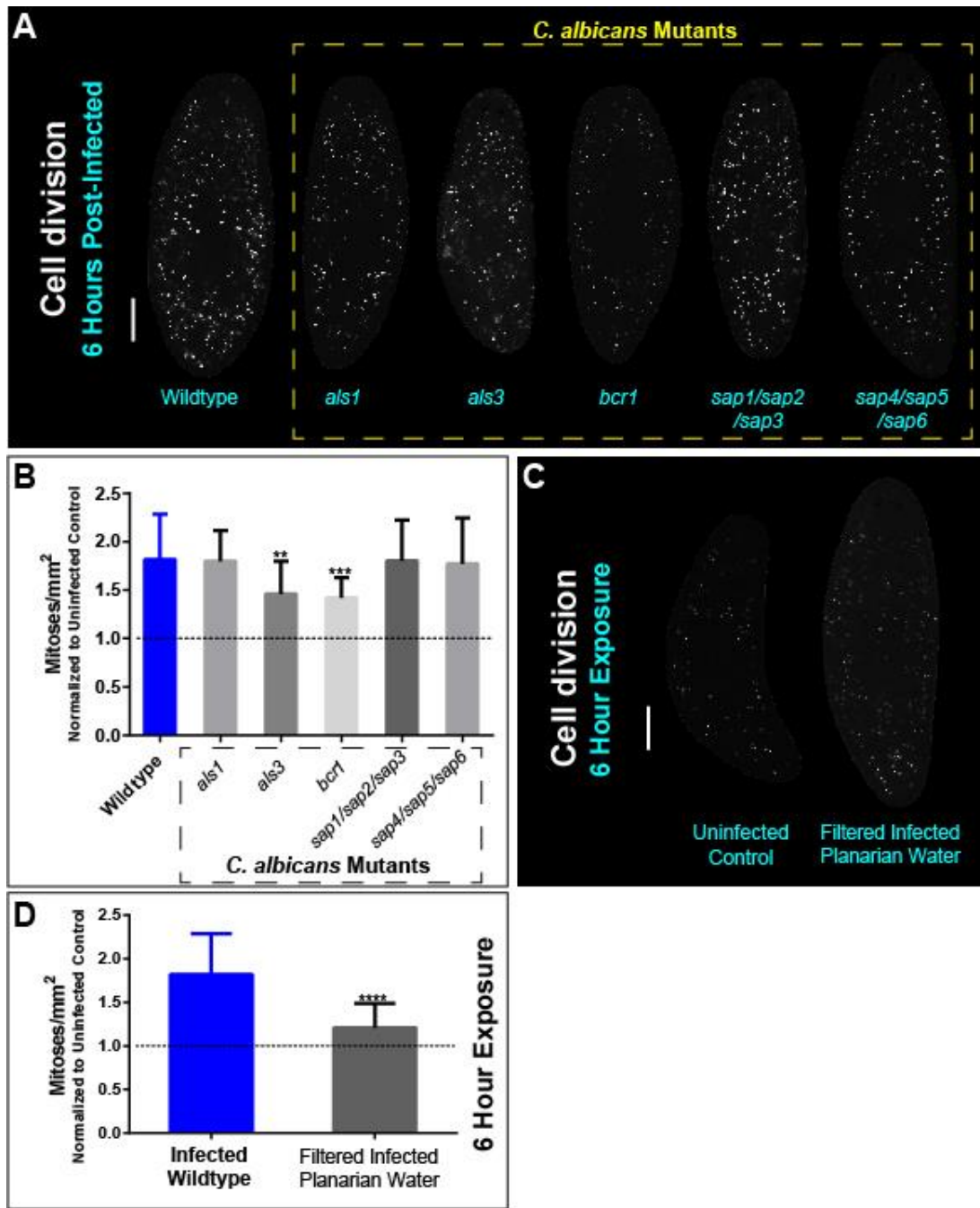


Figure 13: The planarian mitotic response decreases during infections using the *C. albicans* *als3* and *bcr1* mutant strains. (A) Whole-mount immunostaining with anti-phospho-histone H3 (ser10) antibody for planarians, which labels mitotic cells (white foci) at 6 hour post-infection with the *C. albicans* mutant strains indicated. (B) Number of mitotic cells in response to *C. albicans* mutant strains normalized to uninfected planarians at 6 hour post-infection. (C) Whole-mount immunostaining with anti-phospho-histone H3 (ser10) antibody for planarians, which labels mitotic cells (white foci) at 6 hour exposure for animals that were soaked in filtered sterilized cell-free infected planarians media and the uninfected planarians. (D) Amount of mitotic cells in response to filter sterilized cell-free infected media exposed planarians compared to infected planarians normalized to uninfected planarians at 6 hour exposure. Graphs represent mean \pm SEM. All statistical comparisons are against the wildtype strain. The scale bar is 200 μ m for all figures. Two-way ANOVA, ** $P < 0.01$, *** $P < 0.001$, **** $P < 0.0001$

4.7. The planarian Dectin signaling pathway has a role in the clearance of the *C. albicans* infection

C-type lectins play various biological roles, including as a pathogen recognition receptor for cells and tissues¹¹¹. More specifically, there are highly evolutionary conserved C-type lectins that detect *C. albicans*, such as Dectin^{112,113}. Therefore, the role of the planarian Dectin signaling pathway was explored in mediating the host response during the infection. Using qRT-PCR, the gene expression of Dectin components was measured. During a lethal infection with *C. albicans* wildtype strain, I screened a list of genes from the conical Dectin signaling pathway that are found in the planarians: SYK, the adapter protein of Dectin; *Smed-syk* (*syk*) and downstream gene components *Smed-card* (*card*), *Smed-bcl* (*bcl*), *Smed-malt1* (*malt1*), *Smed-tab1* (*tab1*), and *Smed-tak* (*tak*).

Interestingly, as early as 3 hours post-infection, everything slightly increased in expression except for *syk* and *tak1*; which exhibited the most significant increase (Figure 14A). Additionally, 6 and 12 hours post-infection showed the largest expression for all Dectin components. However, this large expression peak decreased after 24 and 48 hours post-infection (Figure 14A). The adaptor protein *syk* presented the most dramatic increase (threefold) during the 6 hours post-infection. The increase in expression was confirmed with fluorescent in situ hybridization (FISH) at 6 hours post-infection. The *syk* probes expression was observed throughout the animal with enrichment in the planarian digestive tract in uninfected controls. During the infection, the planarian *syk* expression was more prominent with the addition of foci appearing in the prepharyngeal area concentrated in the main digestive branch below the eyes (Figure 14B).

The change in expression led me to further analyze the role of *syk* during the fungal infection by disrupting the gene function using RNA interference (RNAi). The RNAi planarians were evaluated in both uninfected and infected animals (Figure 14). The disruption of *syk* demonstrated no morphological defects to uninfected animals. Nevertheless, knockdown of *syk* led to small increases in mitotic activity compared to infected control animals (Figure 14C-D). Furthermore, the downregulation of *syk* slightly affected the clearance rate of the *C. albicans* infection, with RNAi animals needing more than 12 days post-infection to clear the fungi (Figure 14E-F). Though the knockdown did not affect survivability, these findings suggest that *syk* with the accompanying Dectin signaling pathway has a role in mediating the response to an infection.

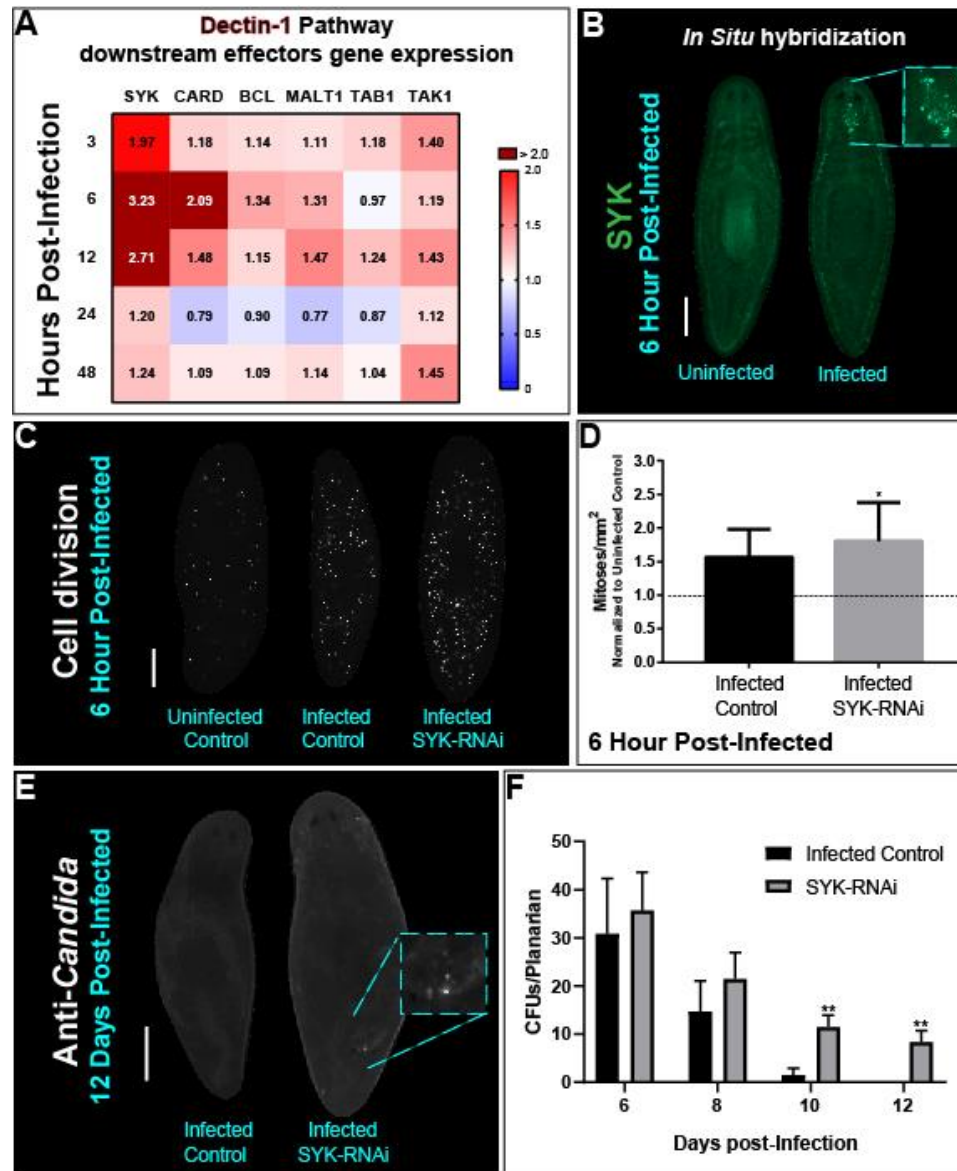


Figure 14: The planarian Dectin signaling pathway plays a role in the clearance of *C. albicans*. (A) Gene expression levels for Dectin signaling pathway homologs during the *C. albicans* infection using 25 million cells/mL. Gene expression represented in a heat map displaying fold change normalized to an uninfected control. Color scale depicts red for upregulation and blue for downregulation; burgundy demonstrates upregulation over twofold. Data were obtained in triplicate per experiment for at least two biological and technical replicates. (B) Fluorescent in situ hybridization showing expression of *syk* in an uninfected and 6 hours post-infected animal. The boxed region are magnifications of the infected animal. This experiment was replicated two times using five animals per experiment. (C) Whole mount immunostaining with anti-phospho-histone H3 (ser10) antibody, which labels mitotic cells (white foci) at 6 hours post-infection. (D) Number of mitoses of control infected animal versus *syk*-RNAi infected animals normalized to an uninfected control at 6 hour post-infection. (E) Representative images of whole mount anti-Candida antibody stain at 12 days post-infection (white foci) of a control animal and *syk*-RNAi animal. Boxed region indicates *C. albicans* aggregates. (F) Number of *C. albicans* colony forming units (CFUs) normalized per planarian of infected control versus infected *syk*-RNAi planarians throughout the infection. All experiments were replicated two times using five animals per experiment. 25 million cells/mL were used for the infections. All graphs represent mean \pm SEM. Scale bar is 200 μ m for all. T-test, * $P < 0.05$, ** $P < 0.01$.

4.8. The *C. albicans* infection elicits a transcriptional varied neoblast response in the planarians leading to a multi-system response.

The planarian model has a heterogeneous neoblast population. Neoblasts differ in a transcriptional set of enriched genes⁶⁰. These transcriptomic changes allow the neoblast to adopt different cellular identities as they further differentiate. To further understand the neoblast dynamics and which subpopulations were affected during the infection, the transcription levels of various genes encoding for different neoblast populations were measured. The neoblast subpopulations are numbered from 1 to 12 (NB1-NB12) based on the amount of *Smed-piwi-1* (*piwi-1*), a universal neoblast marker, where NB1 has the largest amount and NB12 the smallest amount (Figure 15A). Changes in gene expression for six different neoblast lineages were taken during the infection using qRT-PCR. The data demonstrated that specific subsets of neoblast markers were upregulated (Figure 15B). Surprisingly, NB2, which describes the pluripotent clonogenic neoblasts (cNeoblast), was slightly decreased along with *piwi-1* throughout the infection (Figure 15B). As a result, there is no increase in clonogenic neoblast division during the infection. Further, there was a large increase of expression of neoblast subpopulations NB9, NB11, NB4, NB7, and NB5, which possess the lowest amounts of *piwi-1*. The highest expression levels were observed for NB9, NB11, and NB4; these showed a gradual increase that peaked to a 3-8 fold increase at 48 hours post-infection (Figure 15B). These increased neoblast subpopulations belong to the muscle, protonephridia, and neural lineages. Taken together, the results demonstrate that there is a multi-system response to the infection.

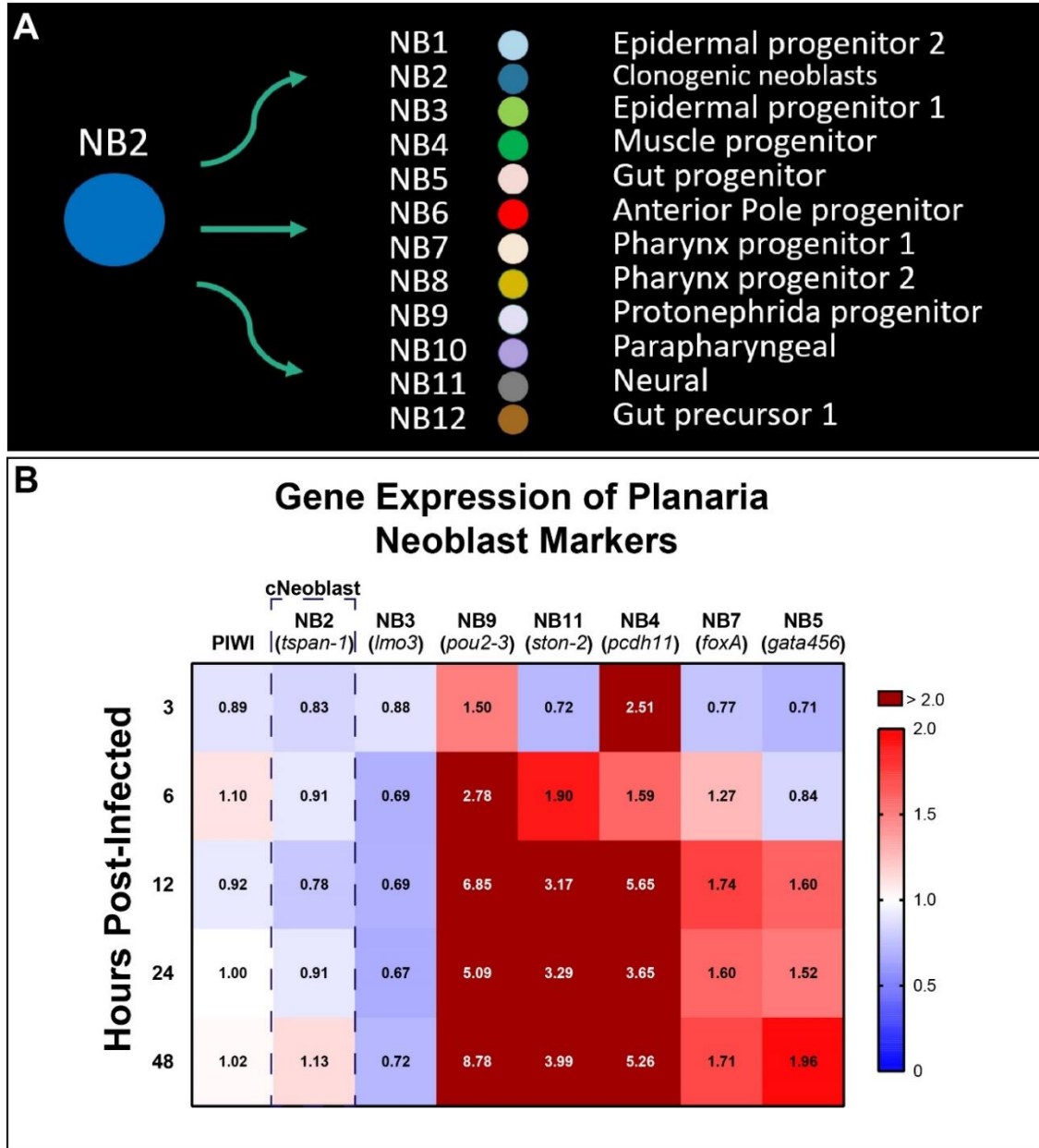


Figure 15: Expression of planarian neoblast subclasses during infection with *C. albicans* infection. (A) Depicts the various neoblast subpopulations found in planarian and the lineage they follow. (B) Gene expression levels of neoblast markers and subclass markers of clonal neoblasts throughout *C. albicans* infection. The expression levels are represented in a heat map, where the color scale depicts red as upregulation and blue as downregulation; burgundy is upregulation greater than twofold. Gene expression is represented by fold change normalized to an uninfected control. Gene expression values represent triplicate samples for at least two biological and three technical replicates.

Afterward, the expression of NB4 was further inspected. The NB4 neoblasts gives rise to the muscle lineage and belongs to the mesoderm lineage. The expression of all NB4 markers available during the infection was measured to compare to the expression of *pcdh11* in Figure 15. Interestingly, just one other NB4 marker, PJ-1b, increased vastly during 6 and 12 hours post infection (Figure 16A). Thus, it seems that only a few mesodermal NB4 neoblasts have a specific response and role during the fungal infection.

To further examine the impact of the NB9 expression in the protonephridia lineage. The gene expression of downstream differentiated cells that are a part of the excretory system of the planarian were measured^{114,115}. The protonephridia makes up the planarian's excretory system, which is branched and widely distributed throughout the body¹¹⁴. Thus, these post-mitotic cells may have essential roles during the infection. To determine the impact of the excretory system by increasing NB9 levels, qRT-PCR was used to measure the markers of the flame cell components, which are segments of the protonephridia¹¹⁴. Flame cells specifically contribute to excretory functions such as electrolyte balance and mucus production¹¹⁴. There was an increase in expression of collecting ducts *Smed-slc9a-3* (*slc9a-3*), distal tubules *Smed-slc4a-6* (*slc4a-6*), and proximal tubules *Smed-slc6a-13* (*slc6a-13*) of the flame cells during 12 and 24 hours post-infection (Figure 16B). These results were confirmed with FISH using the gene *Smed-inx10* (*inx10*), the protonephridia marker was expressed throughout the planarian body¹¹⁴.

The FISH expression showed a gradual increase in flame cells, validating the gene expression (Figure 16C). This indicates that there is an increase in secretions such as mucus by the excretory system of the planarians. To measure the mucus being secreted, I took advantage of the autofluorescence that the planarian mucus has. Mounting live planarians, non-infected and infected planarians were compared by illuminating them, using a blue filter, and observing the fluorescence of the mucus. A significant difference between the mucus secretions of the uninfected and infected planarians was observed. Peak mucus secretions were measured 3 days post-infection (Figure 16D-E). These findings indicate that the excretory system greatly contributes to the planarians response to the *C. albicans* infection by producing large amounts of mucus.

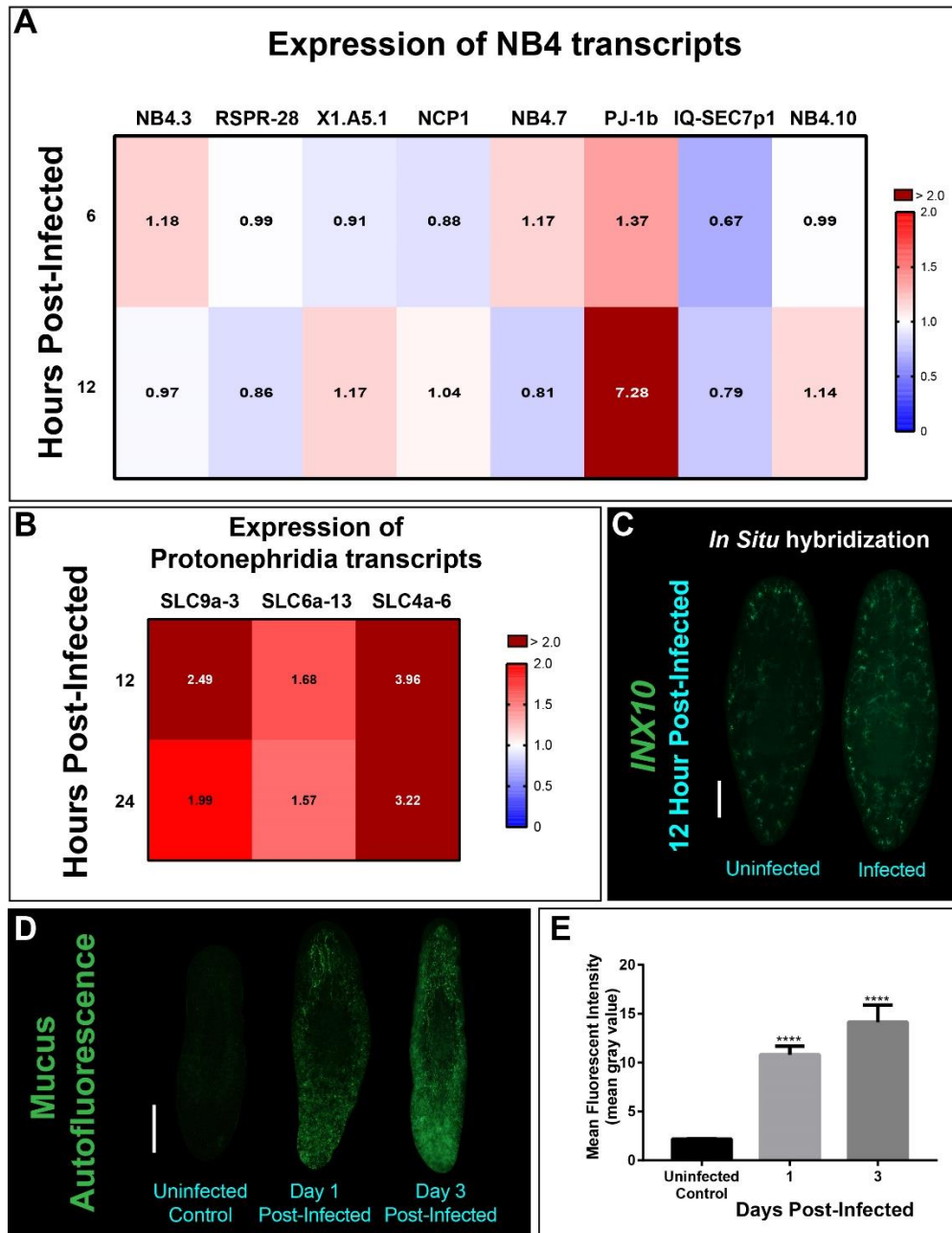


Figure 16: Specific mesenchymal neoblast and protonephridia markers are upregulated in planarians during *C. albicans* infection. (A) Gene expression of eight other markers for NB4 (B) Expression of protonephridia structure markers: *slc9a-3* (collecting ducts), *slc4a-6* (distal tubules), and *slc6a-13* (proximal tubules). (C) Fluorescent *in situ* hybridization showing expression of *inx10* in an uninfected and 24-h infected animal. Scale bar is 200 μ m. Images are representative of eight animals for at least two biological and technical replicates. (D) Whole-mount autofluorescence of the planarian mucus during 1 and 3 day post-infection. Each experiment represents five animals and two biological replicates. (E) Intensity of mucus autofluorescence signal of uninfected and infected animals. Intensity signal quantification involved two biological replicates and 10 animals. The gene expression experiments are represented by at least two technical replicates and three biological replicates. All graphs represent mean \pm SEM. Scale bar is 200 μ m for all. T-test, **** $P < 0.0001$.

Next, the impact of the increased gene expression of NB11 that gives rise to the neural lineage was analyzed during the infection, focusing on the differentiated neurons of the planarians. The planaria's nervous system comprises distinct neuronal subtypes that are categorized by the neurotransmitters that they synthesize¹¹⁶. These neural subtypes are dopaminergic, octopaminergic, GABAergic, serotonergic, and cholinergic neurons, which all have specific markers [Smed-*th* (*th*), Smed-*tbh* (*tbh*), Smed-*gad* (*gad*), Smed-*tph* (*tph*), and Smed-*chat* (*chat*), respectively]. Using qRT-PCR, the expression of each specific neural subtype was investigated to learn if the fungal infection impacts any of these subtypes. Measuring the expression of the neuronal subtypes at 6 and 12 hours post-infection, *chat*+ and *tbh*+ neurons were the only subtypes that increased in expression levels, whereas the rest of the neural subtypes decreased slightly (Figure 17A). In particular, *chat*+ neurons had the highest expression of the two neural subtypes staying above a twofold increase during both time points. Confirming the *chat* expression, FISH was used to validate the qRT-PCR. The expression of the *chat*+ neurons is located explicitly along the brain and ventral cords of the planarian. The *chat* FISH probe showed a larger expression in the infected planarian than in the uninfected animals (Figure 17B).

To further understand the role of the *chat*+ neurons during the infection, *chat* was disrupted with RNAi and the knockdown was observed during the infection. The *chat*-RNAi animals were not more susceptible to the *C. albicans* infection and *chat*-RNAi did not affect survivability. Moreover, there was a slight, albeit insignificant, decrease in mitotic response between *chat*-RNAi and control planarians during the first mitotic peak observed at 6 hours post-infection (Figure 17C-D). It is important to note that disrupting *chat* in planarians results in an abnormally large amount of mucus surrounding the animal. This morphological phenotype seemed to aid the animals against the fungal infection. When the *C. albicans* cells were observed, fungal cells had a more challenging time adhering to the *chat*-RNAi planarians (Figure 17E-F). Overall, these results demonstrate that the nervous system and excretory system contribute to defending against *C. albicans*.

Taken together, all the data presented in this dissertation demonstrated that the human fungal pathogen *C. albicans* utilizes adhesins and filamentation to colonize the planarian flatworm successfully. This leads to a multi-system response from the planarian to counter the fungal infection. An interplay between the planarian model's immune, excretory, and nervous systems was observed in response to *C. albicans*.

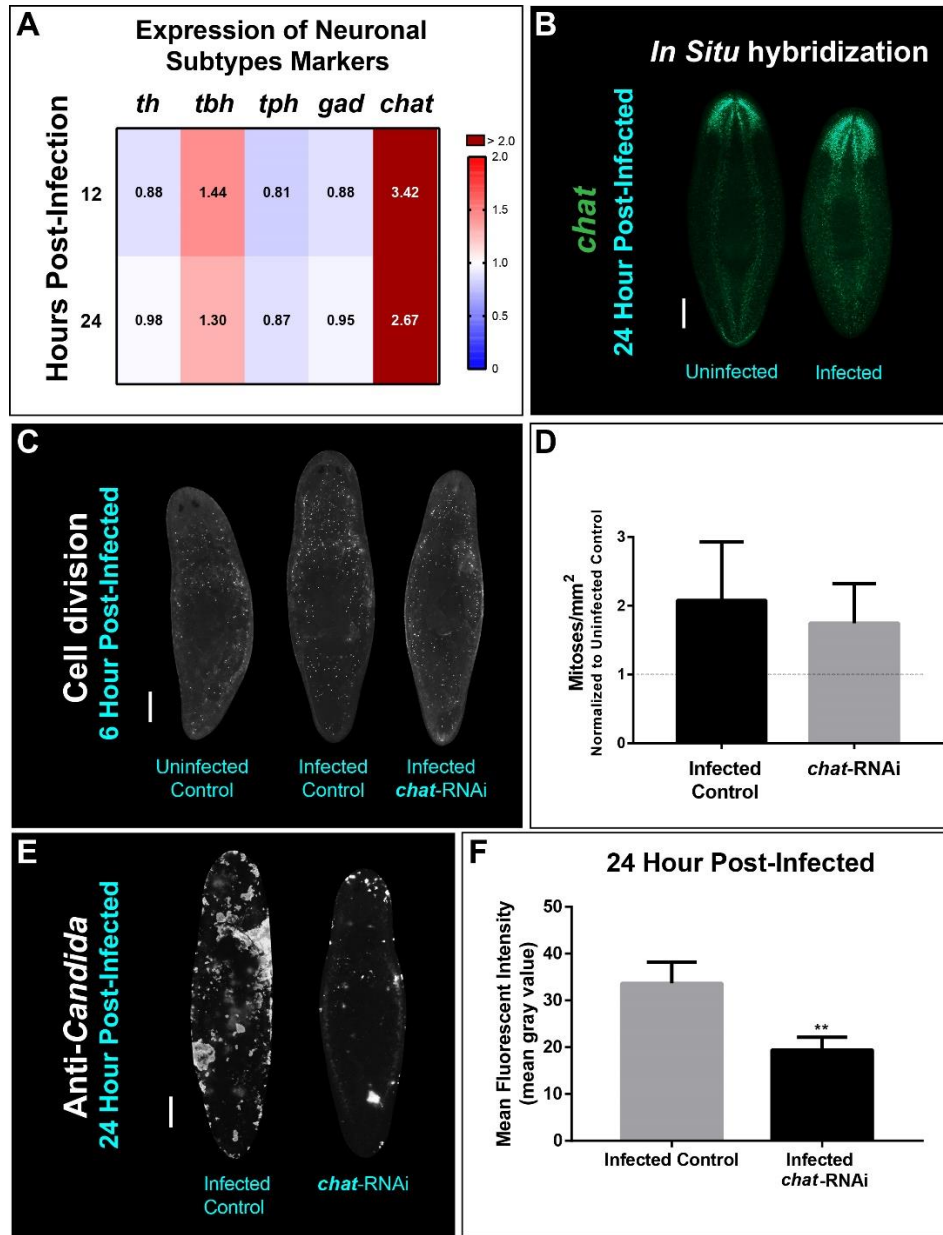


Figure 17: Cholinergic neurons are upregulated in planarians during *C. albicans* infection. (A) Expression of five different neuron subtypes. Gene expression levels throughout the *C. albicans* infection are represented in the heat map. The color scale depicts red as upregulation and blue as downregulation; burgundy is upregulation greater than twofold. Gene expression is represented by fold change normalized to an uninfected control. The experiment is represented by at least two technical replicates and three biological replicates (B) Fluorescent *in situ* hybridization showing expression of cholinergic (*chat*+) neurons in an uninfected and 24 hours post-infected planarian. Scale bar is 200 μ m. Images are representative of eight animals for at least two biological and technical replicates. (C) Whole mount immunostaining with anti-phospho-histone H3 (*ser10*) antibody, which labels mitotic cells (white foci) at 6 hours post-infection comparing infected control with *chat*-RNAi. (D) Number of mitoses of control infected animal versus *chat*-RNAi infected animals normalized to an uninfected control at 6 h post-infection. A total of 10 animals were used. (E) Representative images of whole mount anti-*Candida* antibody stain at 24 hours post-infection (white foci) of a control animal and *chat*-RNAi animal. A total of ten animals were used. (F) Intensity of anti-*Candida* signal of uninfected and infected animals. Intensity signal quantification involved two biological replicates and 10 animals.

5. Discussion

5.1. Development of the planarian infection model for the study of host-pathogen interactions

The first necessity to study the interactions between the planarians and *C. albicans* was development of a consistent infection method. In studying host-pathogen interactions, the ability to observe the responses of both organisms is essential. Further, the method of infection should result in the ability to assay clearance, virulence, survivability, functional analysis, and tractability. All this was considered during development of a reproducible infection protocol based on soaking planarians with *C. albicans* cells that are easily introduced into the media. In addition, the maintenance and cost of planarians are low, and the ability to generate an abundance of animals allows for rapid experimentation and screening of *C. albicans* strains, which takes less than a week. This infection strategy also allows visualization of the different stages of fungal infection, from initial contact, to penetration, to colonization and deep tissue infection of the flatworm (Figure 18).

There are notable disadvantages with two other existing techniques for *C. albicans* infection of planarians. First, the injection or pricking method allows infection of planarians into any desired location, but *C. albicans* cells have difficulty adhering to the planarians. This may be due to the allowance of insufficient time for *C. albicans* to adhere and the ability of planarians to eliminate pathogens rapidly. In contrast, the feeding infection method involves consumption of large amounts of bovine liver and yeast, filling the majority of the digestive branches with yeast. However, the interaction of the pathogen with the liver while inside the host appears to affect the infection. Additionally, the planarians expulse a significant amount of mucus and liver components, resulting in a large reduction of yeast cells after the first day. The scavenger nature of the planarian has likely resulted in an evolutionary advantage to rapidly clear microbes like *C. albicans* with no apparent phenotype. These properties of the planarians make it challenging for use as a model to study *C. albicans* virulence and infection mechanisms.

However, the soaking infection method I developed resulted in the ability of *C. albicans* to kill the planarians, allowing study of the infection from the fungal perspective. The ability to assay virulence, in particular, is one of the greatest advantages our method has when compared to the other infection methods used in the planarian field^{60,67}. The soaking method required different virulence factors of *C. albicans*, including the ability to adhere, change morphologies, and form aggregates. Surprisingly, these changes usually occur after 1-day post-infection, and morphological defects in the planarians accompany these changes (Figure 5). These observations can also be applied to mutant *C. albicans* strains to examine differences in infection (Figure 6).

Furthermore, the soaking infecting strategy also grants the user superior control over the duration of the infection and the amount of yeast cells exposed to the planarians. In addition, it's relatively easy to thoroughly wash away the infecting *C. albicans* cells with fresh media to study clearance of the fungi. Moreover, the soaking strategy provides a valuable tool to observe the interactions of the pathogen and host mucosal surface and

epithelium. Although the feeding infection method results in a robust, rapid clearance of pathogens, characteristics of this method introduce significant confounding problems, which make it challenging to tease apart interactions between host and pathogen. The advantages of infection by soaking are not observed with other infection methods. Thus, the soaking method should be implemented as the standard for future planarian infection studies. Importantly, the planarian infection method has been demonstrated to be as successful as other animal infection methods.

To date, the study of vertebrate and invertebrate *in vivo* models of candidiasis has provided important insight into the pathogenesis of fungal infections. However, limitations to analyzing host-pathogen interactions in the context of the adult body and the stem cell response still exist. For example, although mammalian models, such as the rat, mouse, and rabbit, are the closest species used to mimic human infections, their use is limited by sample size, handling, and cost. However, like all other invertebrate models, the planarians lack adaptive immunity and cannot provide insight into that specific area. Nevertheless, this results in the ability to study the innate response independently of any adaptive immune response. With the planarian model the whole system response of the host can be observed, in contrast to concentrating on a specific organ or tissue as with murine models. When studying the interactions of *C. albicans* in these host models, clinical and mutant strains found to be virulent and avirulent in mice demonstrate similar virulence in planarians. Thus, this model can be used to screen various *C. albicans* mutants and strains at a more rapid pace.

On the other hand, although cost-effective invertebrate models, including *Drosophila melanogaster*, *Caenorhabditis elegans* and *Galleria mellonella*, are limited in their utility for analysis due to embryonic stages influencing host response and infection methodology (e.g., injections cause injury adding another element to consider) and similarity to human tissue. The planarian model also best mimics the mucosal epithelium, with its mucus showing strong homology to that of humans. In addition, the other invertebrate models possess a cuticle that needs to be pierced for infection.

All of these invertebrate models possess genetic tractability and have advantages and disadvantages compared to each other (Table 1). Thus, the optimal infection model depends on the specific investigation being undertaken. If the question involves systemic and mucosal epithelium infections and a cost-effective choice with tractability of both organisms, the planarian model would be the optimal choice. In addition, the planarian is also an ideal choice to visualize the early response and development of a systemic infection. Therefore, although the planarian is still an emerging model and further research is needed, there is great potential for its use as an infection model for *C. albicans*.

5.2. The hyphal growth form and adhesins are critical virulence factors of *C. albicans* that elicit a specific neoblast response in the planarian model

Infecting planarians with the non-filamentous (*efg1*) and hyper-filamentous (*nrg1*) mutant strains compared to the wildtype strain confirmed that switching from yeast to hyphae is important for virulence⁸⁷. The aggressive nature of hyphal cells gives *C. albicans* the capability to produce severe phenotypes and infect the deeper tissues of the planarian

model (Figure 4). The results were similar to that seen in vertebrate infection models, such as mice and rats, demonstrating that filamentation is an essential driver of virulence in systemic infections. Additionally, hyphal defective mutants were found to be attenuated in virulence in both planarian and mice models¹¹⁷⁻¹¹⁹. It is important to note that all mutant strains could adhere to the planarian epithelium. Still, the non-filamentous strain, with the addition of the *als3* and *bcr1* mutant strains, had less adherence and fewer aggregates when infecting these animals (Figure 11). The hyphal growth form thus provided several benefits for colonizing planarians.

The hyphal cells have a hyphae-specific transcriptional program that increases upregulation of several virulence factors. For example, these cells exhibit augmented adherence, biofilm development, and tissue invasion¹¹⁹⁻¹²¹. Moreover, adhesion is crucial for both the induction of endocytosis and active penetration during host invasion by *C. albicans*¹²². Thus, this supports the notion that *efg1*, *asl3*, and *bcr1* mutant strains are not as virulent due to decreased expression of adhesins, which makes it difficult to penetrate the planarian tissue.

The non-filamentous strain was also predicted to be the fastest *C. albicans* strain eliminated. This yeast growth form is the easiest to phagocytose, resulting in increased clearance¹²³. This is due to the inability to escape phagocytosis by physically breaking from the inside of phagocytic cells, which the hyphal growth form can do¹²³. However, this was not the case as the non-filamentous cells were still present 10 days post-infection, with more cells than the wildtype and non-filamentous strains (Figure 6). Thus, it appears that as long there is not significant tissue damage, planarians do not elicit a strong host response and *C. albicans* is cleared more slowly.

Adhesion factors, such as the Als proteins investigated here, allow *C. albicans* to adhere, invade, and damage the epithelium thereby enhancing virulence. Even though these proteins are associated with hyphal properties, they markedly affect the virulence observed in the infecting yeast growth form and its ability to cluster in the planarians. The ability to adhere is the most critical step for successful infection of a host. Further, it is possible that the adhesins are what the planarian model uses to detect infecting *C. albicans* cells.

The planarian model, like all animal models, must be able to detect and respond to pathogens. PRRs are proteins that recognize conserved and frequently found molecules in pathogens^{124,125}. These PRRs are responsible for inducing signals to activate immune cells and pro-inflammatory responses required to contain and eliminate the infection¹²⁵. There are various toll-like receptors and C-type lectins that recognize *C. albicans* and promote an immune response against the fungi^{112,113}. Dectin is a C-type lectin that recognizes β -glucans with conserved downstream effector proteins¹²⁶. The planarians contain several effector proteins known to function downstream of Dectin-1, all of which are upregulated during fungal infections (Figure 14). Specifically, *syk* and *tak* were observed to be dramatically overexpressed at 6 hours post-infection, suggesting that there is a conserved innate immune response in planarians. The increase in expression of dectin downstream effectors is predicted to be responsible for the host responses of the planarians during the infection.

The adherence of *C. albicans* to the planarian epithelial layer was found to induce the dectin signaling cascade, which I speculate leads to the increase in neoblast proliferation (Figure 13). This was dependent on the ability of *C. albicans* to transform to the hyphal

form, which increases the expression of adhesins^{119,120}. The non-filamentous strain possessed a reduced amount of adhesins and therefore could not elicit an increase in neoblast proliferation from the host. The hyper-filamentous strain, locked in the hyphal growth form, exhibits the most abundant expression of adhesins and induced the most marked hyper-proliferation of neoblasts in the host (Figure 9). Furthermore, the response is also dependent on Bcr1, a transcription factor that is an important regulator of adherence and controls the expression of *ALS3*, which is also essential for adherence. Mutation of either of these genes resulted in a reduced adherence, accompanied by a reduced amount of neoblast proliferation at 6 hours post infection (Figure 12-13). Thus, the neoblast response of the planarian is dependent on the amount of adhesins *C. albicans* is expressing during the infection.

Stem cells are essential for renewing tissue and replacing dead cells following injury, infections, and other cell damage¹²⁷. It is known that *C. albicans* infection of the planarians induces proliferation of selective stem cells, both mesenchymal and hematopoietic, leading to maturation of lineage-restricted cells necessary to defend and eliminate the infecting pathogen. In addition, in vertebrates these cells lead to the development of macrophages and specialized lymphocytes, which are essential for phagocytosing and inhibiting the spread of *C. albicans*¹²⁸⁻¹³⁰. This work demonstrated a novel stem cell response to invasive infections in the planarian model. (Figure 8 & 9). In fact, superficial adherence of *C. albicans* was shown to elicit two neoblast proliferation events at 6 and 24 hours post-infection. This is the first report of the mitotic response occurring with no visible signs of injury or increased cell death in a manner independent of any metabolic inputs. The other two, metabolically or injury-induced neoblast hyper-proliferation peaks, occur at 6 and 12 hours post-feeding and 6 and 48 hours post-injury. Thus, occurrence of two hyper-proliferation peaks appears to be typical of induced neoblast events^{82,131}. The infection-induced mitotic response has a similar induction time of 6 hours post-infection with other induced neoblast events. Thus, it is possible that neoblast hyper-proliferation in planarians takes around six hours in response to any stimuli.

Also, the infection-induced neoblast hyper-proliferation included similar transcriptional changes in early wound response genes as observed during injury-induced neoblast proliferation. Early wound response genes, such as *RUNT1* and *EGR2*, are crucial for activating the response to heal and regrow missing tissue in planarians⁸². In addition, these early wound response genes have also been demonstrated to play essential roles in inflammation and antigen-induced proliferation of lymphocytes in other animal models¹³². The observed increase in expression of *egr2* did not peak and fall as in injuries, but remained overexpressed throughout the infection. Moreover, the protein levels of phosphorylated ERK, upstream of *EGR2*, were also increased similar to what is seen after amputation. Like *erg2*, pERK peaks and falls in amputation; however, there were higher levels of pERK throughout the course of infection (Figure 10).

However, the infection did not change the expression of *runt1*, which is another early wound response gene essential for regeneration^{83,94}. Thus, the planarians wound response transcriptomic profile differs from that seen during infections.

Overall, the prolonged increase of *erg2* expression and pERK seems to be dependent on the adherence of *C. albicans* to the planarian epithelium. Thus, the differences in wound response and proliferation peaks indicate that infection promotes hyperproliferation of specific neoblasts dependent on the adhesion of *C. albicans*. Previous studies have classified different neoblast subpopulations based on expression of the transcription

marker, *piwi-1*. The *piwi-1* neoblast subpopulation is NB2, clonogenic neoblasts, which are crucial for regeneration¹³³. Therefore, gene transcription in planarian neoblast subpopulations was assessed following *C. albicans* infection. The high *piwi1* expressing neoblasts (NB1, NB2, and NB3) exhibited no increase in gene expression during the fungal infection, although some genes were slightly downregulated (Figure 15). Thus, with most of the neoblast subpopulations expressing genes at a basal level, these results suggest that only a few neoblast classes are engaged during *C. albicans* infection. The neoblast subclasses with the lowest expression of *piwi1* were the ones upregulated (Figure 14). Specifically, the NB9, NB11, and NB4 neoblast subclasses were upregulated greater than eightfold during the infection. Of note, these three neoblast subclasses contain less than 5% of the total *piwi1* content in the planarians⁶⁰. These results support the idea that specific neoblast subclasses can cycle independently of others. Moreover, the neoblasts with lower *piwi1* expression are the populations with increased proliferation at 6 and 24 hours post-infection. Overall, these results suggest that specific neoblast subpopulations respond to yeast infections, particularly NB9, NB11 and NB4, and this is distinct from what is seen in other instances of induced neoblast hyper-proliferation.

5.3. Increased mucus secretion by planarians counteracts *C. albicans* infection

The planarian neoblast gives rise to several differentiated tissues, including nervous, digestive, excretory and sensory. Given the increased cycling of NB9, NB11 and NB4, which belong to the neural, protonephridia and muscle lineages, I next investigated the distinct transcriptomic expression of differentiated tissues associated with these neoblast lineages. The genes associated with these two systems, excretory and nervous, were found to be overexpressed during the infection. The upregulation of genes associated with the excretory system was observed during the infection; specifically, genes related to the protonephridia structure were largely overexpressed (Figure 15). It is documented that the increase in protonephridia and other excretory components leads to an increase in mucus secretion^{71,134}. Mucus contains several antimicrobial properties that inhibit *C. albicans* infection¹³⁵. Moreover, mucus is easily observed due to its autofluorescence, and was found to increase dramatically as the infection progressed (Figure 15). The planarian mucus both acts as a physical barrier inhibiting pathogen adherence to the epithelium and contains many antimicrobial peptides, zymogens, and proteases to aid in eliminating the pathogen⁷³.

Moreover, gene expression typical of specific neuronal subtypes was also dramatically increased in the planarians. Specifically, both octopaminergic and cholinergic (*tbh+* and *chat+*) neurons were upregulated more than twofold. This implies that specific neural subclasses could be involved in the planarian immune response to the *C. albicans* infection. Several studies have shown the capability of some neurons to act as either, or both, immunocompetent cells and immune system regulators, which is a highly conserved function^{136,137}. In addition, *C. albicans* has been demonstrated to induce nociceptive neurons in murine models, which are essentially innate immune cells¹³⁸. Thus, it appears that planarians use *chat+* and *tbh+* neurons for organismal communication to defend against *C. albicans*. Moreover, *chat+* neurons may be particularly important in this process, as this neuronal subtype is expressed from the anterior to the posterior of the animal (Figure 16). Further investigation revealed that disruption of *chat* gene expression with RNAi causes planarians to be overwhelmingly covered with mucus. Therefore, it

seems that *chat+* neurons help regulate the production of mucus independently of any infection. Thus, when *chat-RNAi* planarians are infected, they start with the advantage of having an excess amount of mucus, which interferes with the ability of *C. albicans* to adhere and colonize the epithelium (Figure 17). Therefore, one immune function of *chat+* neurons maybe to regulate the excretory system to increase mucus secretion in response to fungal infections.

5.4. Concluding remarks

The results of this study shown that the planarians are a competent model for *C. albicans* infection. The human fungal pathogen *C. albicans* was able to infect and colonize the flatworm while expressing various virulence factors at different stages of infection. The planarian model also displayed the capability to recognize the infection and mount a multi-system response involving stem cells as well as differentiated tissues of the nervous and excretory systems. Once the infection media containing the *C. albicans* cells was removed, the flatworm effectively eliminated and cleared the infection in a short amount of time, even when severe disease phenotypes resulted. Therefore, this investigation establishes the planarian as a cost-effective fast throughput model to perform host-pathogen interaction studies. A collection of various host models can provide wide-ranging insights into the mechanisms underlying the development of infection and subsequent elimination of pathogens. Thus, I advocate implementing the planarian model to study the early stages of a mucosal and systemic *C. albicans* infections.

I suggest the host-pathogen model described in this work bears strong resemblance to early mucosal infections in mammals, and can be a powerful tool to gain additional insights about fungal infections (Figure 18). The planarian soaking infection method demonstrated consistency in virulence associated with fungal filamentation and biofilm development observed with other animal models. Moreover, this infection method allows numerous experiments to be conducted with a rapid turnaround, as analysis of the pathogen's virulence, host immune response, and the observation of infection can all be accomplished within one week. It also allows systemic analysis of host responses and study of the complex interplay of several tissues in response to a superficial infection. Future experiments will address the precise interplay between neoblasts, differentiated tissues, and the molecular cascade orchestrated by the planarian innate immune system to defend against invading pathogens. In addition, analyzing transcriptomic changes in both the host and pathogen will provide more knowledge about the interactions occurring in both organisms, as well as the immune responses in planarians.

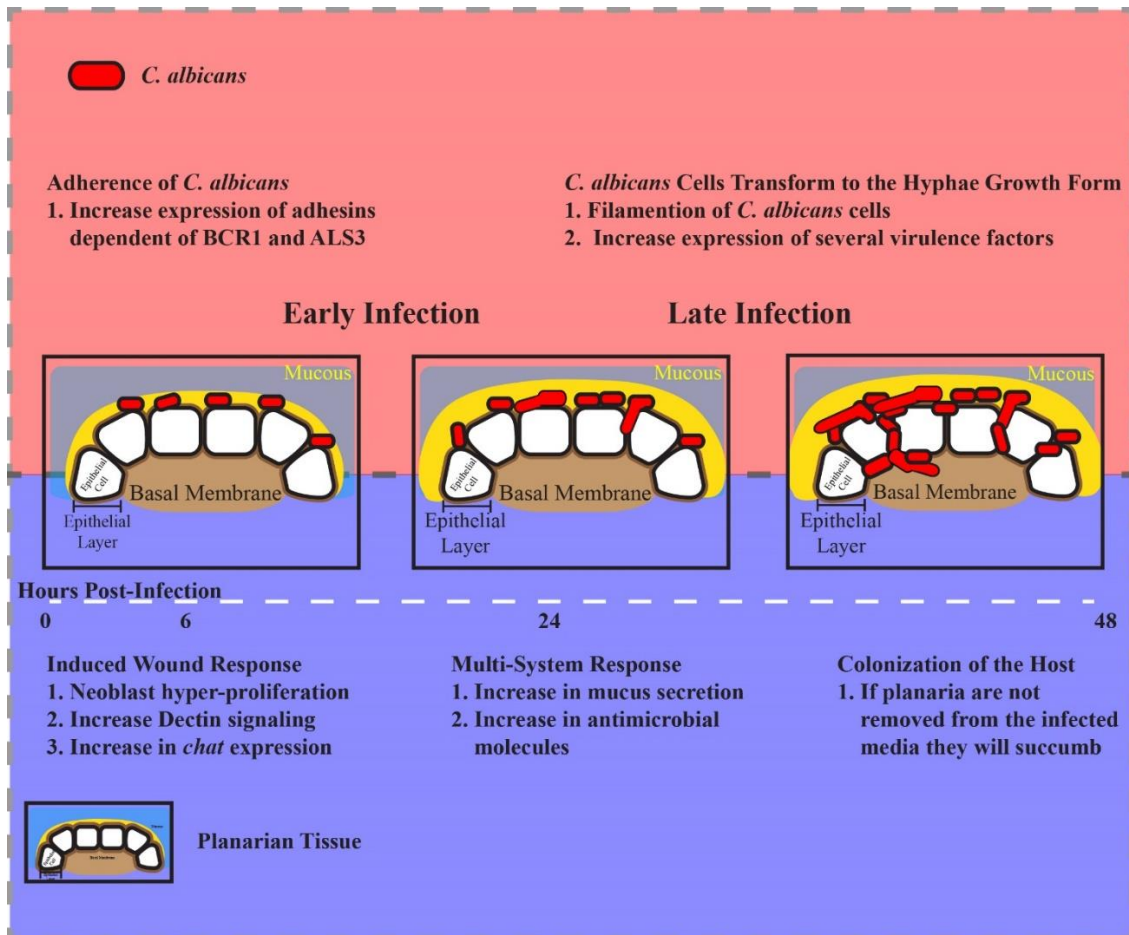


Figure 18: Summary model of interactions occurring during *C. albicans* infection of planarians, using the soaking infection method. The top (salmon color) section indicates the roles of *C. albicans* during the early and late stages of infection. The bottom (blue color) indicates the planarian responses to *C. albicans* during the infection. The middle images describe the stages of infection, demonstrating the *C. albicans* cells adhering to the planarian epithelial layer to colonize and infect the planarian's deep tissue.

5.5. Future directions

This study is the first to describe the use of the planarian flatworm as an infection model to investigate host-pathogen interactions with the fungal pathogen *C. albicans*. The emerging model has provided insight into the planarian immune response and proven useful as an additional tool to study *C. albicans* infection. To further develop this planarian-*C. albicans* infection model, additional classification of the immune system and phagocytic cells of the planarian flatworm will be required. In addition, no upstream PRRs have been identified in planarians; however, I believe there are specific C-type lectins, homologous to the dectin PRR, responsible for this function.

Because the planarian dectin signaling pathway was not thoroughly analyzed, it would be interesting to functionally assess this pathway and the effector proteins identified here. Disruption of canonical dectin signaling components found in the planarian would define the importance of this pathway and indicate whether the planarian relies on other signaling mechanisms during *C. albicans* infection. Further, of the six dectin signaling components in planarians, only the SYK gene has been disrupted. In addition, the expression of *chat+* neurons and genes involved in mucus secretion during infection could also be assessed in the absence of dectin pathway proteins. This would reveal possible regulatory mechanisms eliciting the neural responses during fungal infection.

Future research avenues may also involve, high-throughput analysis of the transcriptomic responses in both host and pathogen at different stages of infection. Although, omics studies are needed, there are a few problems with this approach. Notably, the number of *C. albicans* cells is vastly outnumbered by host cells, so finding a method to obtain and differentiate RNA from *C. albicans* would be crucial. Once a strategy is identified to effectively sequence RNA from both organisms, potential identifying markers of planarian phagocytic cells that respond to the infecting yeast can be identified to observe their roles in eliminating *C. albicans*. This would help improve the planarian as an infection model, adding the ability to visualize the phagocytic cells responding to the yeast and assay the ability of different *C. albicans* strains to avoid or inhibit phagocytosis. Additionally, *C. albicans* transcription factor mutants could then be screened to observe the transcriptomic changes that result from successful *in vivo* infections to determine novel virulence factors¹³⁹. Lastly, the omics strategy will also help identify genes within *C. albicans* responsible for colonizing and evading the planarian immune system. These studies are expected to identify molecular targets with potential for clinical applications.

The influence of the planarian microbiome during the *C. albicans* infection requires further attention. In preliminary studies, I found that disrupting the bacterial flora with a cocktail of antibiotics leads to increased resistance to lethal concentrations of *C. albicans*. To further these results, a combination of *in vitro* and *in vivo* experimentation and transcriptomic sequencing can be done to uncover why removing the bacterial microbiome increases fungal infection resistance. *In vitro* experiments, for example, include homogenizing the planarians and plating the homogenate in both complex media and minimal media, to grow the microbiome, followed by streaking of *C. albicans* to observe morphological characteristics of the yeast as a competition assay. In addition, antibiotic filter paper disks can be introduced to compare the growth of *C. albicans* in the presence and absence of the microbiome. These *C. albicans* cells can then be collected and transcriptomic differences compared. In additional experiments, planarians exposed to antibiotics would be infected with *C. albicans* and collected to assess transcriptomic changes in both

organisms during the infection. These results could identify what is causing the increased fungal resistance in the host.

Importantly, these investigations can also be expanded to other fungal pathogens. *Candida glabrata* is another major human pathogen and *Candida auris* has become problematic due to its multi-resistant properties^{29,33,140}. These *Candida* pathogens can also be analyzed in the planarian model to observe and compare their infection mechanisms. Further, the results obtained from fungal pathogens can be compared to bacterial pathogens to determine if the planarian response is specific for microbial pathogens or if it is a general response to all pathogens. Thus, the potential of the planarian model is only beginning, and my pioneering doctoral work set the basis of this intriguing new paradigm and I expect to see future work capitalizing on it with long-term goals reaching into clinical applications.

Works Cited

1. Hart, B. L. Behavioural defences in animals against pathogens and parasites: parallels with the pillars of medicine in humans. *Philos. Trans. R. Soc. Lond. B. Biol. Sci.* **366**, 3406–3417 (2011).
2. Trinh, P., Zaneveld, J. R., Safranek, S. & Rabinowitz, P. M. One Health Relationships Between Human, Animal, and Environmental Microbiomes: A Mini-Review. *Front. Public Health* **6**, 235 (2018).
3. Sampath, V. Bacterial endotoxin-lipopolysaccharide; structure, function and its role in immunity in vertebrates and invertebrates. *Agric. Nat. Resour.* **52**, 115–120 (2018).
4. Loker, E. S., Adema, C. M., Zhang, S.-M. & Kepler, T. B. Invertebrate immune systems - not homogeneous, not simple, not well understood. *Immunol. Rev.* **198**, 10–24 (2004).
5. Flajnik, M. & Dupasquier, L. Evolution of innate and adaptive immunity: can we draw a line? *Trends Immunol.* **25**, 640–644 (2004).
6. Marcos, C. M. *et al.* Anti-Immune Strategies of Pathogenic Fungi. *Front. Cell. Infect. Microbiol.* **6**, (2016).
7. van Kooyk, Y. & Geijtenbeek, T. B. H. DC-SIGN: escape mechanism for pathogens. *Nat. Rev. Immunol.* **3**, 697–709 (2003).
8. Zecconi, A. & Scali, F. Staphylococcus aureus virulence factors in evasion from innate immune defenses in human and animal diseases. *Immunol. Lett.* **150**, 12–22 (2013).
9. Hohl, T. M. Overview of vertebrate animal models of fungal infection. *J. Immunol. Methods* **410**, 100–112 (2014).
10. Conti, H. R., Huppler, A. R., Whibley, N. & Gaffen, S. L. Animal models for candidiasis. *Curr. Protoc. Immunol.* **105**, 19.6.1-19.6.17 (2014).
11. Capilla, J., Clemons, K. V. & Stevens, D. A. Animal models: an important tool in mycology. *Med. Mycol.* **45**, 657–684 (2007).
12. Russell, J. J. *et al.* Non-model model organisms. *BMC Biol.* **15**, 55, s12915-017-0391-5 (2017).
13. Rauta, P. R., Nayak, B. & Das, S. Immune system and immune responses in fish and their role in comparative immunity study: A model for higher organisms. *Immunol. Lett.* **148**, 23–33 (2012).
14. Rolff, J. Invertebrate Ecological Immunology. *Science* **301**, 472–475 (2003).
15. Kollias, C. M., Huneke, R. B., Wigdahl, B. & Jennings, S. R. Animal models of herpes simplex virus immunity and pathogenesis. *J. Neurovirol.* **21**, 8–23 (2015).
16. Imler, J. L. & Hoffmann, J. A. Toll receptors in Drosophila: a family of molecules regulating development and immunity. *Curr. Top. Microbiol. Immunol.* **270**, 63–79 (2002).
17. Chauhan, A. *et al.* A Rat Model of Central Venous Catheter to Study Establishment of Long-Term Bacterial Biofilm and Related Acute and Chronic Infections. *PLoS ONE* **7**, e37281 (2012).
18. Netea, M. G., Quintin, J. & van der Meer, J. W. M. Trained Immunity: A Memory for Innate Host Defense. *Cell Host Microbe* **9**, 355–361 (2011).
19. Whiteway, M. & Bachewich, C. Morphogenesis in *Candida albicans*. *Annu. Rev. Microbiol.* **61**, 529–553 (2007).
20. Ott, L. *et al.* Evaluation of invertebrate infection models for pathogenic corynebacteria. *FEMS Immunol. Med. Microbiol.* **65**, 413–421 (2012).

21. Lebeaux, D., Chauhan, A., Rendueles, O. & Beloin, C. From in vitro to in vivo Models of Bacterial Biofilm-Related Infections. *Pathog. Basel Switz.* **2**, 288–356 (2013).
22. Wilson-Sanders, S. E. Invertebrate models for biomedical research, testing, and education. *ILAR J.* **52**, 126–152 (2011).
23. Arvanitis, M., Glavis-Bloom, J. & Mylonakis, E. Invertebrate models of fungal infection. *Biochim. Biophys. Acta BBA - Mol. Basis Dis.* **1832**, 1378–1383 (2013).
24. Bongomin, F., Gago, S., Oladele, R. & Denning, D. Global and Multi-National Prevalence of Fungal Diseases—Estimate Precision. *J. Fungi* **3**, 57 (2017).
25. Kullberg, B. J. & Arendrup, M. C. Invasive Candidiasis. *N. Engl. J. Med.* **373**, 1445–1456 (2015).
26. d’Enfert, C. *et al.* The impact of the Fungus-Host-Microbiota interplay upon *Candida albicans* infections: current knowledge and new perspectives. *FEMS Microbiol. Rev.* **45**, fuaa060 (2021).
27. Gabaldón, T. & Carreté, L. The birth of a deadly yeast: tracing the evolutionary emergence of virulence traits in *Candida glabrata*. *FEMS Yeast Res.* **16**, fov110 (2016).
28. Ksiezopolska, E. & Gabaldón, T. Evolutionary Emergence of Drug Resistance in *Candida* Opportunistic Pathogens. *Genes* **9**, 461 (2018).
29. Jackson, B. R. *et al.* On the Origins of a Species: What Might Explain the Rise of *Candida auris*? *J. Fungi* **5**, 58 (2019).
30. Schwartz, I. S., Smith, S. W. & Dingle, T. C. Something wicked this way comes: What health care providers need to know about *Candida auris*. *Can. Commun. Dis. Rep. Releve Mal. Transm. Au Can.* **44**, 271–276 (2018).
31. Perltroth, J., Choi, B. & Spellberg, B. Nosocomial fungal infections: epidemiology, diagnosis, and treatment. *Med. Mycol.* **45**, 321–346 (2007).
32. Yang, B. & Rao, R. Emerging Pathogens of the *Candida* Species. in *Candida Albicans* (ed. Sandai, D.) (IntechOpen, 2019). doi:10.5772/intechopen.80378.
33. Arendrup, M. C. & Patterson, T. F. Multidrug-Resistant *Candida*: Epidemiology, Molecular Mechanisms, and Treatment. *J. Infect. Dis.* **216**, S445–S451 (2017).
34. Calderone, R. A. & Fonzi, W. A. Virulence factors of *Candida albicans*. *Trends Microbiol.* **9**, 327–335 (2001).
35. Odds, F. C. Pathogenesis of *Candida* infections. *J. Am. Acad. Dermatol.* **31**, S2–S5 (1994).
36. Jacobsen, I. D. *et al.* *Candida albicans* dimorphism as a therapeutic target. *Expert Rev. Anti Infect. Ther.* **10**, 85–93 (2012).
37. Sudbery, P., Gow, N. & Berman, J. The distinct morphogenic states of *Candida albicans*. *Trends Microbiol.* **12**, 317–324 (2004).
38. Duvenage, L. *et al.* Inhibition of Classical and Alternative Modes of Respiration in *Candida albicans* Leads to Cell Wall Remodeling and Increased Macrophage Recognition. *mBio* **10**, e02535-18 (2019).
39. Kumamoto, C. A. Inflammation and gastrointestinal *Candida* colonization. *Curr. Opin. Microbiol.* **14**, 386–391 (2011).
40. Miller, M. G. & Johnson, A. D. White-opaque switching in *Candida albicans* is controlled by mating-type locus homeodomain proteins and allows efficient mating. *Cell* **110**, 293–302 (2002).
41. Noble, S. M., Gianetti, B. A. & Witchley, J. N. *Candida albicans* cell-type switching and functional plasticity in the mammalian host. *Nat. Rev. Microbiol.* **15**, 96–108 (2017).

42. Ene, I. V. *et al.* Phenotypic Profiling Reveals that *Candida albicans* Opaque Cells Represent a Metabolically Specialized Cell State Compared to Default White Cells. *mBio* **7**, (2016).
43. Pande, K., Chen, C. & Noble, S. M. Passage through the mammalian gut triggers a phenotypic switch that promotes *Candida albicans* commensalism. *Nat. Genet.* **45**, 1088–1091 (2013).
44. Cotter, G. & Kavanagh, K. Adherence mechanisms of *Candida albicans*. *Br. J. Biomed. Sci.* **57**, 241–249 (2000).
45. Verstrepen, K. J. & Klis, F. M. Flocculation, adhesion and biofilm formation in yeasts. *Mol. Microbiol.* **60**, 5–15 (2006).
46. Mayer, F. L., Wilson, D. & Hube, B. *Candida albicans* pathogenicity mechanisms. *Virulence* **4**, 119–128 (2013).
47. Murciano, C. *et al.* Evaluation of the role of *Candida albicans* agglutinin-like sequence (Als) proteins in human oral epithelial cell interactions. *PloS One* **7**, e33362 (2012).
48. Sundstrom, P. Adhesion in *Candida* spp. *Cell. Microbiol.* **4**, 461–469 (2002).
49. Monod, M., Togni, G., Hube, B. & Sanglard, D. Multiplicity of genes encoding secreted aspartic proteinases in *Candida* species. *Mol. Microbiol.* **13**, 357–368 (1994).
50. Naglik, J. R. *et al.* In vivo analysis of secreted aspartyl proteinase expression in human oral candidiasis. *Infect. Immun.* **67**, 2482–2490 (1999).
51. Schaller, M., Schäfer, W., Korting, H. C. & Hube, B. Differential expression of secreted aspartyl proteinases in a model of human oral candidosis and in patient samples from the oral cavity. *Mol. Microbiol.* **29**, 605–615 (1998).
52. Li, W. *et al.* Role of *Candida albicans*-secreted aspartyl proteinases (Saps) in severe early childhood caries. *Int. J. Mol. Sci.* **15**, 10766–10779 (2014).
53. Koh, A. Y. Murine models of *Candida* gastrointestinal colonization and dissemination. *Eukaryot. Cell* **12**, 1416–1422 (2013).
54. Capilla, J., Clemons, K. V. & Stevens, D. A. Animal models: an important tool in mycology. *Med. Mycol.* **45**, 657–684 (2007).
55. Gentile, L., Cebrià, F. & Bartscherer, K. The planarian flatworm: an in vivo model for stem cell biology and nervous system regeneration. *Dis. Model. Mech.* **4**, 12–19 (2011).
56. Newmark, P. A. & Sánchez Alvarado, A. Not your father's planarian: a classic model enters the era of functional genomics. *Nat. Rev. Genet.* **3**, 210–219 (2002).
57. Cebrià, F. Planarian Body-Wall Muscle: Regeneration and Function beyond a Simple Skeletal Support. *Front. Cell Dev. Biol.* **4**, 8 (2016).
58. Pellettieri, J. & Sánchez Alvarado, A. Cell turnover and adult tissue homeostasis: from humans to planarians. *Annu. Rev. Genet.* **41**, 83–105 (2007).
59. Reddien, P. W. & Sánchez Alvarado, A. Fundamentals of planarian regeneration. *Annu. Rev. Cell Dev. Biol.* **20**, 725–757 (2004).
60. Abnave, P. *et al.* Screening in Planarians Identifies MORN2 as a Key Component in LC3-Associated Phagocytosis and Resistance to Bacterial Infection. *Cell Host Microbe* **16**, 338–350 (2014).
61. Maciel, E. I. & Oviedo, N. J. Platyhelminthes: Molecular Dissection of the Planarian Innate Immune System. in *Advances in Comparative Immunology* (ed. Cooper, E. L.) 95–115 (Springer International Publishing, 2018). doi:10.1007/978-3-319-76768-0_4.

62. Pang, Q. *et al.* De Novo Transcriptome Analysis Provides Insights into Immune Related Genes and the RIG-I-Like Receptor Signaling Pathway in the Freshwater Planarian (*Dugesia japonica*). *PLOS ONE* **11**, e0151597 (2016).
63. Vásquez-Doorman, C. & Petersen, C. P. *zic-1* Expression in Planarian Neoblasts after Injury Controls Anterior Pole Regeneration. *PLoS Genet.* **10**, e1004452 (2014).
64. Peiris, T. H., Hoyer, K. K. & Oviedo, N. J. Innate immune system and tissue regeneration in planarians: an area ripe for exploration. *Semin. Immunol.* **26**, 295–302 (2014).
65. Rozanski, A. *et al.* PlanMine 3.0—improvements to a mineable resource of flatworm biology and biodiversity. *Nucleic Acids Res.* **47**, D812–D820 (2019).
66. Arnold, C. P. *et al.* Pathogenic shifts in endogenous microbiota impede tissue regeneration via distinct activation of TAK1/MKK/p38. *eLife* **5**, (2016).
67. Maciel, E. I., Jiang, C., Barghouth, P. G., Nobile, C. J. & Oviedo, N. J. The planarian *Schmidtea mediterranea* is a new model to study host-pathogen interactions during fungal infections. *Dev. Comp. Immunol.* **93**, 18–27 (2019).
68. Maciel, E. I., Valle Arevalo, A., Ziman, B., Nobile, C. J. & Oviedo, N. J. Epithelial Infection With *Candida albicans* Elicits a Multi-System Response in Planarians. *Front. Microbiol.* **11**, 629526 (2020).
69. Cone, R. A. Barrier properties of mucus. *Adv. Drug Deliv. Rev.* **61**, 75–85 (2009).
70. Fahy, J. V. & Dickey, B. F. Airway mucus function and dysfunction. *N. Engl. J. Med.* **363**, 2233–2247 (2010).
71. Zanin, M., Baviskar, P., Webster, R. & Webby, R. The Interaction between Respiratory Pathogens and Mucus. *Cell Host Microbe* **19**, 159–168 (2016).
72. King, S. M. & Patel-King, R. S. Planaria as a Model System for the Analysis of Ciliary Assembly and Motility. *Methods Mol. Biol. Clifton NJ* **1454**, 245–254 (2016).
73. Bocchinfuso, D. G. *et al.* Proteomic profiling of the planarian *Schmidtea mediterranea* and its mucous reveals similarities with human secretions and those predicted for parasitic flatworms. *Mol. Cell. Proteomics MCP* **11**, 681–691 (2012).
74. Zayas, R. M., Cebrià, F., Guo, T., Feng, J. & Newmark, P. A. The use of lectins as markers for differentiated secretory cells in planarians. *Dev. Dyn. Off. Publ. Am. Assoc. Anat.* **239**, 2888–2897 (2010).
75. Muta, T. & Iwanaga, S. The role of hemolymph coagulation in innate immunity. *Curr. Opin. Immunol.* **8**, 41–47 (1996).
76. Lu, A. *et al.* Insect prophenoloxidase: the view beyond immunity. *Front. Physiol.* **5**, 252 (2014).
77. Gao, L. *et al.* Innate and intrinsic immunity in planarians. *Invertebr. Surviv. J.* 443–452 Pages (2017) doi:10.25431/1824-307X/ISJ.V14I1.443-452.
78. Tsoum TSA, L. L. *et al.* Antimicrobial capacity of the freshwater planarians against *S. aureus* is under the control of Timeless. *Virulence* **8**, 1160–1169 (2017).
79. Mer, M., Zumla, A. & Dünser, M. W. Limiting consumption in tuberculosis: current concepts in anti-tuberculosis treatment in the critically ill patient. *Intensive Care Med.* **44**, 2229–2231 (2018).
80. Morita, M. Phagocytic response of planarian reticular cells to heat-killed bacteria. *Hydrobiologia* **227**, 193–199 (1991).
81. Scimone, M. L., Kravarik, K. M., Lapan, S. W. & Reddien, P. W. Neoblast specialization in regeneration of the planarian *Schmidtea mediterranea*. *Stem Cell Rep.* **3**, 339–352 (2014).
82. Wenemoser, D. & Reddien, P. W. Planarian regeneration involves distinct stem cell responses to wounds and tissue absence. *Dev. Biol.* **344**, 979–991 (2010).

83. Wenemoser, D., Lapan, S. W., Wilkinson, A. W., Bell, G. W. & Reddien, P. W. A molecular wound response program associated with regeneration initiation in planarians. *Genes Dev.* **26**, 988–1002 (2012).
84. Oviedo, N. J., Nicolas, C. L., Adams, D. S. & Levin, M. Establishing and Maintaining a Colony of Planarians. *Cold Spring Harb. Protoc.* **2008**, pdb.prot5053-pdb.prot5053 (2008).
85. Homann, O. R., Dea, J., Noble, S. M. & Johnson, A. D. A phenotypic profile of the *Candida albicans* regulatory network. *PLoS Genet.* **5**, e1000783 (2009).
86. Nobile, C. J. *et al.* Complementary adhesin function in *C. albicans* biofilm formation. *Curr. Biol. CB* **18**, 1017–1024 (2008).
87. Felk, A. *et al.* *Candida albicans* hyphal formation and the expression of the Efg1-regulated proteinases Sap4 to Sap6 are required for the invasion of parenchymal organs. *Infect. Immun.* **70**, 3689–3700 (2002).
88. Ye, J. *et al.* Primer-BLAST: a tool to design target-specific primers for polymerase chain reaction. *BMC Bioinformatics* **13**, 134 (2012).
89. Oviedo, N. J., Nicolas, C. L., Adams, D. S. & Levin, M. Gene knockdown in planarians using RNA interference. *CSH Protoc.* **2008**, pdb.prot5054 (2008).
90. Rouhana, L. *et al.* RNA interference by feeding in vitro-synthesized double-stranded RNA to planarians: methodology and dynamics. *Dev. Dyn. Off. Publ. Am. Assoc. Anat.* **242**, 718–730 (2013).
91. Pellettieri, J. *et al.* Cell death and tissue remodeling in planarian regeneration. *Dev. Biol.* **338**, 76–85 (2010).
92. Peiris, T. H. *et al.* Regional signals in the planarian body guide stem cell fate in the presence of genomic instability. *Dev. Camb. Engl.* **143**, 1697–1709 (2016).
93. King, R. S. & Newmark, P. A. In situ hybridization protocol for enhanced detection of gene expression in the planarian *Schmidtea mediterranea*. *BMC Dev. Biol.* **13**, 8 (2013).
94. Wurtzel, O. *et al.* A Generic and Cell-Type-Specific Wound Response Precedes Regeneration in Planarians. *Dev. Cell* **35**, 632–645 (2015).
95. Robb, S. M. C., Gotting, K., Ross, E. & Sánchez Alvarado, A. SmedGD 2.0: The *Schmidtea mediterranea* genome database: The Planarian Genome Database. *genesis* **53**, 535–546 (2015).
96. Gao, L. *et al.* The role of a novel C-type lectin-like protein from planarian in innate immunity and regeneration. *Dev. Comp. Immunol.* **67**, 413–426 (2017).
97. Torre, C. *et al.* *Staphylococcus aureus* Promotes Smed-PGRP-2/Smed-setd8-1 Methyltransferase Signalling in Planarian Neoblasts to Sensitize Anti-bacterial Gene Responses During Re-infection. *EBioMedicine* **20**, 150–160 (2017).
98. Khalil, S., Jacobson, E., Chambers, M. C. & Lazzaro, B. P. Systemic bacterial infection and immune defense phenotypes in *Drosophila melanogaster*. *J. Vis. Exp. JoVE* e52613 (2015) doi:10.3791/52613.
99. Shagin, D. A. *et al.* Identification and characterization of a new family of C-type lectin-like genes from planaria *Girardia tigrina*. *Glycobiology* **12**, 463–472 (2002).
100. Lo, H. J. *et al.* Nonfilamentous *C. albicans* mutants are avirulent. *Cell* **90**, 939–949 (1997).
101. Pukkila-Worley, R., Peleg, A. Y., Tampakakis, E. & Mylonakis, E. *Candida albicans* hyphal formation and virulence assessed using a *Caenorhabditis elegans* infection model. *Eukaryot. Cell* **8**, 1750–1758 (2009).

102. Lohse, M. B., Gulati, M., Johnson, A. D. & Nobile, C. J. Development and regulation of single- and multi-species *Candida albicans* biofilms. *Nat. Rev. Microbiol.* **16**, 19–31 (2018).
103. Nobile, C. J. & Johnson, A. D. *Candida albicans* Biofilms and Human Disease. *Annu. Rev. Microbiol.* **69**, 71–92 (2015).
104. Agata, K., Tasaki, J., Nakajima, E. & Umesono, Y. Recent identification of an ERK signal gradient governing planarian regeneration. *Zool. Jena Ger.* **117**, 161–162 (2014).
105. Tasaki, J. *et al.* ERK signaling controls blastema cell differentiation during planarian regeneration. *Dev. Camb. Engl.* **138**, 2417–2427 (2011).
106. Owlarn, S. *et al.* Generic wound signals initiate regeneration in missing-tissue contexts. *Nat. Commun.* **8**, 2282 (2017).
107. Hoyer, L. L. The ALS gene family of *Candida albicans*. *Trends Microbiol.* **9**, 176–180 (2001).
108. Roudbarmohammadi, S. *et al.* ALS1 and ALS3 gene expression and biofilm formation in *Candida albicans* isolated from vulvovaginal candidiasis. *Adv. Biomed. Res.* **5**, 105 (2016).
109. Nobile, C. J. *et al.* Critical role of Bcr1-dependent adhesins in *C. albicans* biofilm formation in vitro and in vivo. *PLoS Pathog.* **2**, e63 (2006).
110. Jackson, B. E., Wilhelmus, K. R. & Hube, B. The Role of Secreted Aspartyl Proteinases in *Candida albicans* Keratitis. *Investig. Ophthalmology Vis. Sci.* **48**, 3559 (2007).
111. Drickamer, K. & Taylor, M. E. Recent insights into structures and functions of C-type lectins in the immune system. *Curr. Opin. Struct. Biol.* **34**, 26–34 (2015).
112. Tang, J., Lin, G., Langdon, W. Y., Tao, L. & Zhang, J. Regulation of C-Type Lectin Receptor-Mediated Antifungal Immunity. *Front. Immunol.* **9**, 123 (2018).
113. Mayer, S., Raulf, M.-K. & Lepenies, B. C-type lectins: their network and roles in pathogen recognition and immunity. *Histochem. Cell Biol.* **147**, 223–237 (2017).
114. Rink, J. C., Vu, H. T.-K. & Sánchez Alvarado, A. The maintenance and regeneration of the planarian excretory system are regulated by EGFR signaling. *Dev. Camb. Engl.* **138**, 3769–3780 (2011).
115. Issigonis, M. & Newmark, P. A. Planarian ‘kidneys’ go with the flow. *eLife* **4**, e09353 (2015).
116. Ross, K. G., Currie, K. W., Pearson, B. J. & Zayas, R. M. Nervous system development and regeneration in freshwater planarians. *Wiley Interdiscip. Rev. Dev. Biol.* **6**, (2017).
117. Moyes, D. L., Richardson, J. P. & Naglik, J. R. *Candida albicans*-epithelial interactions and pathogenicity mechanisms: scratching the surface. *Virulence* **6**, 338–346 (2015).
118. Jabra-Rizk, M. A. *et al.* *Candida albicans* Pathogenesis: Fitting within the Host-Microbe Damage Response Framework. *Infect. Immun.* **84**, 2724–2739 (2016).
119. Sudbery, P. E. Growth of *Candida albicans* hyphae. *Nat. Rev. Microbiol.* **9**, 737–748 (2011).
120. Azadmanesh, J., Gowen, A. M., Creger, P. E., Schafer, N. D. & Blankenship, J. R. Filamentation Involves Two Overlapping, but Distinct, Programs of Filamentation in the Pathogenic Fungus *Candida albicans*. *G3 Bethesda Md* **7**, 3797–3808 (2017).
121. Desai, J. V. *Candida albicans* Hyphae: From Growth Initiation to Invasion. *J. Fungi Basel Switz.* **4**, (2018).

122. Gow, N. A. R., van de Veerdonk, F. L., Brown, A. J. P. & Netea, M. G. *Candida albicans* morphogenesis and host defence: discriminating invasion from colonization. *Nat. Rev. Microbiol.* **10**, 112–122 (2011).
123. Oliver, J. C., Ferreira, C. B. R. J., Silva, N. C. & Dias, A. L. T. *Candida* spp. and phagocytosis: multiple evasion mechanisms. *Antonie Van Leeuwenhoek* **112**, 1409–1423 (2019).
124. Wang, X.-W. & Wang, J.-X. Pattern recognition receptors acting in innate immune system of shrimp against pathogen infections. *Fish Shellfish Immunol.* **34**, 981–989 (2013).
125. Amarante-Mendes, G. P. *et al.* Pattern Recognition Receptors and the Host Cell Death Molecular Machinery. *Front. Immunol.* **9**, 2379 (2018).
126. Brown, G. D. Dectin-1: a signalling non-TLR pattern-recognition receptor. *Nat. Rev. Immunol.* **6**, 33–43 (2006).
127. Aboobaker, A. A. Planarian stem cells: a simple paradigm for regeneration. *Trends Cell Biol.* **21**, 304–311 (2011).
128. Yáñez, A., Megías, J., O'Connor, J.-E., Gozalbo, D. & Gil, M. L. *Candida albicans* Induces Selective Development of Macrophages and Monocyte Derived Dendritic Cells by a TLR2 Dependent Signalling. *PLoS ONE* **6**, e24761 (2011).
129. Beno, D. W., Stöver, A. G. & Mathews, H. L. Growth inhibition of *Candida albicans* hyphae by CD8+ lymphocytes. *J. Immunol. Baltim. Md 1950* **154**, 5273–5281 (1995).
130. Megías, J., Maneu, V., Salvador, P., Gozalbo, D. & Gil, M. L. *Candida albicans* stimulates *in vivo* differentiation of haematopoietic stem and progenitor cells towards macrophages by a TLR2-dependent signalling: *C. albicans* activates *in vivo* HSPCs through TLRs. *Cell. Microbiol.* **15**, 1143–1153 (2013).
131. Ziman, B., Karabinis, P., Barghouth, P. & Oviedo, N. J. Sirtuin-1 regulates organismal growth by altering feeding behavior and intestinal morphology in planarians. *J. Cell Sci.* jcs.239467 (2020) doi:10.1242/jcs.239467.
132. Li, S. *et al.* The transcription factors Egr2 and Egr3 are essential for the control of inflammation and antigen-induced proliferation of B and T cells. *Immunity* **37**, 685–696 (2012).
133. Zeng, A. *et al.* Prospectively Isolated Tetraspanin+ Neoblasts Are Adult Pluripotent Stem Cells Underlying Planaria Regeneration. *Cell* **173**, 1593-1608.e20 (2018).
134. Kavanaugh, N. L., Zhang, A. Q., Nobile, C. J., Johnson, A. D. & Ribbeck, K. Mucins Suppress Virulence Traits of *Candida albicans*. *mBio* **5**, (2014).
135. Antoni, L. *et al.* Human colonic mucus is a reservoir for antimicrobial peptides. *J. Crohns Colitis* **7**, e652-664 (2013).
136. Godinho-Silva, C., Cardoso, F. & Veiga-Fernandes, H. Neuro-Immune Cell Units: A New Paradigm in Physiology. *Annu. Rev. Immunol.* **37**, 19–46 (2019).
137. Klimovich, A. *et al.* Prototypical pacemaker neurons interact with the resident microbiota. *Proc. Natl. Acad. Sci. U. S. A.* **117**, 17854–17863 (2020).
138. Kashem, S. W. *et al.* Nociceptive Sensory Fibers Drive Interleukin-23 Production from CD301b+ Dermal Dendritic Cells and Drive Protective Cutaneous Immunity. *Immunity* **43**, 515–526 (2015).
139. Noble, S. M., French, S., Kohn, L. A., Chen, V. & Johnson, A. D. Systematic screens of a *Candida albicans* homozygous deletion library decouple morphogenetic switching and pathogenicity. *Nat. Genet.* **42**, 590–598 (2010).
140. Li, L., Redding, S. & Dongari-Bagtzoglou, A. *Candida glabrata*: an emerging oral opportunistic pathogen. *J. Dent. Res.* **86**, 204–215 (2007).